Combining phosphoproteomics and high-throughput phenotyping for the identification of gravitropism-related proteins in *Arabidopsis thaliana*

Dissertation

zur Erlangung des Doktorgrades

der Naturwissenschaften

vorgelegt beim Fachbereich Biowissenschaften

der Johann Wolfgang-Goethe-Universität

in Frankfurt am Main

von

GUANGWEI XING

Frankfurt am Main 2023

(D 30)

vom Fachbereich Biowissenschaften der Johann Wolfgang-Goethe-Universität als Dissertation angenommen.

Erster Gutachter: Prof. Dr. Maik Böhmer

Zweiter Gutachter: Prof. Dr. Jörg Soppa

Datum der Disputation: …….

Zusammenfassung

Der Gravitropismus ist ein grundlegender Prozess in Pflanzen, der es Sprossen ermöglicht, nach oben zu wachsen, und Wurzeln, nach unten zu wachsen. Die Phosphorylierung spielt eine zentrale Rolle bei der Regulierung des pflanzlichen Gravitropismus, da sie als entscheidender Mechanismus für die Übertragung und Modulation von Signalen dient, die an diesem grundlegenden biologischen Prozess beteiligt sind (Schepetilnikov *et al.*, 2013; Van Leene *et al.*, 2019). Mehrere Kinasen, darunter PID (Grones *et al.*, 2018), D6PK (Tan *et al.*, 2020), und TOR (Schepetilnikov *et al.*, 2013) wurden als potenzielle Schlüsselfaktoren für die Vermittlung der gravitropischen Reaktion in Pflanzen identifiziert. Darüber hinaus wird die Gravitropismus-Reaktion schnell eingeleitet und tritt in der Regel innerhalb von Sekunden nach der gravitropischen Stimulation auf (Zheng *et al.*, 2015).

Um tiefere Einblicke in die molekularen Vorgänge zu gewinnen, die in den ersten Sekunden der Schwerelosigkeit auftreten, wurde in dieser Studie eine Phosphoproteomik-Studie an Arabidopsis-Keimlingen durchgeführt. Durch die Konzentration auf diese frühe Zeitspanne sollten die dynamischen Phosphorylierungsereignisse erfasst werden, die eine entscheidende Rolle bei der Reaktion der Pflanze auf die veränderten Schwerkraftbedingungen spielen.

Für diese Studie wurden zwei bewährte Plattformen verwendet: der Fallturm und die Parabelflugplattform, die vom Zentrum für angewandte Raumfahrttechnologie und Mikrogravitation (ZARM) in Bremen und von Novespace in Bordeaux, Frankreich, zur Verfügung gestellt wurden. Die umfassende Analyse in dieser Studie ergab insgesamt 4.266 Phosphosites. Die in dieser Studie beobachteten Phosphorylierungsmuster und Rückstandsverhältnisse stimmten mit früheren Arabidopsis-Phosphoproteomik-Studien überein, was die Zuverlässigkeit und Reproduzierbarkeit der Ergebnisse bestätigte (Yang *et al.*, 2020; Andrea Vega *et al.*, 2021; Rayapuram *et al.*, 2021).

Die Analyse der signifikant unterschiedlich phosphorylierten Peptide in der Hypergravitationsbehandlung sowie in den 3 s und 22 s Mikrogravitationsbehandlungen ergab interessante Überschneidungsmuster. Insgesamt 85 Peptide wurden in allen drei Versuchsgruppen gemeinsam gefunden, was auf eine gemeinsame Reaktion unter diesen Bedingungen hindeutet. Abgesehen von den 85 Peptiden, die alle drei Gruppen gemeinsam hatten, wurden 53 Peptide sowohl in der Hypergravitations- als auch in der 3-Sekunden-Mikrogravitationsbehandlung gefunden, während weitere 53 Peptide sowohl in der Hypergravitations- als auch in der 22-Sekunden-Mikrogravitationsbehandlung zu finden waren. Darüber hinaus wurden 130 Peptide zwischen der 3-Sekunden- und der 22-Sekunden-Behandlung unter Mikrogravitation gefunden. Diese Ergebnisse deuten darauf hin, dass bestimmte Proteine konsistente Veränderungen in ihren Phosphorylierungszuständen über die verschiedenen Dauern der Mikrogravitations- und Hypergravitationsexposition aufweisen, was

auf eine gemeinsame Reaktion und potenzielle Regulierungsmechanismen als Reaktion auf die Schwerkraftänderungen hindeutet.

Zu den angereicherten Gene Ontology (GO)-Begriffen für die signifikant unterschiedlich phosphorylierten Proteine in der 3-Sekunden-Mikrogravitationsbehandlung gehörten "Signaltransduktion", "Mikrotubuli-Zytoskelett-Organisation" und "Protein-Targeting zur Vakuole, beteiligt am Ubiquitin-abhängigen Proteinkatabolismus über den multivesikulären Körpersortierweg". Diese Ergebnisse unterstreichen die rasche Aktivierung von Signalwegen und die Beteiligung von Zytoskelett- und Lipid-Signalproteinen in den frühen Stadien der Gravitropismus-Reaktion.

Im Gegensatz dazu zeigte die 22-s-Mikrogravitationsbehandlung eine Anreicherung nur in Bezug auf biologische Prozesse, insbesondere bei der zellulären Reaktion auf Hormonreize und Salicylsäure-vermittelte Signalwege. Dies deutet darauf hin, dass eine längere Mikrogravitations-Exposition spezifische biologische Prozesse im Zusammenhang mit Hormonreaktionen und Signalübertragung auslösen kann.

Die Analyse von Phosphorylierungsmustern bei verschiedenen Behandlungen liefert wertvolle Informationen über die dynamische Regulierung der Proteinphosphorylierung als Reaktion auf bestimmte Versuchsbedingungen. Durch den Vergleich der Phosphorylierungsprofile von Proteinen in verschiedenen Behandlungsgruppen können Forscher Einblicke in die Signalwege und zellulären Prozesse gewinnen, die an den beobachteten Reaktionen beteiligt sind. In dieser Studie wurden die identifizierten signifikant unterschiedlich phosphorylierten Peptide mithilfe einer Clusteranalyse in zwei verschiedene Cluster eingeteilt, die jeweils einzigartige Phosphorylierungsmuster aufwiesen. Auf der Ebene der biologischen Prozesse wurden innerhalb dieser Cluster faszinierende Präferenzen beobachtet. Insbesondere Phosphoproteine des Clusters 1 reicherten sich im biologischen Prozess des "Protein-Targeting zur Vakuole, das am Ubiquitin-abhängigen Proteinkatabolisierungsprozess über den multivesikulären Körpersortierungsweg beteiligt ist" an, zu dem auch TOM-LIKE (TOL) Phosphoproteine gehören. Frühere Forschungen haben bereits die Beteiligung von TOL-Proteinen am Gravitropismus nachgewiesen (Anon, 2013), während diese Arbeit darüber hinaus interessante Veränderungen in ihren Phosphorylierungsniveaus aufgedeckt hat. Dies deutet darauf hin, dass die Phosphorylierung eine regulierende Rolle im Gravitropismus-Weg der TOL-Proteine spielen könnte. Im Gegensatz dazu deutet die Anreicherung von Phosphoproteinen des Clusters 2 im biologischen Prozess der "Regulierung der Genexpression" auf ihre Rolle bei der Modulation der Genaktivität als Reaktion auf die Stimulation durch die Mikrogravitation hin. Dieses Ergebnis impliziert, dass Veränderungen in den Phosphorylierungsmustern der Proteine die Expression spezifischer Gene beeinflussen und dadurch die zellulären Reaktionen auf die Mikrogravitation beeinflussen können. Darüber hinaus zeigten die Phosphoproteine des Clusters 2 auch eine Anreicherung in der Kategorie

der zellulären Komponenten, insbesondere im Gene Ontology (GO) Begriff "Mikrotubuli". Mikrotubuli sind ein integraler Bestandteil des Zytoskeletts, eines Netzwerks fadenförmiger Proteine, das strukturelle Unterstützung bietet, die zelluläre Bewegung erleichtert und an verschiedenen zellulären Prozessen beteiligt ist (Soga *et al.*, 2018). Die Rolle des Zytoskeletts beim Gravitropismus ist in Arabidopsis gut belegt. Ein bemerkenswertes Beispiel ist die Verwendung von Latrunculin B (Lat B), einem depolymerisierenden Mittel, das spezifisch auf das Mikrofilament-Zytoskelett (Drøbak *et al.*, 2004). Studien haben gezeigt, dass die Anwendung von Lat B die Krümmungsreaktion von Arabidopsis-Wurzeln durch Hemmung der Zellstreckung erleichtert (Xu *et al.*, 2021). Darüber hinaus ist eines der Schlüsselproteine, die am Gravitropismus beteiligt sind, ARG1. Interessanterweise wurde nachgewiesen, dass ARG1 *in vivo* physisch mit Aktin interagiert (B., Harrison und Masson, 2008). Die Anreicherung von mit Mikrotubuli assoziierten Proteinen in den identifizierten Clustern deutet auf ihre potenzielle Rolle bei der Regulierung der Mikrotubuli-Dynamik und -Organisation hin, die beide für verschiedene zelluläre Prozesse von entscheidender Bedeutung sind, einschließlich der Neuordnung des Zytoskeletts und des gerichteten Wachstums als Reaktion auf gravitropische Reize.

Proteinsequenzmotive dienen als Unterscheidungsmerkmale von Proteinfamilien und sind wertvolle Werkzeuge für die Vorhersage von Proteinfunktionen (Bork und Koonin, 1996). In dieser Studie wurden die angereicherten Motive der signifikant unterschiedlich phosphorylierten Proteine analysiert, die in den 3s und 22s Mikrogravitationsbehandlungen identifiziert wurden. Es wurden zwei angereicherte Motive, nämlich [-R-x-x-pS-] und [-pS-P-], innerhalb der signifikant hochregulierten phosphorylierten Peptide entdeckt. Es ist jedoch wichtig anzumerken, dass nur das [-R-x-x-pS-] Motiv in den hochregulierten Proben der 3-s-Mikrogravitationsbehandlung vorhanden war. Dieses Ergebnis stimmt mit einer kürzlich durchgeführten Studie überein, in der Arabidopsis kurzzeitig mit 120 Sekunden Schwerkraftschwankungen behandelt wurde. Sie identifizierten drei Arten von Motiven: ein acidophiles Motiv (p[S/T][D/E] oder p[S/T]xx[D/E]), ein basophiles Motiv (Rxxp[S/T]) und ein Prolin-gesteuertes Motiv (p[S/T]P) (Yang *et al.*, 2020). In Übereinstimmung mit ihren Ergebnissen wurde bei dieser Untersuchung auch das Vorhandensein der Motive [-R-x-x-pS-] und [-pS-P-] festgestellt. Das Fehlen des acidophilen Motivs in dieser Untersuchung könnte auf die unterschiedlichen Versuchsbedingungen zurückzuführen sein. Während in dieser Studie Mikrogravitationsbehandlungen für 3 Sekunden und 22 Sekunden durchgeführt wurden, wurde in der oben genannten Studie eine längere Dauer von 120 Sekunden verwendet, obwohl sie sich ausschließlich auf die Änderung der Richtung der Schwerkraft in einer bodengebundenen Umgebung konzentrierte.

Zur weiteren Aufklärung der Phosphorylierungsereignisse wurde ein Netzwerk von Phosphorylierungsereignissen auf der Grundlage der Kinase-Substrat-Beziehung erstellt.

Interessanterweise wurden mehrere Proteine vorgeschlagen, die am Gravitropismus in Arabidopsis beteiligt sind, wie BZR1 und TOC120. Frühere Studien haben die Beteiligung von *TOC120* am Gravitropismus nahegelegt, insbesondere im Zusammenhang mit mutiertem ARG1 (Strohm *et al.*, 2014). Angesichts der Plastiden-Lokalisierung von TOC120 könnte die Phosphorylierung von TOC120 möglicherweise eine Rolle bei der schnellen Auslösung gravitropischer Signale durch die Bewegung von Amyloplasten spielen. Während der genaue Mechanismus der gravitropischen Stimulationswahrnehmung unbekannt bleibt, ist es plausibel, dass die Sedimentation der Amyloplasten eine Kinaseaktivierung und eine anschließende Phosphorylierungssignalisierung durch TOC120 auslöst.

Die motivbasierte Kinase-Substrat-Analyse deckte mehrere Kinase-Familien auf, die potenziell am Gravitropismus beteiligt sein könnten, insbesondere CK II und CDK. Um die Beteiligung dieser Kinasen am Gravitropismus zu untersuchen, wurden Kinase-Inhibitor-Tests mit TTP 22 als CK-II-Inhibitor und Dinaciclib als CDK-Inhibitor durchgeführt. Die Ergebnisse zeigten, dass die Auswirkungen auf den Gravitropismus der Wurzeln von der Konzentration der Inhibitoren abhingen. Wurde TTP 22 in Konzentrationen von 20 µM und 40 µM verabreicht, wurde eine signifikante hemmende Wirkung auf den Wurzelgravitropismus beobachtet, was auf eine dosisabhängige Reaktion hindeutet. Höhere Konzentrationen von TTP 22 führten zu einer ausgeprägteren Wirkung auf den Wurzelgravitropismus. Darüber hinaus wiesen die beiden Inhibitoren unterschiedliche Wirkungsmuster auf. Die Behandlung mit TTP 22 bei 20 µM oder 40 µM führte zu einer Verringerung der Gesamtkrümmung der Wurzeln. Bei einer Konzentration von 10 nM wurde jedoch festgestellt, dass Dinaciclib die Wurzelkrümmung in den frühen Stadien des Wurzelwachstums, wenn die Länge weniger als 0,4 cm beträgt, deutlich reduziert. In den späteren Stadien war die hemmende Wirkung von Dinaciclib nicht mehr so ausgeprägt und die Wurzelkrümmung ähnelte der von unbehandelten Pflanzen. Wurde die Konzentration von Dinaciclib jedoch auf 100 nM erhöht, wurde eine drastischere Hemmwirkung auf die Wurzelkrümmung beobachtet, was auf eine teilweise Blockierung der gesamten Krümmungsreaktion hinweist. Es wurde vorgeschlagen, dass CK II eine entscheidende Rolle bei der Transkriptionsregulierung in Pflanzen spielt (Stone und Walker, 1995)während Cyclin-abhängige Kinasen (CDKs) eine zentrale Rolle bei der Regulierung des Zellzyklus spielen (De Veylder *et al.*, 2001). Die Verwendung von TTP 22 und Dinaciclib in dieser Studie könnte die Transkriptions- und Zellzyklusaktivitäten gehemmt haben, die an der gravitropischen Reaktion der Wurzeln beteiligt sind. Dies unterstützt die Annahme, dass CDK- und CK-II-Kinasen eine entscheidende Rolle bei der Regulierung der gravitropischen Reaktion spielen und dass ihre Hemmung beobachtbare Auswirkungen auf das gerichtete Wachstum von Pflanzenwurzeln hat.

In mehreren Studien wurde die Wirksamkeit von Kurzzeitstimulationstests unter Mikrogravitation mit verschiedenen Forschungsplattformen wie Falltürmen, Parabelflügen und

Schallraketen umfassend nachgewiesen (Oluwafemi und Neduncheran, 2022; Böhmer und Schleiff, 2019). In dieser Arbeit wurden diese Plattformen genutzt, um die Auswirkungen der verschiedenen Plattformen auf die Phosphoproteomanalyse zu untersuchen, und es wurde festgestellt, dass in den Fallturmproben weniger Phosphopeptide beobachtet wurden als in den Proben der Parabelflugplattform. Darüber hinaus führte die Fallturm-Plattform zu einem Rückgang der Anzahl der signifikant unterschiedlich phosphorylierten Peptide. Diese Unterschiede können auf technische Variationen bei der Durchführung der 3-Sekunden-Mikrogravitationsinduktionsexperimente auf verschiedenen Plattformen zurückgeführt werden. Nach dem Entfernen der Peptide, die bereits in der Hypergravitationsphase der Parabelflugplattform eine signifikante differentielle Phosphorylierung aufwiesen, wurde festgestellt, dass sich nur fünf der verbleibenden signifikant differentiell phosphorylierten Peptide in der 3-Sekunden-Mikrogravitationsbehandlung mit den 71 Peptiden überschnitten, die mit der Fallturmplattform identifiziert wurden. Darüber hinaus zeigte die Klassifizierungsanalyse auch, dass die Hypergravitationsbehandlung einen erkennbaren Einfluss auf die Proteinphosphorylierung vor der 3-s-Mikrogravitationsbehandlung hatte. Diese Ergebnisse deuten insgesamt darauf hin, dass die beobachteten Phosphorylierungsänderungen während der 3-s-Mikrogravitationsbehandlung bei Verwendung der Parabelflugplattform durch die vorherige Exposition gegenüber Hypergravitationsbedingungen beeinflusst werden können.

Trotz dieser plattformbedingten Unterschiede wurden im Rahmen dieser Untersuchung 12 Phosphoproteine identifiziert, die bei beiden Plattformen signifikante Überschneidungen aufweisen. Das Vorhandensein dieser Proteine und ihrer entsprechenden Phosphosites deutet auf eine robuste und konsistente Beteiligung der Phosphorylierung während der Mikrogravitationsbehandlung hin.

Mehrere Mutanten wurden für den Gravitropismusversuch ausgewählt, darunter *suo-1*, *patl2*, *pck1*, *med26c*, *villin3*, *smo4-2*, *hyaluronan*, *map65-1*, *naip1*, *tpx2*, *toc120* und *tzf3*. Das Ergebnis zeigte, dass die Kinetik der gravitropischen Biegung bei verschiedenen Mutanten im Vergleich zum WT unterschiedlich ist ($p < 0,05$), mit Ausnahme von *map65-1*, *hyaluronan* und *villin3*. Mutanten wie *patl2-1*, *med26c*, *naip1*, *tpx2* und *tzf3* zeigten eine verzögerte Phase zu Beginn der Biegung, während die Mutanten *suo-1* und *pck1 eine* schnellere anfängliche Biegereaktion zeigten. Insbesondere *toc120 wies* während der mittleren Krümmungsphase einen signifikanten Unterschied auf.

Die Identifizierung sich überschneidender Phosphoproteine, auf die TOR abzielt, untermauert die Annahme, dass die TOR-Signalübertragung eine entscheidende Rolle bei der Modulation der durch Mikrogravitation ausgelösten Phosphorylierungsvorgänge in Arabidopsis spielt.

Die Phänotypisierung ist ein entscheidender Aspekt der Forschung zum Pflanzentropismus, und in dieser Studie wurde der Bedarf an einem zugänglichen und zuverlässigen Instrument

zur Phänotypisierung erkannt. Um diese Anforderung zu erfüllen, wurde im Rahmen dieser Studie GraviPi entwickelt, eine neuartige Plattform, die bildgebende Hardware und Messsoftware (PlANgle.py, entwickelt von Freya Arthen) umfasst. Ziel war es, eine kostengünstige Alternative zu teuren Geräten und manuellen Messinstrumenten (z. B. ImageJ) zu schaffen und gleichzeitig Stabilität und Genauigkeit zu gewährleisten. Durch strenge Tests und Validierung bestätigte diese Studie die Robustheit der Hardware und die Präzision der Software. GraviPi zeigte bei der Messung der Tropismusreaktionen von Pflanzen eine konstante Leistung und eine zuverlässige Datenerfassung. Mit seiner benutzerfreundlichen Schnittstelle und seinen automatisierten Analysemöglichkeiten hat GraviPi das Potenzial, experimentelle Arbeitsabläufe im Bereich der Pflanzentropismusforschung zu rationalisieren und zu verbessern. Durch das Angebot einer kostengünstigen und leicht zugänglichen Lösung eröffnet GraviPi einem breiteren Spektrum von Forschern die Möglichkeit, Phänomene des Pflanzentropismus zu untersuchen, ohne die Einschränkungen, die durch teure Geräte oder zeitaufwändige manuelle Messungen entstehen. Darüber hinaus machen die einfache Handhabung und die zuverlässige Leistung des GraviPi es zu einem wertvollen Instrument sowohl für Experimente in kleinem Maßstab als auch für groß angelegte Phänotypisierungsstudien.

ARG1, ein DnaJ-ähnliches Protein, wurde zusammen mit seinem Paralog ARL2 in die Signaltransduktion bei Veränderungen des Schwerkraftvektors einbezogen (B., R., Harrison und Masson, 2008; B., Harrison und Masson, 2008). Frühere Studien haben nahegelegt, dass der ARG1/ARL2-Komplex aufgrund seiner chaperonähnlichen Eigenschaften das zytosolische HSC70 an eine Membran rekrutieren und somit als membranassoziiertes Muster für die Gravitropismus-Signalgebung fungieren könnte (B., Harrison und Masson, 2008). Alternativ könnte es HSC70 rekrutieren, um die Aktindynamik als Reaktion auf gravitropische Stimulation zu modulieren. Es ist auch möglich, dass die Aktivität des ARG1/ARL2-Komplexes unabhängig von HSC70 und dem Zytoskelett ist. Das Fehlen von Informationen über neue Interaktionspartner für ARG1 hat jedoch das weitere Verständnis seines Mechanismus bei der gravitropischen Signaltransduktion behindert.

In dieser Studie wurden ARL1 und HSP70-1 als Interaktionspartner von ARG1 identifiziert, was die Frage aufwirft, ob ARL1 und HSP70-1 an demselben Gravitropismus-Signalweg wie ARG1 beteiligt sind. Die HSP70-Proteine in Arabidopsis weisen ein hohes Maß an funktioneller Redundanz auf, was durch das Vorhandensein von 14 weiteren HSP70-Proteinen im Arabidopsis-Genom belegt wird (Sung *et al.*, 2001). In den Daten der Immunpräzipitation-Massenspektrometrie (IP-MS) wurde in dieser Studie eine deutliche Anreicherung von fünf HSP70-Proteinen festgestellt. Um weitere Erkenntnisse zu gewinnen, ist es wichtig, die Interaktion zwischen ARG1 und anderen HSP70-Proteinen, einschließlich der in unserer IP-MS-Analyse identifizierten, zu untersuchen.

In dieser Studie wurde auch die Interaktion zwischen ARL1 und ARG1 entdeckt und verifiziert. Der in dieser Studie mit Arabidopsis durchgeführte BIFC-Assay zeigte eine Kerninteraktion zwischen ARG1-YN/ARL1-YC oder ARG1-YC/ARL1-YN. Es ist möglich, dass ARL1 und ARG1 innerhalb des Zellkerns interagieren, um die Transkription oder sogar Abbauprozesse (z. B. Ubiquitin-vermittelter Proteinabbau) zu regulieren; weitere Experimente sind jedoch erforderlich, um diese Hypothese zu bestätigen.

ARG1 wurde in verschiedenen zellulären Kompartimenten, die am Proteinhandel beteiligt sind, nachgewiesen (Boonsirichai *et al.*, 2003). Die IP-MS-Ergebnisse haben mehrere interessante Kandidaten aufgedeckt, die an der ARG1-vermittelten Gravitropismus-Signaltransduktion beteiligt sein könnten. Unter diesen Kandidaten wurden MEMBRANE STEROID BINDING PROTEIN 1 (MSBP1), PHOSPHOLIPASE D DELTA (PLDDELTA) und PATELLIN 2 (PATL2) bereits früher mit dem Vesikeltransport in Verbindung gebracht, was sie besonders interessant macht (Tejos *et al.*, 2018; Yang *et al.*, 2008; Wang, 2005). Es ist denkbar, dass der ARG1/HSP70-1-Komplex eine Rolle bei der Erleichterung des Trafficking eines unbekannten Proteins durch den Vesikel-Trafficking-Weg spielt. Mögliche Kandidatenproteine, die an diesem Prozess beteiligt sein könnten, sind MSBP1, PLDDELTA und PATL2. Weitere Untersuchungen sind erforderlich, um ihre Beteiligung zu bestätigen und die genauen Mechanismen zu klären, durch die der ARG1/HSP70-1-Komplex seinen Transport vermittelt.

Darüber hinaus wurde in dieser Studie erfolgreich nachgewiesen, dass die Interaktion zwischen ARL1 und ARG1 im Zellkern stattfindet. Die spezifische Funktion dieser Lokalisierung bleibt jedoch unbekannt. Es wird spekuliert, dass diese Kernlokalisierung des ARL1/ARG1-Komplexes möglicherweise an Prozessen wie dem Abbau oder der Transkription beteiligt sein könnte. Weitere Experimente und Untersuchungen sind erforderlich, um die genaue Rolle und Bedeutung dieser Interaktion innerhalb des Zellkerns und ihre Auswirkungen auf zelluläre Prozesse wie den Proteinabbau und die Gentranskription zu bestimmen.

Darüber hinaus werden derzeit Anstrengungen unternommen, um die Beteiligung anderer potenzieller Partner von ARG1 zu bestätigen, darunter MSBP1, Phospholipase D delta, HSP70-2, HSP70-3, HSP70-4 und cpHSP70-1. Durch die Entschlüsselung der Interaktionen und Rollen dieser Proteine soll diese zukünftige Studie ein umfassendes Verständnis der ARG1-vermittelten Gravitropismus-Signaltransduktion erlangen und Licht auf die molekularen Mechanismen werfen, die dieser wesentlichen Pflanzenreaktion zugrunde liegen.

Insgesamt wirft diese Arbeit ein Licht auf die molekularen Komponenten und Signalereignisse, die am pflanzlichen Gravitropismus beteiligt sind. Sie trägt zum bestehenden Wissen bei und eröffnet neue Wege zur Erforschung dieses faszinierenden Bereichs der Pflanzenbiologie.

Abstract

Gravitropism is a fundamental process in plants that allows shoots to grow upward and roots to grow downward. Protein phosphorylation has been postulated to participate in the intricate signaling cascade of gravitropism. In order to elucidate the underlying mechanisms governing the gravitropic signaling and unearth novel protein constituents, an exhaustive investigation employing microgravity-induced phosphoproteomics was undertaken. The significantly phosphorylated proteins unraveled in this study can be effectively divided into two groups through clustering analysis. Furthermore, the elucidation of Gene Ontology (GO) enrichment analysis disclosed the conspicuous overrepresentation of these clustered phosphoproteins in cytoskeletal organization and in hormone-mediated responses intimately intertwined with the intricate phenomenon of gravitropism. Motif enrichment analysis unveiled the overrepresentation of [-pS-P-] and [-R-x-x-pS-] motifs. Notably, the [-pS-P-] motif has been suggested as the substrate for the Casein kinase II (CK II) and Cyclin-dependent kinase (CDK). Kinase-inhibitor assays confirmed the pivotal role played by CK II and CDK in root gravitropism. Mutant gravitropism assays validated the functional significance of identified phosphoproteins, with some mutants exhibiting altered bending kinetics using a custom-developed platform. The study also compared phosphoproteomics data from different platforms, revealing variations in the detected phosphopeptides and highlighting the impact of treatment differences. Furthermore, the involvement of TOR signaling in microgravity-induced phosphorylation changes was uncovered, expanding the understanding of plant gravitropism responses.

To fulfill the large-scale verification of interesting candidates from the phosphoproteomics study, a novel root and hypocotyl gravitropism phenotyping platform was developed. This platform integrated cost-effective hardware, including Raspberry Pi, a high-quality camera, an Arduino board, a rotation stage (obtained from Prof. Dr. Maik Böhmer), and programmable green light (modified by Sven Plath). In addition, through collaboration with a software developer, machine-learning-based software was developed for data analysis. This platform tested the gravitropic response of candidate mutants identified in the phosphoproteomics study. Furthermore, the capabilities of this platform were expanded to investigate tropisms in other species and organs. To find novel proteins that might act as partners of a key protein that is involved in gravitropism signaling, ALTERED RESPONSE TO GRAVITY 1 (ARG1), immunoprecipitation coupled with Mass Spectrometry (IP-MS) was performed and identified ARG1-LIKE1 (ARL1) as a potential interacting protein with ARG1. This interaction was further confirmed through *in vivo* pull-down assays and bimolecular fluorescence complementation assays. In addition, the interaction between ARG1 and HSP70-1 was also validated.

Overall, this thesis sheds light on the molecular components and signaling events involved in plant gravitropism. It contributes to existing knowledge and opens up new ways to investigate this fascinating area of plant biology.

Table of contents

List of Figures

Chapter 1

Chapter 2

Chapter 3

6 Supplement file

List of Tables

Chapter 2

Chapter 3

7 Supplement file

Abbreviations

ABP1: AUXIN BINDING PROTEIN 1

ARG1: ALTERED RESPONSE TO GRAVITY 1

ARL1: ARG1-LIKE 1

ARL2: ARG1-LIKE 2

AUX1: AUXIN RESISTANCE 1

DOC: Deoxycholate

DTT: Dithiothreitol

EIN2: ETHYLENE INSENSITIVE 2

ER: Endoplasmic Reticulum

ESA: European Space Agency

ESCRT: Endosomal Sorting Complexes Required for Transport

FA: Formic Acid

GO: Gene Ontology

GraviPi: Gravitropism Raspberry Pi

H2O2: Hydrogen peroxide

Hg: Hyper-gravity

HSP70:HEAT SHOCK 70-kDa

IBP: Image-Based Phenotyping

IDD: Indeterminate Domain

InsP3: Inositol 1, 4, 5-trisphosphate

IP: Immunoprecipitation

IP-MS: Immunoprecipitation coupled with Mass Spectrometry

KEGG: Kyoto Encyclopedia of Genes and Genomes

Lat-B: Latrunculin B

LED: Light-emitting diode

µg: Microgravity

MS: Murashige and Skoog medium

NASC: Nottingham Arabidopsis Stock Centre

PCA: Principle component analysis

PDK1: PHOSPHOINOSITIDE-DEPENDENT PROTEIN KINASE 1

PGM1: PHOSPHOGLUCOMUTASE 1

PhosPhAt: The Arabidopsis Protein Phosphorylation Sites Database

PHOT1: PHOTOTROPIN 1

PIN: PIN-FORMED

PM: Plasma Membrane

PP2A: PROTEIN PHOSPHATASE 2 A

RNAi: RNA interference

S6K1: PROTEIN KINASES OF RPS6 1

SE: Standard Error

SEX1: STARCH EXCESS1

TAIR: The Arabidopsis Information Resource

TCA: Trichloroacetic Acid

TiO2: Titanium Dioxide

TOC: Translocon at the Outer membrane of Chloroplasts

TOL: TOM1-LIKE

TOR: TARGET OF RAPAMYCIN

VSP: Vesicular Sorting Bodies

WT: Wild Type

ZARM: Center of Applied Space Technology And Microgravity

Chapter 1 Introduction

1.1 Gravitropism

Plants, being stationary organisms, have developed the ability to adapt and acquire scarce natural resources such as water and light in diverse environments [1]. Tropism involves the growth of plant organs toward or away from a stimulus. The growth of plant organs' toward or away from the direction of gravity is known as gravitropism [2,3]. Research on plants gravitropism has gained significant attention in recent years. On the one hand, studying plant gravitropism provides insights into how plants respond and adapt to environmental cues, aiding in understanding plant development and optimizing agricultural practices. For instance, in the case of barley, the regulatory role of ENHANCED GRAVITROPISM 2 in controlling root growth angle has been established, highlighting its potential significance in crop enhancement [4]. On the other hand, the significance of studying plant gravitropism extends beyond terrestrial applications. With the growing interest in space exploration and the potential for human settlement on celestial bodies such as the Moon and Mars, understanding plant gravitropism responses becomes crucial for sustaining life and establishing self-sufficient habitats in extraterrestrial environments [5].

1.2 Role of amyloplasts and columella cells in gravitropism

Gravitropism encompasses three distinct phases: the perception of gravitropic stimulation, signal transduction, and the differential growth of organs [3]. The starch-statolith model stands as a widely embraced hypothesis that comprehensively elucidates the mechanism of plant gravitropism. This model states that the sedimentation of starch-enriched amyloplasts (Figure 1.1 A & B) induces a signaling process and further causes an asymmetric growth. Amyloplasts specifically localized in root cap columella cells, or stem endodermal cells in higher plants, act as statoliths [6,7]. These specialized cells possess statoliths that undergo sedimentation in response to gravitational force. Disrupting or removing the innermost columella cells, root gravitropism curvature was strongly inhibited without changing root growth rates [8], emphasizing the crucial role of amyloplasts specifically localized in these columella cells in mediating gravitropism.

In addition to physiological evidence implicating the role of amyloplasts in gravitropism, molecular findings provide further support by highlighting the significance of starch metabolism, including starch synthesis and degradation, which is closely linked to the composition and function of amyloplasts. For instance, *PHOSPHOGLUCOMUTASE 1 (PGM1)* mutation disrupts starch synthesis, resulting in defective starch production by altering the activity of PGM1, a key enzyme involved in the interconversion of glucose-1-phosphate and glucose-6-phosphate during starch biosynthesis [9]. Conversely, mutation in *STARCH EXCESS 1* (*SEX1*)

lead to an excessive accumulation of starch due to impaired starch degradation, resulting in an excess of starch [10]. Interestingly, these genetic alterations have opposite effects on gravitropism. The *PGM1* mutation is linked to a decreased gravitropic stimulation response [9], conversely, the *SEX1* mutation enhances gravitropism curvature [10]. These findings provide valuable insights into the intricate relationship between starch accumulation and gravitropism in Arabidopsis, highlighting the pivotal role of these genetic factors in modulating plant growth responses to gravity stimuli.

From lower to higher plants, statoliths have evolved to assume various forms. An illustrative example is *Chara globularis* Thuill, a genus of green algae, which employs barium sulfate ($BaSO_4$) crystals as statoliths within their vacuoles. These crystals serve as dense structures that enable the *Chara globularis* Thuill to sense gravitropic stimuli and guide its growth orientation [11], while in *Phycomyces sporangiophores* vacuole, protein crystals function as statoliths [12]. In flowering plants, the dense starch-enriched amyloplasts are well characterized as statoliths, such as in the dicot *Arabidopsis thaliana*, or the monocot, *Oryza sativa*, amyloplasts specifically localized at the apex of root or endodermis of the stem and function as statoliths [13]. The utilization of different forms of statoliths demonstrates the adaptability and diversity of gravitropic mechanisms across plant species. From the perspective of evolution, in lower plants, such as algae, the choice of BaSO4 crystals as statoliths is likely due to the availability of barium and sulfate ions in their natural habitat, these ions can be readily absorbed by the algae from the surrounding water, facilitating the formation of the dense crystals within the cells. While in flowering plants, plants synthesize a large amount of starch through photosynthesis, which provides a foundation for plants to use amyloplasts as statoliths, except for the role of statoliths, amyloplasts also provide a function of energy reserve, the multiple functions of amyloplasts might help flowering plants optimize their organelle utilization and expand their environmental adaptation.

Interestingly, columella cells in plants have undergone subcellular organelle rearrangement, leading to a distinctive polar distribution that enhances their ability to function as gravitropic stimulation sensing cells. Recent investigations have unveiled a polar organization within these cells, wherein the nucleus is positioned on the proximal side, while the peripheral side is occupied by the endoplasmic reticulum (ER) [14]. This polar subcellular arrangement likely facilitates the efficient perception and transduction of gravitropic signals within the columella cells [14]. Remarkably, a specialized form of the ER, referred to as nodal ER (Figure 1.1 C), has been discovered in columella cells, localized in a peripheral layer adjacent to the plasma membrane [14]. The identification of the nodal ER provides further evidence of the unique subcellular organization within columella cells, emphasizing their specialized role in gravitropic stimulation perception.

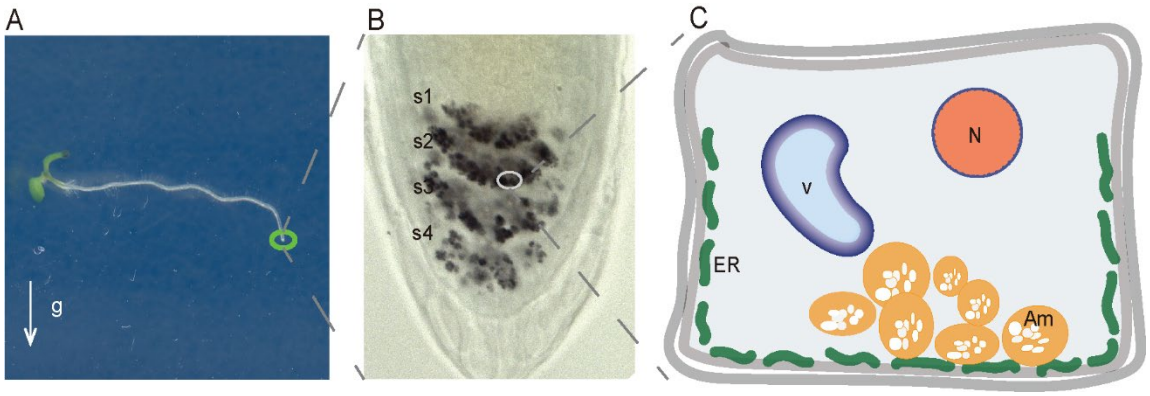

Figure 1.1 Arabidopsis root gravistimulation, root cap staining, and a schematic model of amyloplast sedimentation. (A) A wild-type (Col-0) seedling was grown vertically for 7 days and subsequently subjected to a 90-degree rotation for 10 hours to induce gravistimulation. The direction of gravity is indicated by the white arrow; (B) Lugol staining was performed on 7-day-old Arabidopsis wild-type (Col-0) root caps. The different layers of columella cells, denoted as s1-s4, were observed. Amyloplasts, indicated by their black color, were visualized within the root cap; (C) The schematic model depicts the sedimentation of amyloplasts within a columella cell. The key components include the nucleus (N), vacuole (V), amyloplasts (Am), and nodal endoplasmic reticulum (ER).

1.3 Gravitropism signaling

1.3.1 Role of second messengers in plant gravitropism signaling

The precise mechanism by which amyloplast sedimentation within the statocytes generates a biochemical signal remains elusive. However, one hypothesis proposes the presence of ligands on the surface of amyloplasts, which could interact with specific receptors embedded in the adjacent membranes of the statocytes [11]. This model provides a framework for understanding the intricate interplay between physical forces and molecular signaling events during the perception of gravitropic stimulation, although further investigation is required to unravel the precise mechanisms involved. Nonetheless, extensive research has provided compelling evidence for the involvement of diverse second messengers in the signaling pathways triggered by gravity stimuli. Intracellular calcium ion changes are closely related to gravitropism, as the cytosolic calcium concentration can increase in response to gravitropic stimulation [15]. This response is suggested to be mediated by calcium channels in the plasma membrane or intracellular calcium pools, such as the endoplasmic reticulum [16,17]. Cytosolic calcium transients were observed in Arabidopsis young seedlings after reorientation, using the calcium indicator aequorin [15]. Treatment with 10−3 M EGTA for 8 hours has been observed to effectively inhibit gravitropism in 70-80% of oat coleoptiles, while not affecting growth [18]. In addition, significant inhibition of root curvature in Arabidopsis was observed upon treatment

with 0.1 μM thapsigargin, a specific inhibitor of SERCA-type calcium pumps [19]. RED GENETICALLY ENCODED CALCIUM INDICATOR 1 (R-GECO1), a widely used genetically encoded calcium indicator, enables monitoring of intracellular calcium levels. This red fluorescent protein-based probe undergoes a conformational change upon binding to calcium, leading to a shift in its fluorescence emission spectrum [20]. In living root cells of *Arabidopsis thaliana*, the use of R-GECO1 as a calcium monitor revealed the detection of asymmetric calcium spikes during the early stage of gravitropism [21]. However, the exact role of calcium in the regulation of plant gravitropism has yet to be fully understood.

In addition to calcium changes as a second messenger in response to gravitropic stimulation, it has been proposed that the level of inositol trisphosphate (InsP3), which is another second messenger, undergoes dynamic changes in response to gravitropic stimulation [22]. In Arabidopsis, it has been observed that upon 5 minutes of gravitropic stimulation, the level of InsP3 exhibits the first peak, followed by a second peak at approximately 15 to 20 minutes after the initiation of the gravitropic stimulation.[23]. Furthermore, emerging evidence points towards a close interplay between amyloplast sedimentation and the modulation of InsP3 levels in plant cells. Notably, in tissues lacking amyloplasts, the expected changes in InsP3 levels following gravitropic stimulation are absent [22,24]. This observation suggests that the presence of amyloplasts and their sedimentation play a pivotal role in initiating the cascade of events leading to InsP3-mediated signaling during gravitropism.

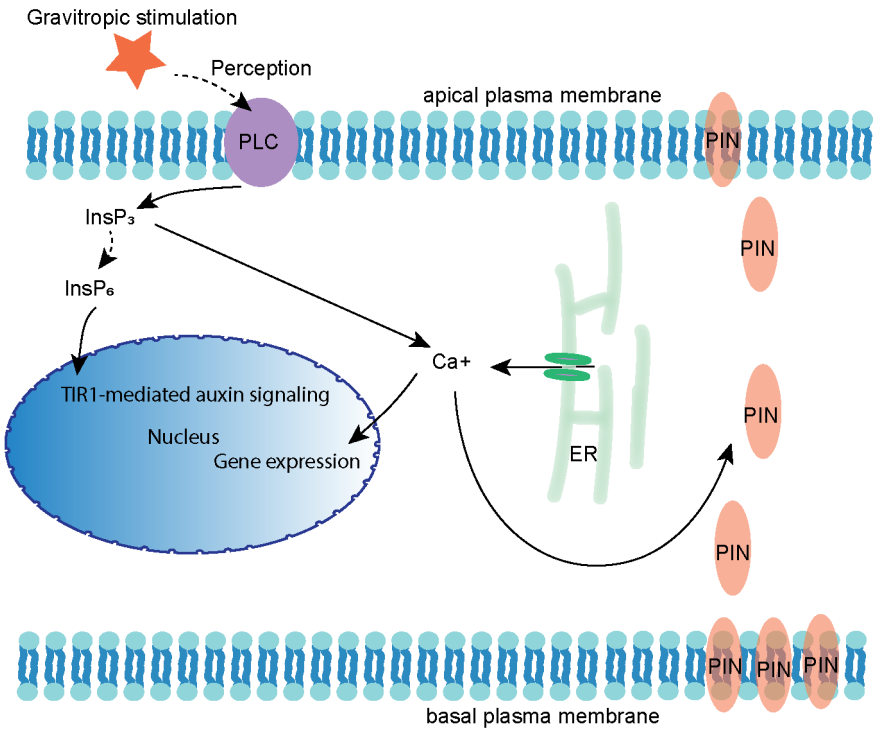

Figure 1.2 Gravitropic stimulation induces $InsP_3$ and calcium signaling. PLC represents phospholipase C, $InsP_3$ represents Inositol 1, 4, 5-trisphosphate, $InsP_6$ represents inositol

hexakisphosphate, ER represents endoplasmic reticulum, PIN represents PIN-FORMED proteins, TIR1 represents TRANSPORT INHIBITOR RESPONSE 1.

Evidence has also revealed the interplay between calcium and InsP3 signaling, as well as the involvement of auxin efflux transporters. Gravitropic stimulation has the ability to activate phospholipase C (PLC) as shown in Figure 1.2. The activation of PLC leads to the hydrolysis of phosphatidylinositol 4,5-bisphosphate (PIP2), which is localized in the plasma membrane. This hydrolysis process results in the production of inositol trisphosphate (InsP3) and diacylglycerol (DAG) [22,25]. As a downstream product, InsP3 induces the release of calcium ions from intracellular reservoirs into the cytoplasm [26]. PIN-FORMED (PIN)-mediated polar auxin transport (PAT) plays a crucial role in the process of gravitropism curvature. Calcium signaling has been demonstrated to be involved in the regulation of PIN trafficking, specifically through the action of CALCIUM-DEPENDENT PROTEIN KINASE 29 (CPK29). CPK29 is capable of phosphorylating specific target residues on the PIN-HL domain [27]. The loss function of CPK29 has a noticeable impact on hypocotyl gravitropism [27]. This finding highlights the intricate interplay between calcium signaling and the proper subcellular distribution of auxin transporters. Furthermore, emerging evidence suggests that inositol hexakisphosphate (InsP6) serve as a structured co-factor for the auxin receptor TRANSPORT INHIBITOR RESPONSE 1 (TIR1) [28]. TIR1, a key component of the auxin signaling pathway, plays a crucial role in the recognition and degradation of AUXIN/INDOLE-3-ACETIC ACID (AUX/IAA) proteins, thereby regulating auxin-responsive gene expression [29]. $InsP_6$ interacts with TIR1, stabilizing its binding pocket and facilitating the formation of the TIR1-Aux/IAA complex. This interaction enhances the efficiency and specificity of auxin-mediated signaling, highlighting the significance of InsP6 as a potential co-factor in regulating auxin responses [28]. However, despite significant progress in understanding the role of calcium and InsP3 signaling in auxin transport and associated developmental processes, the precise molecular mechanisms underlying these interactions remain elusive. Although the connection between calcium and InsP3 signaling and auxin transporter localization and function is well established, the specific molecular interactions and downstream signaling events involved in this process are not fully comprehended. Therefore, further research is required to unravel the intricate crosstalk among calcium and InsP3 signaling as well as auxin transport pathways.

1.3.2 Key proteins in plant gravitropism signaling

So far, researchers have made significant progress in identifying several crucial proteins that play pivotal roles in gravitropic signal transduction (Figure 1.3). Among the various proteins studied, one protein that has gained significant attention is ALTERED RESPONSE TO GRAVITY 1 (ARG1). ARG1 has been identified as a crucial player in the signal transduction process of gravitropism [30]. The knock-out of ARG1 has been shown to significantly reduce

the curvature of both roots and hypocotyls during gravitropic responses [31]. Despite the reduced curvature observed in *arg1-1* mutant plants, they continue to exhibit phytohormonal responsiveness and demonstrate similar behavior to wild-type plants when subjected to phytohormonal treatments [30]. This includes treatments with indoleacetic acid (IAA) at 1 X 10^{-6} and 1 X 10^{-7} M, abscisic acid at 1 X 10^{-5} and 1 X 10^{-6} M, gibberellins at 1 X 10^{-5} and 1 X 10^{-6} M. This finding suggests that ARG1 is involved in the perception/signal transduction phase of gravitropism [31]. The ARG1 protein possesses a highly conserved DnaJ-like domain, which is known to play a critical role in protein folding and molecular chaperone activities. The presence of this domain suggests that ARG1 may function as a co-chaperone, facilitating the ATPase activity of HSP70 proteins [31,32]. In addition to its DnaJ-like domain, ARG1 is predicted to contain a coiled-coil domain in the C-terminus. This coiled-coil domain is involved in protein-protein interactions and is often found in proteins that interact with cytoskeleton components [33]. Sequence similarities between the coiled-coil domain of ARG1 and other cytoskeleton-interacting proteins have led to the suggestion that ARG1 may interact with cytoskeletal proteins to facilitate the transduction of gravitropism signals [31]. Recent studies have revealed the involvement of various cytoskeleton-related proteins in the regulation of gravitropism. Actin filaments, as fundamental components of the cytoskeleton, have been proposed to have a crucial role in gravitropism regulation [34]. Notably, Arabidopsis ACTIN-RELATED PROTEIN 3 (ARP3) has been identified as a key player influencing amyloplast movement and the trafficking of PIN proteins, which are essential for auxin transport and distribution in plant cells [35]. These findings highlight the significance of cytoskeletal dynamics, particularly actin filaments, in modulating gravitropic responses and the proper localization of key molecules involved in the process.

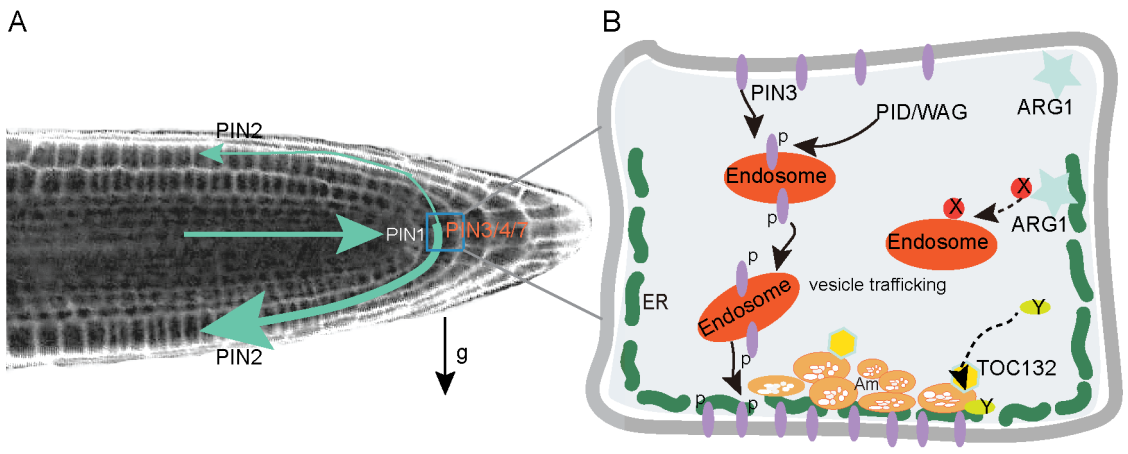

Figure 1.3 Key proteins in gravitropism signaling and phosphorylation. (A) Model of Arabidopsis root marked with auxin flow after gravitropism stimulation. Auxin efflux transporters such as PIN-FORMED 1 (PIN1), PIN-FORMED 2 (PIN2), PIN-FORMED 3 (PIN3), PIN-FORMED 4

(PIN4), and PIN-FORMED 7 (PIN7) are labeled; (B) Key proteins involved in gravitropism signaling via vesicle trafficking and phosphorylation, including ALTERED RESPONSE TO GRAVITY 1 (ARG1), PIN3, PINOID/WAVY ROOT GROWTH (PID/WAG) kinases, TRANSLOCON AT THE OUTER ENVELOPE MEMBRANE OF CHLOROPLASTS 132 (TOC132), UNKNOWN PROTEIN X and Y. ER represents for the endoplasmic reticulum, Am represents for the amyloplast, p represents for phosphorylation.

The disrupted phenotype observed in the *arg1-2* null mutants was successfully restored through the targeted expression of *ARG1* in the statocytes using specific promoters. The utilization of the root-cap target expression *RCP1* promoter in the *pRCP1:ARG1* construct and the endodermis target expression *SCR* promoter in the *pSCR:ARG1* construct effectively rescued the phenotypic defects in the *arg1-2* mutants. These findings underscore the critical role of expressing *ARG1* in the appropriate cell types via specific promoters for the normal functioning of gravitropism in Arabidopsis [36]. During gravistimulation in columella cells, a significant physiological response is cytoplasmic alkalinization. In this context, it was observed that the *arg1-2* mutants lacked the pH increase in the cytoplasm following gravistimulation, in contrast to the wild-type (WT) plants. This intriguing finding suggests that *ARG1* likely plays a crucial role in regulating the pH dynamics within columella cells during the process of gravitropism [36]. To gain insights into the role of *ARG1* in auxin dynamics during gravitropism, researchers employed a *DII-INDUCED 5* (*DR5):: β-Glucuronidase* (*GUS*) reporter system to investigate the changes in auxin distribution in *arg1-2*. The *DR5::GUS* reporter provides a visual readout of auxin levels in plant tissues, by fusing the *DR5* promoter to the *GUS* gene, researchers can monitor and assess the spatial and temporal distribution of auxin signaling in plant tissues. When the *DR5* promoter is active in response to auxin, the *GUS* gene is expressed, resulting in the production of the GUS enzyme and the subsequent blue coloration in the plant tissues. In comparison to the wild-type plants, the researchers observed a distinct alteration in auxin accumulation patterns in the root cap of *arg1-2* following gravistimulation. This observation suggests that *ARG1* plays a significant role in regulating the auxin dynamics during gravitropism, particularly in the root cap [36]. To investigate the subcellular localization of ARG1 and its potential involvement in vesicle trafficking, researchers conducted confocal microscopy and immunofluorescence experiments using *GFP-ARG1* and *cMYC-ARG1* transgenic plants. In the *GFP-ARG1* transgenic plants, root tip cells displayed a distinct subcellular localization pattern characterized by a diffuse and reticulated distribution of GFP-ARG1. This localization pattern is consistent with ARG1's association with the endoplasmic reticulum (ER), suggesting its involvement in ER-related processes, including vesicle trafficking. To further confirm the role of ARG1 in vesicle trafficking, the researchers performed an immunoblot experiment using fractionation techniques. By fractionating cellular components, researchers were able to detect the presence of cMYC-ARG1 in specific fractions that are associated with vesicle trafficking[36]. These findings provide strong evidence

supporting the involvement of ARG1 in vesicle trafficking processes within plant cells. In addition to ARG1, Arabidopsis possesses other homologous proteins called ARG1-LIKE 1 (ARL1) and ARG1-LIKE 2 (ARL2) [31]. Studies have proposed that *ARL2* may function within the same signal pathway as *ARG1*, but it plays a distinct role compared to PGM1. Roots of the *arl2-1 arg1-2* double mutant exhibit gravitropic kinetics comparable to those of the individual single mutants [37]. However, an intriguing observation emerged in *arl2-1 pgm-1* mutations in the homozygous state, as it displayed a more prominent defect in root gravitropism compared to the single mutants [37]. This suggests that *ARL2* may have specific functions and interactions within the gravitropism signaling cascade that are separate from those of *PGM1.* Unlike ARL2, ARL1 does not seem to play a critical role in gravitropism, seedlings with a null mutation in ARL1 exhibited gravitropic behavior similar to wild-type plants [37].

Further research has revealed a potential functional relationship between ARG1, ARL2, and PIN3 within the gravitropism pathway. Gravitropic kinetics, which involve the quantitative analysis of plant growth and curvature in response to gravity, were examined in mutant combinations such as *arl2-4 pin3-3* and *arg1-3 pin3-3*. Interestingly, the gravitropic kinetics observed in these double mutants were similar to those of the corresponding single mutants, *arl2-4* and *arg1-3*, respectively. This finding suggests that ARG1, ARL2, and PIN3 may operate within the same signaling pathway or share common downstream components that contribute to the regulation of gravitropism in plants [36]. A co-immunoprecipitation experiment with transgenic plants expressing *ARG1-GFP* and *ARL2-GFP* has revealed the interaction between ARG1 and ARL2 [38]. Moreover, the co-immunoprecipitation experiments have uncovered additional interactions between ARG1 and other significant proteins, specifically HSP70s and actin proteins [38]. These findings strongly suggest that ARG1, together with ARL2, HSP70s, and actin proteins, forms a complex network of molecular interactions crucial for the regulation of gravitropism. The involvement of HSP70 and actin proteins in the signal transduction pathway mediated by ARG1/ARL2 suggests a potential mechanism where HSP70 is recruited by ARG1/ARL2, leading to conformational changes in actin and subsequent modulation of cellular processes. However, it is also possible that ARG1/ARL2 may function independently of HSP70 and actin, indicating the presence of other yet unidentified proteins that contribute to the pathway's functionality. These intriguing findings highlight the need for further investigation to unravel the complete molecular mechanism and identify additional components involved in the regulation of gravitropism [38].

Emerging evidence suggests a close genetic association between *ARG1* and *MODIFIER OF ARG1 1* (*MAR1*) and *MODIFIER OF ARG1 2* (*MAR2*). In contrast to the moderate defect in gravitropic response observed in the *arg1-2* single mutant, the double mutants *mar1-1arg1-2* and *mar2-1arg1-2* exhibited a pronounced phenotype characterized by a significant alteration in root growth direction. On the other hand, the single mutants *mar1-1* or *mar2-1* exhibited

normal gravitropic responses [39]. This discovery suggests a significant genetic connection between *MAR1* or *MAR2* with *ARG1* in modulating the gravitropic response. Indeed, *MAR1* encodes the TRANSLOCON AT THE OUTER MEMBRANE OF CHLOROPLASTS (TOC) 75 III, and *MAR2* encodes TRANSLOCON AT THE OUTER MEMBRANE OF CHLOROPLASTS 132 (TOC132). The TOC complex plays a crucial role in the translocation of proteins across the outer membrane of plastid, facilitating their import into the organelle [40]. In the *mar1-1arg1-2* and *mar2-1arg1-2* mutants, the morphology and movement of amyloplasts were found to be unchanged and exhibited no significant alterations when compared to wild-type plants. [39]. This finding suggest that the role of TOC132 in gravitropic signaling is likely not related to changes in the sedimentation behavior of columella amyloplasts. Instead, it implies that TOC132 may contribute to gravitropic signaling through signal transducer translocation [39].

The TOC complex is well characterized as a protein import machinery, and the TOC core complex consists of three functional subunits, TRANSLOCON AT THE OUTER ENVELOPE MEMBRANE OF CHLOROPLASTS 34 (TOC34), TOC75, and TRANSLOCON AT THE OUTER ENVELOPE MEMBRANE OF CHLOROPLASTS 159 (TOC159), while TOC132 belongs to the TOC159 family [40]. The TOC159 is known for its involvement in the import of photosynthetic proteins into chloroplasts. TOC132 is associate with the import of non-photosynthetic proteins [41,42]. The absence of ARG1 and ARL2 from plastids indicates that the genetic interactions observed between *arg1* and *toc132*, as well as between *arl2* and *toc132*, may not be attributed to direct physical interaction between these proteins within the plastid compartment. A ligand interaction model has proposed that TOC132, either directly or through a TOC132-mediated transducer, functions as a ligand that interacts with an unknown receptor protein [39]. And the interaction between TOC132 and the receptor protein is facilitated by ARG1/ARL2 [39]. Together, these signal transducers, including ARG1/ARL2 and the components of the TOC complex, collaborate to promote gravitropism signaling [39]. However, further research discovered that TOC132 is unlikely to directly interact with the ARG1/ARL2-mediated unknown protein because deletion of the acidic cytoplasmic domain of TOC132, which is supposed to function as the direct interaction domain, still permitted rescuing the root gravitropism defect in the *mar2-1arg1-2* double mutant [43].

Interestingly, the loss of function of TRANSLOCON AT THE OUTER ENVELOPE MEMBRANE OF CHLOROPLASTS 120 (TOC120), a paralogue of TOC132, was also found to increase the defect of *arg1-2* gravitropism. Overall, studies of ARG1 have contributed significantly to our understanding of the mechanisms underlying gravitropism. In addition, the discovery of genetic interactions between ARG1, TOC75-III, and TOC132 has provided valuable insights into potential ligand interactions and signal transduction pathways involved in gravitropism [39].

Despite extensive investigations into the involvement of ARG1/ARL2 and the components of the TOC complex in gravitropism signaling, there is still a knowledge gap regarding the

identification of additional components within the same pathway. Unraveling these novel components associated with gravitropism signaling will provide valuable insights into the complexity of plant growth responses to gravity and further enhance our comprehension of this fundamental biological phenomenon.

1.3.3 Role of protein phosphorylation in plant gravitropism response

Protein posttranslational modifications, such as phosphorylation, are vital in gravitropism signaling (Figure 1.3). Gravity-induced auxin redistribution is well known to contribute to the curvature of organs, which is mediated by auxin transporters [44]. Auxin efflux carriers, such as PIN-FORMED (PIN) proteins, have specific subcellular localization patterns. In the root, PIN-FORMED 2 (PIN2) exhibits predominant localization in the shootward membranes of lateral root cap cells [45]. This subcellular distribution pattern of PIN2 suggests its involvement in the shootward auxin transport. PIN-FORMED 3 (PIN3) and PIN-FORMED 7 (PIN7) are localized to the plasma membrane of root columella cells [46,47]. PIN-FORMED 4 (PIN4), functioning as an auxin sink generator, exhibits localization at the boundaries between the quiescent center and the surrounding cells [48]. In contrast, AUXIN TRANSPORTER PROTEIN 1 (AUX1), an auxin influx transporter, was found to be localized explicitly within the root apex, where it plays a crucial role in regulating gravitropic root curvature [49].

One way that PIN proteins undergo relocation is through vesicular transport, involving cycling between the plasma membrane and endosomal vesicles and sorting for degradation in the vacuole [50–52]. This process relies on the activity of the endosomal sorting complexes required for transport (ESCRT), which assemble from various vesicular sorting bodies (VSPs). For instance, PIN2 can be recognized at the plasma membrane and sorted as cargo by the TARGET OF MYB1 LIKE (TOL) protein, ultimately leading to its degradation [53].

Another way to influence PIN localization is via reversible phosphorylation. Kinase-mediated phosphorylation or phosphatase-regulated dephosphorylation as a conserved mechanism controls PIN's localization. *In vivo* studies have revealed that PINOID (PID) partially phosphorylates PIN3 [54]. The introduction of phosphorylation-mimicking mutations in PIN3 at either phosphorylation sites P1 (S226D, S243D, and S283D) or phosphorylation sites P2 (S316D, S317D, and S321D) resulted in significant impairment of PIN3 polarization in root columella cells following gravitropic stimulation [54]. In contrast, protein phosphatase 2A (PP2A) has been identified as a negative regulator of PIN hydrophilic loop phosphorylation. Mutant plants deficient in PP2AA1, in combination with either PP2AA2 or PP2AA3, exhibited an enhanced capacity to phosphorylate the hydrophilic loop of PIN2 [55,56].

In addition to the PID kinase, several other kinases have also been identified as important regulators of PIN protein function and localization. For example, the AGC group of protein kinases is named after its constituent families, which include protein kinase A, G, and C

families [57]. One of the key regulators in this signaling pathway is the 3-PHOSPHOINOSITIDE-DEPENDENT PROTEIN KINASE 1 (PDK1), which can activate AGC1 kinase to facilitate PIN phosphorylation [58,59]. A recent discovery revealed that MEMBRANE ASSOCIATED KINASE REGULATOR 2 (MAKR2) functions as a negative regulator of TRANSMEMBRANE KINASES 1 (TMK1) activity, which in turn influences the dynamics of PIN2 accumulation during gravitropism [60]. The interaction between MAKR2 and TMK1 provides a mechanism for fine-tuning the signaling pathway involved in gravity-induced responses by modulating the levels and localization of PIN2 protein.

The asymmetric distribution of auxin is crucial in promoting differential growth, characterized by acid growth-mediated cell elongation. The acid growth theory demonstrates that activation of the plasma membrane-localized H^+-ATPase by auxin triggers the efflux of protons, leading to apoplastic acidification [61,62]. Recent studies have confirmed that the TMK1 plays a crucial role in the activation of the H^+-ATPase by phosphorylating specific C-terminal threonine residues of these proton pumps [62].

Apart from auxin signaling, the TARGET OF RAPAMYCIN (TOR) signaling pathway has emerged as a crucial regulatory pathway governing plant development and response to various abiotic stresses, including gravitropism. The TOR signaling pathway exerts its regulatory function by phosphorylating downstream proteins, which in turn modulates their activity and influences cellular responses [63,64]. The alteration of gravitropism response has been observed when inhibiting TOR signaling using Torin-1, an ATP-competitive inhibitor of TOR kinase, or in *TOR RNA interference* (RNAi) seedlings [65]. Recent research has discovered that TOR can phosphorylate and stabilize PLETHORA 2 (PLT2), a transcription factor critical in maintaining columella development and promoting gravitropism [66].

Significant advancements have been made in understanding the role of phosphorylation-mediated signaling in gravitropism, specifically regarding the phosphorylation events that regulate the localization and activity of PIN proteins and H+-ATPase, as well as the involvement of TOR signaling. However, our knowledge of the comprehensive phosphorylation landscape during the initial stages of microgravity response remains limited.

1.4 Gravitropic stimulation-induced curvature, imaging, and measurement tools

In order to facilitate the study of tropisms, advanced hardware and software systems, such as Image-based platforms, are crucial for accurately measuring and analyzing plant organ curvature. Features related to plant tropisms, such as root, stem, and hypocotyl characteristics, can be extracted and processed. It is essential to consider that these features, including size, color, and shape, vary across different plant species [67]. To optimize feature extraction in plant tropism studies, algorithms should be designed with parameter configurations that accommodate diverse plant characteristics. Consistency in image parameters, such as white

balance and exposure, is essential for robust image processing algorithms. By addressing these challenges, the reliability and effectiveness of image analysis and interpretation can be improved, leading to enhanced performance in image-based processes for studying plant tropisms.

Furthermore, it is noteworthy that certain plant species, particularly poaceae's coleoptiles, exhibit an excellent repositioning response upon gravitropic stimulation. These specialized plant structures demonstrate a robust ability to adjust their orientation in response to gravitropic stimulation, which can be observed as they actively reposition themselves to align with the gravitational force [68], characterized by heightened velocity and magnitude. Consequently, these dynamic movements can challenge the efficacy of conventional path-tracking models. The unpredictable repositioning and readjustment exhibited by plant structures during gravitropic responses may deviate from the expected trajectory, making it difficult for traditional path-tracking models to accurately predict and track the movement of plants. Therefore, it is crucial to develop alternative modeling approaches that can account for and adapt to the inherent variability and complexity of plant movements.

Over the past few years, researchers have designed a range of devices, some specifically for the phenotyping of the movement of tropisms and others with broader functions that are not limited to monitoring tropism movement. For example, the MultipleXLab can incessantly track many seeds encompassing the entire process of germination and development [69]. The D-root device is designed for detecting root systems in the dark [70]. In addition, many studies mentioned using digital cameras and scanners [51,54]. Despite advancements, these devices still have restricted factors such as their high cost, lack of specialization, low throughput, and inadequate downstream software capabilities for comprehensive analysis of tropism movement.

In the past decades, hand-operated measuring was widely accepted in analyzing acquired images of phenotypes, especially the measurement of root or hypocotyl bending angle [39,71–73]. Manual measurements in plant tropism studies are prone to human bias and can be time-consuming, especially when dealing with many images captured over short intervals or long durations. In addition, manual measurements are subjective, leading to potential errors and inconsistencies. In order to mitigate these issues, automated image analysis techniques and computer algorithms can provide objective and efficient measurements, reducing human bias and enhancing the accuracy and reliability of data analysis in plant tropism research. Researchers have developed a series of software in place of hand-based measurements, e.g., RootTrace [74], BRAT [75], KineRoot [76], and ACORBA [77]. These tools have been used to analyze root gravitropism bending angle auto or semi-automatically from the camera, scanner, or microscope images. However, these tools still possess certain limitations. For example, KineRoot needs graphite particles to mark the root bending region, which might influence plant

growth. The BRAT pipeline can only measure the root angle between the whole root vector and the vertical axis of the picture, but the root bending occurs at the root tip [1,78]. While RootTrace needs a manually set starting point for every seedling, this is time-consuming.

Furthermore, the newly developed Acorba is designed for images from a scanner and microscope. To a certain extent, limitations become evident due to the intrinsic impact that light emitted by the flatbed scanner may have on plant tropism [70]. Obtaining the desired light source for imaging purposes can be a complex task, and having precise control over the lighting conditions is crucial.

Decades ago, Arabidopsis was chosen as a model plant species for studying tropisms in laboratory settings, which has provided valuable insights into the underlying molecular mechanisms. While Arabidopsis has been instrumental in uncovering fundamental principles of tropism, it is crucial to recognize that a single species cannot fully capture the intricacies of tropism across all plant species [13]. The image-based phenotype study will boost other species' tropism research. Despite other software claims to measure other species' tropism movement [77], a comprehensive exploration of other species' tropism still lacks. In parallel with the advancement of our understanding of molecular mechanisms, it is of equal importance to develop advanced and efficient platforms for high-throughput methods aimed at studying the numerous potential candidates identified through omics screens. Therefore, investing in developing high-resolution imaging techniques, sophisticated data analysis algorithms, and standardized experimental protocols will significantly contribute to our understanding of gravitropism.

1.5 Research Objectives

This thesis aims to enhance our comprehension of Arabidopsis gravitropism by exploring additional proteins that play a role in this intricate process. Specifically, it will investigate protein phosphorylation as a crucial regulatory mechanism and discover new partners of ARG1 that might be involved in signaling. The research will be organized around the following subtopics to accomplish these objectives:

Identification of proteins involved in phosphorylation-mediated gravitropism signaling. Through a comprehensive phosphoproteomics approach, the thesis aims to identify and quantify protein phosphorylation changes during gravitropism signaling. The investigation will involve subjecting Arabidopsis plants to microgravity conditions using specialized platforms such as the drop tower and parabolic flight, enabling precise time-course analysis of phosphorylation dynamics.

Development of a high-throughput plant gravitropism phenotyping platform. This platform will serve as a high-throughput system for conducting gravitropism physiological experiments, particularly focused on the investigation of the numerous potential candidates identified

through phosphoproteomics screens. A robust high-throughput phenotyping platform will be established to enhance our ability to study and measure gravitropic bending with accuracy and efficiency. This platform will provide a reliable and scalable tool for quantifying and analyzing gravitropic responses across many plant samples, facilitating the identification of novel genetic and molecular factors involved in the process.

Identification of interaction partners of the essential gravitropism signaling protein ARG1. Through the use of ARG1-YFP transgenic plants, an integrated approach combining immunoprecipitation followed by mass spectrometry (IP-MS) will be employed to identify potential interaction partners of ARG1. The identified candidates will then be further validated using co-immunoprecipitation assays.

By pursuing these research objectives, this thesis aims to contribute significant insights into the molecular basis of gravitropism in Arabidopsis. The findings will expand our knowledge of phosphorylation-mediated signaling, evaluate the influence of different microgravity platforms on phosphoproteomics study, establish advanced tools for phenotyping gravitropic responses, and shed light on the protein-protein interactions that regulate gravitropism. Ultimately, these endeavors will enhance our understanding of plant growth and responses to gravity, with potential implications for agriculture, horticulture, and space exploration.

Chapter 2 Methods

2.1 DNA and RNA extraction

Plant materials, including leaves and roots, were collected and homogenized using a pestle. DNA and RNA extraction were carried out using a NucleoSpin Plant II purification kit obtained from MACHEREY-NAGELThe concentration of DNA and RNA was quantified using a Nanodrop 1000 spectrophotometer (https://www.thermofisher.com).

2.2 cDNA synthesis

For cDNA synthesis,the Bio-Rad iScript™ cDNA Synthesis Kit was used according to manufacturer's protocol. The PCR program was performed using the Thermo Fisher Scientific StepOnePlus PCR system, following the established protocol: 5 minutes of priming at 25 °C, 20 minutes of reverse transcription at 46 °C, 1 minute of RT inactivation at 95 °C, and holding at 4 °C.

2.3 Polymerase chain reaction

Two types of polymerases were used in this thesis: *Thermus aquaticus* (Taq) Polymerase and Phusion polymerase from New England Biolabs (NEB, M0273S, M0530S). The Taq polymerase PCR protocol involved an initial denaturation step at 95 °C for 30 seconds (1 cycle), followed by denaturation at 95 °C for 15 seconds (30 cycles), annealing at 58 °C for 30 seconds (30 cycles), extension at 72 °C for 1 minute per kilobase (30 cycles), a final extension at 72 °C for 5 minutes (1 cycle), and holding at room temperature (1 cycle). For Phusion polymerase, the PCR protocol included an initial denaturation at 98 °C for 30 seconds (1 cycle), denaturation at 98 °C for 10 seconds (25 cycles), annealing at 55 °C for 15 seconds (25 cycles), extension at 72 °C for 15 seconds per kilobase (25 cycles), a final extension at 72 °C for 5 minutes (1 cycle), and holding at 4 °C (1 cycle).

2.4 Cloning method

Gateway cloning technology was employed, and the Gateway cloning kit (Gateway™ LR Clonase™ Enzyme Mix, Gateway™ BP Clonase™ Enzyme Mix) was obtained from Thermo Fisher Scientific Both the BP (recombination reaction between the donor vector and the entry clone) and LR (recombination reaction between the entry clone and the destination vector) experiments were conducted following the manufacturer's protocol provided with the kit.

2.5 Agarose gel electrophoresis

A 1% agarose gel was prepared using Agarose Standard ordered from Carl Roth in TAE buffer (0.4 M tris acetate, 0.01 M EDTA, pH 8). The DNA samples were mixed with 6 X loading buffer (30% (v/v) glycerol, 0.25% (w/v) bromophenol blue dye, and (w/v) 0.25% xylene cyanol FF

dye). A GeneRuler DNA Ladder Mix was obtained from Thermo Scientific. Electrophoresis was performed using the PHERO-stab-500 system at 100 volts for 20 minutes.

2.6 Gel extraction and plasmid extraction

The desired DNA fragment was cut first and purified with NucleoSpin Gel and PCR Clean-up kit (MACHEREY-NAGEL, 740609.50).Overnight incubated bacterium contains construct used or generated in this study (Table 2.1) was harvested by centrifugation at 14.000 g, and plasmid was isolated with a NucleoSpin Plasmid EasyPure kit (MACHEREY-NAGEL, 740727.250).

Table 2.1 DNA constructs used or genetrated in this study.

Construct	Tag	Resistance	Reference
pDONR221	Not applicable	Kanamycin	Gateway™ pDONR™221
pXCSG-mYFP	mYFP	Ampicillin	[79]
pXCSG-ARG1-mYFP	mYFP	Ampicillin	This study
pGWB402-omega	Not applicable	Spectinomycin	[80]
pGWB402-omega-Twin-strepII	Twin-strepII	Spectinomycin	This study
pGWB402-omega-GFP	GFP	Spectinomycin	This study
pGWB402-ARL1-Twin-strepII	Twin-strepII	Spectinomycin	This study
pGWB402-HSP70-1-Twin-strepII	Twin-strepII	Spectinomycin	This study
pGWB402-ARG1-GFP	GFP	Spectinomycin	This study
pXCSG-YC84	YC84	Ampicillin	[81]
pXCSG-YN155	YN155	Ampicillin	[81]
pXCSG-ARG1-YC84	YC84	Ampicillin	This study
pXCSG-ARG1-YN155	YN155	Ampicillin	This study
pXCSG-ARL1-YC84	YC84	Ampicillin	This study
pXCSG-ARL1-YN155	YN155	Ampicillin	This study
pRTdsEnp1-mCherry	mCherry	Ampicillin	Stavros Vraggalas

2.7 E. coli and Agrobacterium tumefaciens transformation

For *E. coli* transformation, the heat-shock method was employed [82]. The cells were subjected to a heat shock at 42 °C using a Thermomixer comfort from Eppendorf for 45 seconds, then cooled on ice for 30 seconds. Immediately after, 1 ml of LB medium was added to the cells. On the other hand, the electroporation method was used for *Agrobacterium tumefaciens* transformation [83].

2.8 Restriction enzyme digestion and ligation

GFP and Twin-strepII sequences with STOP codon were cloned and inserted into the pGWB402-omega vector [80] between AfeI (NEB, R0652S) and SacI (NEB, R3156S) restriction sites to create pGWB402-omega-GFP and pGWB402-omega-Twin-strepII. The

digestion reaction was performed as per the protocol from NEB. Subsequently, a ligation reaction was performed using T4 ligase obtained from NEB (M0202S), with 100 ng of linear vector DNA and the prepared insertion fragment.

2.9 Sodium-dodecyl sulfate polyacrylamide gel (SDS-PAGE) electrophoresis

The plant material was harvested and ground using liquid nitrogen. Protein extraction was performed by adding Laemmli sample buffer, which contained 65.8 mM Tris-HCl (pH 6.8), 2.1% SDS, 26.3% (w/v) glycerol, and 0.01% bromophenol blue. The protein samples were then denatured by heating at 95 °C for 5 minutes. The SDS-PAGE gel was prepared according to protocol [84], consisting of a 4% stacking gel and a 12% standard gel. Electrophoresis was carried out using the Mini-PROTEAN Tetra Vertical Electrophoresis Cell.

2.10 Plant lines and growth conditions for phosphoproteomics study

Arabidopsis thaliana lines used in this study, including WT (Col-0), *suo-1* (N67882), *patl2-1* (N663195), *pck1* (N665690), *med26c* (N666414), *villin3* (N673278), *smo4-2* (N677609), *hyaluronan* (N682375), *map65-1* (N684785), *naip1* (N692946), *tpx2* (N868104), *tzf3* (*TZF3,* N927237) and *toc120* (N668738) were ordered from the Nottingham Arabidopsis Stock Centre (NASC, Nottingham, UK).

The dry sterilization method sterilized the seeds' surface [85]. After vernalization at 4 °C for 2-3 days, the seeds were placed on half-strength Murashige and Skoog (MS) agar medium. Subsequently, the plates were transferred to a growth chamber with standard growth conditions, including a photoperiod of 16 hours of light and 8 hours of darkness, with a light intensity of 100 umol m^{-2} s^{-1}.

2.11 Drop tower assay for 3 s microgravity treatment

The drop tower campaign was done at the Center of Applied Space Technology And Microgravity (ZARM) in Bremen. Wild-type (WT) *Arabidopsis thaliana* Col-0 seeds were surface sterilized with a dry sterilization method. After stratification at 4 °C for three days, these seeds were sown on meshes and put in the standard growth condition for seven days. The fine-growing seedlings were then transferred to a hardware designed for microgravity treatment, called ARABIDOMICS [86] for 3 s microgravity treatment. Ten seconds before the drop, non-treated seedlings were fixed by methanol inside ARABIDOMICS as controls. After 3 s microgravity treatment, treated samples were collected (Figure 2.1). Two separate campaigns were conducted, and eight biological samples were collected by [87].

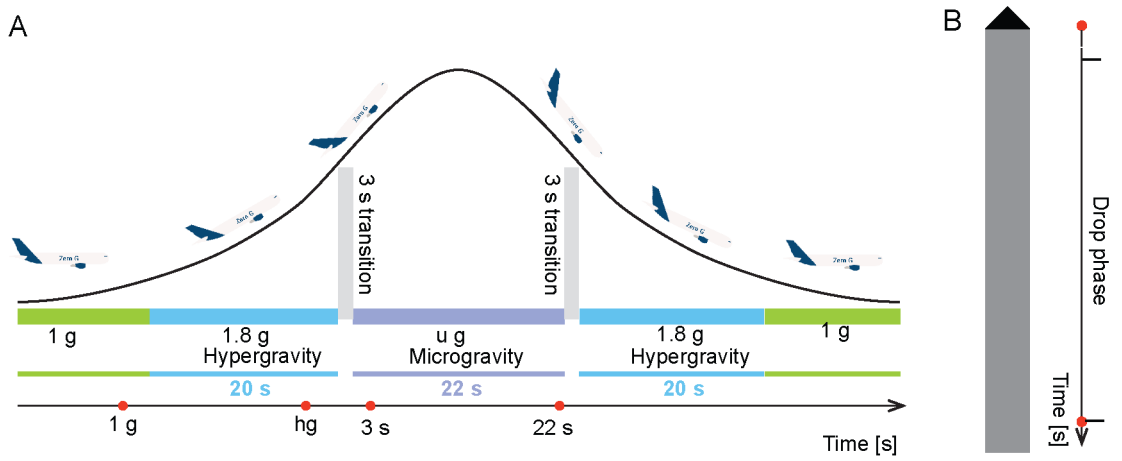

Figure 2.1 Schematic diagram of microgravity platform. (A) Scheme of parabolic flight. 1g represents 1 g control (5 s before hypergravity), hg represents hypergravity control (18 s after the start of hypergravity phase), 3 s represents 3 s microgravity (3 s after the start of microgravity phase), 22 s represents 22 s microgravity (22 s after the start of microgravity phase); (B) Scheme of the drop tower. 1 g control means the sample collected 10 s before drop, and 3 s microgravity represents the sample collected 3 s after drop. Red points represent sample collected time points.

2.12 Parabolic flight assay from 3 s to 22 s microgravity treatment

The parabolic flight campaign was performed at Novespace in Bordeaux, France. Following surface sterilization, *Arabidopsis thaliana* ecotype Col-0 seeds were carefully placed onto mesh surfaces using a pipette. After stratification at 4 °C for three days, these seeds were sown on meshes and put in the standard growth condition for seven days. The seven-day-old seedlings were carefully transferred to the ARABIDOMICS hardware [86] and moved onboard for microgravity treatment. Before the first parabola, a first set of plants was fixed at 1 g (5 seconds before the hypergravity phase) as control. During the first parabola, samples were fixed in the hypergravity phase (18 s after the start of the hypergravity phase) as hypergravity technical control. During the microgravity phase, samples were fixed under microgravity stimulation at 3 and 22 seconds (Figure 2.1). All plant materials were fixed with methanol. In total, five biological replicates were collected in two parabolic flight campaigns.

2.13 Phosphopeptide identification and label-free quantification

MaxQuant (version 2.0.1.0) [88,89] was used to process raw data from the Orbitrap analyzer, the Arabidopsis protein database was downloaded from The Arabidopsis Information Resource (TAIR, https://www.arabidopsis.org/, Araport11, 201606), and used for mapping peptides. Oxidation (M), Acetyl (Protein N-term), and Phospho (STY) were selected as variable modifications, and Carbamidomethyl (C) as fixed modification. Label-free quantification was set with default parameters. Trypsin was set as a specific digestion enzyme with a maximum

of 2 missed cleavages. The match between runs was enabled. The minimum peptide length was set to 7. The maximum peptide mass was set to 4600 Da, the minimum peptide length for the unspecific search was 8, the maximum was set to 25, and no variation mode was selected.

2.14 Bioinformatic analysis for phosphoproteome data

The Phospho (STY)Sites.txt file acquired from the MaxQuant was submitted to the Differential Enrichment analysis of Proteomics data (DEP) package for downstream analysis [88]. Data preprocessing, including data filtering, normalization, handling missing values, and imputation, is necessary to quantify proteins given the nature of the peptide-level data [90]. In brief, reverse hits and contaminants were initially removed. Less stringent filtering for missing values was done by keeping proteins identified in 3 out of 5 replicates of at least one condition. To reduce potential systematic variations arising from technical factors, the data was normalized using the variance stabilizing transformation method, which is suitable for count-based data [91]. The variance stabilizing transformation is particularly suitable for proteomics data normalization due to the nature of the data. Proteomics data often exhibit count-based characteristics, where the abundance of proteins or peptides is measured by the number of identified spectral counts or peptide fragments. Count-based data often display heteroscedasticity, meaning that the variance of the measurements increases with the mean, this can lead to biased statistical analysis and inaccurate interpretation of the data [91]. To evaluate the impact of normalization, a boxplot was created to compare the distributions of samples before and after the normalization process. The issue of missing value in label-free quantitative proteomics has raised broad concerns [92,93]. To assess the presence of missing values in this study, a bar plot was created to visualize the distribution of identified phosphopeptides across the 20 samples. The missed values were imputed with globally observed minimum value in the data set. To assess whether there are statistically significant differences between the group means, protein-wise linear models combined with empirical Bayes statistics (moderate Analysis of Variance, ANOVA) statistical analysis was performed using the DEP package (Significance: p-value < 0.05). The principal component analysis was performed using the ggplot2 [94] and ggrepel packages [95]. The venn diagram was generated using the VennDiagram package [96]. Pattern analysis was performed using the TCseq package with the default settings [97]. A paired-t test was used to analyze the differential phosphorylation proteins for the drop tower samples. The significance level was set to p-value < 0.05. The visualization and integrated discovery (DAVID) was used for Gene Ontology (GO) analysis with all of the identified proteins as background, the significance level was set to p-value < 0.05 [98,99]. String database was used to predict protein-protein interaction with default settings (https://string-db.org/). After data normalization (variance stabilizing transformation) with the DEP package, principle component analysis was done using ggplot2. A volcano plot was done with the DEP package to visualize

the differential phosphorylated proteins (-log10 transformed p-value vs log2 fold-change).
To identify enriched motifs, a set of significant upregulated and downregulated phosphopeptides were extracted based on the positions of phosphosites. In detail, a 13 amino acids window was chosen with the phosphosites located in the center. Subsequently, the motif file was submitted to the MoMo website to identify motifs representing amino acid preferences flanking the phosphosites using the motif-x algorithm with settings of motif width = 13, minimum occurrences for residue = 20 and binomial probability threshold for residue = 0.000001 [100].

2.15 Kinase-inhibitor root gravitropism assay

Casein kinase 2 inhibitor TTP22 and Cyclin-dependent Kinase Inhibitor Dinaciclib were ordered from biomol. Seeds were first sterilized via the dry sterilization method. Seeds were then sown on half-strength MS plates (0.22 %, (w/v) Murashige and Skoog salts (incl. vitamins), 0.8% (w/v) phyto agar), then stratification at 4 °C for 2-3 days. After stratification, the plates were placed in a growth chamber under standard growth conditions and allowed to grow vertically for 5-7 days. And seedlings were treated with TTP 22 (20uM and 40uM), or Dinaciclib (10 nM, 100nM) with pipette and placed in the growth chamber under the standard growth condition vertically for 1 h, subsequently, the plates were rotated 90° to induce gravitropic stimulation. Images were captured at 10-minute intervals using the custom-built GraviPi imaging platform, and the root bending angle was measured using the software integrated with the GraviPi system.

2.16 Description of GraviPi

The GraviPi system comprises a Raspberry Pi (Raspberry Pi 4 model B), an Arduino board (Arduino Zero), a rotational stage (customed by Prof. Dr. Maik Böhmer), a raspberry Pi high quality camera (7.9mm Diagonale, 4056x3040, Sony IMX477R, variabler focus)., and a programmable green LED light (obtained from Amazon). In detail, the initialization of raspberry pi was done according to the protocol (https://www.raspberrypi.com/documentation/computers/getting-started.html). Briefly, the raspberry pi was powered by an official raspberry pi power supply, which provides +5.1 voltage. An 8 GB SD card was used to install an operating system. The rotation stage was built by a combination of a laser-curve stage, a stepper motor, and a NEMA17 Smart Stepper controlling board (https://misfittech.net/). The green LED stripe light was modified to be programming controllable by Sven Plath The Raspberry Pi controls the camera and the programmable LED light, while the rotation stage is connected to the Arduino board and controlled by the Raspberry Pi, as depicted in Figure 2.2. The system utilizes software called PlANgleT.py, developed by Freya Arthen. The PLANgleT.py python script was implemented to allow semi-automatic detection of object (root, hypocotyl) ridges in images. The script is based on the

unbiased detector Fiji plugin for ridge-detection to scan the images for multiple objects like in this case roots or hypocotyls.

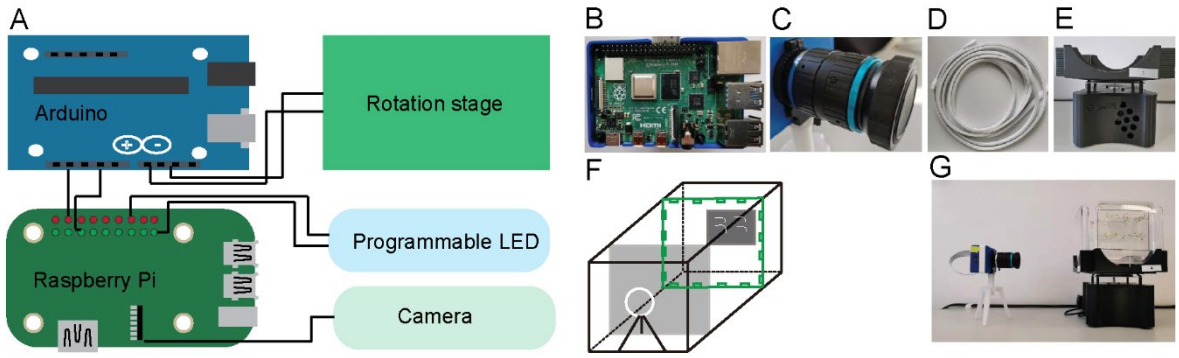

Figure 2.2 Schematic diagram of the GraviPi controlling system and the components of GraviPi hardware. (A) The GraviPi controlling system; (B) Raspberry pi board; (C) Raspberry pi high-quality camera; (D) Programmable LED; (E) Rotation stage; (F) Schematic of integrated hardware; (G) Schematic of the high-quality camera with rotation stage.

2.17 Tropism assay for other species and Arabidopsis hydrotropism

Nicotiana benthamiana, *Solanum lycopersicum*, *Triticum aestivum*, *Zea mays*, *Pisum sativum*, *Brassica napus*, and *Glycine max* seeds were surface sterilized by dry sterilization. Seeds were first sown on a half-strength MS plate for the Arabidopsis hydrotropism assay. Then plates were put at 4 °C for three days for stratification. After that, plates were vertically placed in a growth chamber under standard growth conditionfor five days. Pick delicate grown seedlings to split agar plate prepared according to Antoni et al. [101]. For the Arabidopsis hypocotyl gravitropism assay, after seeds stratification, plates were put in a growth chamber under standard growth conditions for two days, and covered with aluminum foil for another three days, then plates were orientated 90 ° and imaged by GraviPi. For *Nicotiana benthamiana*, *Solanum lycopersicum*, *Triticum aestivum*, *Zea mays*, *Pisum sativum*, *Brassica napus*, and *Glycine max* root gravitropism assay, the germinated seeds were transferred to half MS plate and grown for three to five days, then rotated plate 90 ° and imaging by the GraviPi. For wheat coleoptiles gravitropism assay, two days after vertically grown, rotated plate 90° for gravitropic stimulation and imaging. Manual angle (angle between root tip and gravity direction) measurement was done with Fiji (https://imagej.net/software/fiji/, version 20221201-1017).

2.18 Sucrose treatment assay

WT Col-0 seeds were sown on half-strength MS plate, supplied with 0%, 1%, and 3% sucrose. After three days at 4 °C , seeds germinated and grew at the standard growth condition in the growth chamber. Then, the plates were rotated 90 ° for imaging. The gravitropism and root

growth rate quantification was conducted following a method described in [102].

2.19 Plant materials and growth conditions for ARG1-mYFP

Arabidopsis thaliana Col-0 was used as the wild-type control in this study. The *arg1-3* mutant was ordered from the Nottingham Arabidopsis Stock Center (NASC) with NASC ID N67419. Polymerase chain reaction (PCR)-based genotyping (Table 2.2, primers) was carried out to verify the homozygosity of *arg1-3.* To generate the *ARG1* overexpression (*ARG1 OE*) line, the *ARG1* coding sequence was cloned into pXCSG-YFP binary vector [79] by Gateway cloning technology. pXCSG-ARG1-YFP was then transformed into *Agrobacterium tumefaciens* strain GV3101pmp90 RK cells [103]. After that, the floral dipping method [104] was used to transform the pXCSG-ARG1-YFP into the *arg1-3* mutant. Homozygous transgenic *ARG1-mYFP* plants were selected. In this study, all the seeds used were surface sterilized with the dry sterilization method. Seeds were placed onto half MS medium without sucrose at pH 5.7 in standard growth condition.

Table 2.1 Oligonucleotides used in this study.

Description	name	sequence 5' -> 3'
arg1-3 homozygous identificaition	LB3_SALK	ATTTTGCCGATTTCGGAAC
	ARG1_LP	CATCAATCCACCATCACAATG
	ARG1_RP	CGGTATGCAAGTTTTGAGCTC
ARG1 amplification	ARG1_cds_F	GGGGACAAGTTTGTACAAAAAAGCAGGCTATGAGCGCGAAAAAG CTTGA
	ARG1_cds_R	GGGGACCACTTTGTACAAGAAAGCTGGGTCACCAAGCTTCTTAT CAGATCCTT
ARL1 amplification	ARL1_cds_F	GGGGACAAGTTTGTACAAAAAAGCAGGCTATGCCAGGTCATAGA TCCAAGTCG
	ARL1_cds_R	GGGGACCACTTTGTACAAGAAAGCTGGGTCACAAGGTTTTTTCT TGTCCAATTTC
HSP70-1 amplification	HSP70-1-F	GGGGACAAGTTTGTACAAAAAAGCAGGCTATGTCGGGTAAAGGA GAAGGAC
	HSP70-1-R	GGGGACCACTTTGTACAAGAAAGCTGGGTCGTCGACCTCCTCGA TCTTAGGTC
GFP amplification	GFP-F	AAAGCGCTTCCGGTAAAGGAGAAGAACTTTTCACTGG
	GFP-R	AACGAGCTCCTAATCTAGTTCATCCATGCCATGTG
Twin-strepII amplification	Twin_s_F	ACCTCTGACTTGAGCGTCG
	Twin_s_R	AACGAGCTCTACTTATTTCTCGAACTGC

2.20 Immunoprecipitation-mass spectrometry (IP-MS) experiment

Both *arg1-3* and *ARG1-mYFP* seedlings were grown on half-strength MS medium without sucrose for three weeks at the standard growth condition. Plants were harvested and ground

in liquid nitrogen using a mortar and pestle. The ground plant materials were resuspended with lysis buffer containing 50 mM Tris-HCl, pH 7.5, 150 mM NaCl, 10% (v/v) glycerol, 2 mM EDTA, 1 mM DTT, 1% (v/v) Triton X-100, and 1 X protease inhibitor cocktail. 3 ml lysis buffer was used per 1 g powder. Afterward, the resuspended extracts were centrifuged at 20.000g for 20 min twice. The supernatants were collected and incubated with GFP-Trap agarose beads (GFP-Trap, Agarose, gta-20, ChromoTek). Each sample was incubated with 25 ul beads slurry at 4 °C for 1 h. . The agarose beads were washed with washing buffer containing 50 mM Tris-HCl, pH 7.5, 150 mM NaCl, 10% (v/v) glycerol, 2 mM EDTA, and 1 mM DTT 3 times. One-tenth beads were eluted with 20ul Laemmli sample buffer (65.8 mM Tris-HCl, pH 6.8, 2.1% (w/v) SDS, 26.3% (w/v) glycerol, 0.01% (v/v) bromophenol blue) and the eluted samples were used for Colloidal Coomassie blue staining (0.08% (w/v) coomassie brilliant blue G250 (cbb G250), 10% (v/v) citric acid, 8% (w/v) ammonium sulfate, 20% (v/v) methanol) and western blot with anti-GFP primary antibody (Sigmaaldrich, anti-GFP, 1:1000), and anti-mouse secondary antibody (Proteintech, HRP-conjugated Affinipure Goat Anti-Mouse, 1:5000). The rest of the beads were used for Mass Spectrometry sample preparation.

Briefly, 25 ul Sodium deoxycholate (SDC) buffer (2% (w/v) deoxycholate (DOC), 1 mM TCEP, 4 mM CAA, and 50 mM Tris-HCl, pH 8.5) was added to the beads, heated for 10 min at 60 °C , then digested with 25 ul Trypsin overnight at 37 °C . A self-assembly Stage tip was used to clean up the peptides, after which the peptides were eluted with 60ul 80% ACN/1.25% ammonia and speed-vac to dryness. At last, the dried peptides were resuspended in 10ul 2% ACN/0.1% TFA. The Mass Spectrometry analysis was done with Orbitrap Exploris mass spectrometry (Thermo Fisher Scientific).

2.21 Mass spectrometry data analysis

MaxQuant software (version 2.0.3.1) was used for raw data analysis. Oxidation and Acetyl were set as variable modifications, while Carbamidomethyl was set as fixed modification. Label-free quantification was set with default parameters. Arabidopsis TAIR_pep_201606 sequences were used as protein database (https://www.arabidopsis.org/download_files/Proteins/Araport11_protein_lists/archived/Araport11_genes.201606.pep.fasta.gz), the Min. peptide length was set to 7, Max. peptide mass [da] was set to 4600. A match between runs was selected in the global parameters.

2.22 Statistical analysis of the IP-MS samples

The DEP package [105] was used for the downstream statistical analysis. The proteinGroups file was read into RStudio (https://rstudio.com), and potential contamination was removed. LFQ values were used for quantification. The LFQ values were filtered first, and only values that were identified in all replicates of at least one condition were kept. The selected LFQ intensity

values were normalized. T-test was used for the differential enrichment analysis with defined cutoffs of adjust p-value < 0.05 and logFC = 2. Microsoft Excel was used to filter the proteins further. The number of unique peptides present in IP samples was higher than in control samples.

2.23 Bioinformatic analysis for IP-MS samples

A volcano plot was created with the DEP package to visualize the differential enriched proteins (-log10 transformed adjust p-value vs log2 fold-change). The DAVID was used for GO analysis with all of the identified proteins as background, the significance level was set to p-value < 0.05.

2.24 In vivo pull-down assay

ARG1, *ARL1*, and *HSP70-1* coding sequences without the STOP codon were amplified by PCR (Table 2.2, primers). The amplified sequences were first cloned into the pDONR221 vector and then into pGWB402-omega-GFP or pGWB402-omega-Twin-strep vector by gateway cloning. The *ARG1*, *ARL1*, and *HSP70-1* in pGWB402-omega-GFP, or pGWB402-omega-Twin-strep vector were transformed into *Agrobacterium tumefaciens* GV3101pmp90 cell by electroporation transformation. To avoid gene silencing, the expression vector plus P19 [106] was transformed into 4-week-old tobacco leaves through agrobacterium-mediated transformation [107]. After two days of growth, the transformed leaves were harvested for pull-down assay.

For the pull-down assay, 1 gram of tobacco leaves was homogenized in lysis buffer (50 mM Tris-HCl, pH 7.5, 150mM NaCl, 10% (v/v) glycerol, 2mM EDTA, 1mM DTT, 1% (v/v) TritonTM X-100, and 1 X protease inhibitor cocktail). Afterward, the extracts were centrifuged at 20 000g for 10 min at 4 °C twice. The supernatant was collected, 50ug/ml avidin was added, and incubated for 30 min at 4 °C . Then, 25ul MagStrep “type3” XT beads (IBA, 2-4090-002) were added to the supernatant and incubated for 1 h at 4 ℃. After three times washing with washing buffer (50 mM Tris-HCl, pH 7.5, 150mM NaCl, 10% (v/v) glycerol, 2mM EDTA, 1mM DTT, 1% (v/v) TritonTM X-100, and 1 X protease inhibitor cocktail), the protein was eluted from the beads with 40ul Laemmli sample buffer (65.8 mM Tris-HCl, pH 6.8, 2.1% (w/v) SDS, 26.3% (w/v) glycerol, 0.01% (v/v) bromophenol blue).

2.25 Bimolecular fluorescence complementation (BIFC) assay and confocal microscopy

The BiFC assay was conducted on Arabidopsis leaf protoplasts following the previously described protocol [108]. For protoplast transfection, a total of 40 µg of each plasmid DNA was utilized to express the fusion proteins. The incubation period was set to 12 hours under low

light conditions. At least three replicates of distinct protoplasts were examined using a Zeiss LSM 780 confocal microscope, employing preset sequential scan settings for YFP (Ex: 514 nm, Em: 517–553 nm), GFP (Ex: 488 nm, Em: 510 nm) and mCherry (Ex: 587 nm, Em: 610 nm).

Chapter 3 Results

3.1 Microgravity-induced phosphorylation changes in *Arabidopsis thaliana*

3.1.1 Data preprocessing

A phosphoproteomics analysis using a parabolic flight platform was conducted to identify phosphorylation events associated with microgravity. WT Col-0 seedlings were subjected to microgravity treatments of 3 s and 22 s, with onboard samples at 1 g serving as the control, and hypergravity samples used as a technical control (Figure 3.1.1). Two campaigns (67th and 70th) were carried out, and a total of five biological replicates were collected. Phosphopeptides were enriched using titanium dioxide (TiO_2) before being identified through liquid chromatography-tandem mass spectrometry (LC-MS/MS).

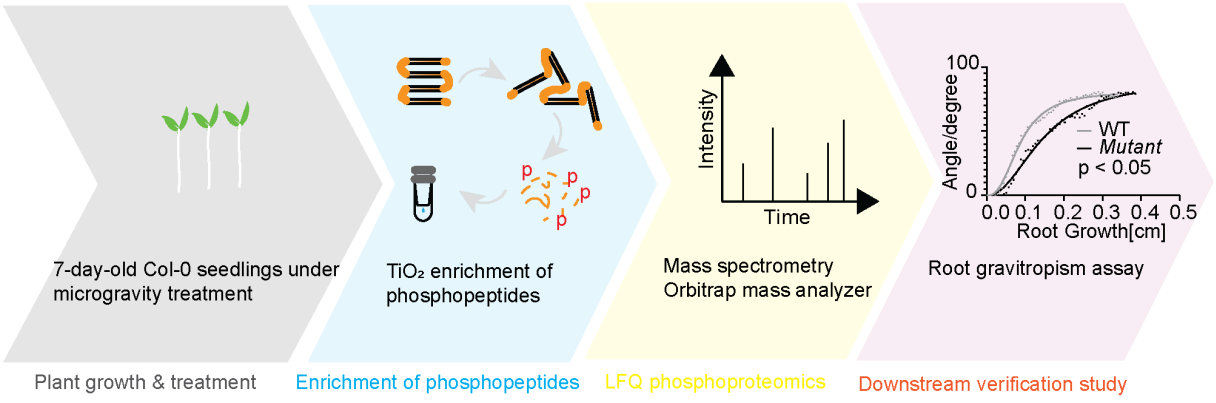

Figure 3.1.1 Phosphoproteomics experimental workflow and data analysis. Several-day-old Arabidopsis Col-0 seedlings were subjected to microgravity conditions for treatment. Samples were collected, and phosphopeptides were enriched using TiO2. Subsequently, Mass Spectrometry analysis was performed, followed by downstream physiological experiments.

In the parabolic flight experiment, 7,631 phosphopeptides were identified across all 20 samples. Data preprocessing, including data filtering, normalization, handling missing values, and imputation, is necessary to quantify proteins given the nature of the peptide-level data [90]. As depicted in supplement Figure 3.1.1 A, the identification of phosphopeptides is inconsistent between the replicates. Only approximately 1,250 phosphopeptides were identified in all 20 replicates, indicating the presence of missing values. To mitigate the impact of missing values, a less stringent filtering approach was implemented, in contrast to a more stringent approach where only phosphopeptides identified in all five replicates would be retained. Instead, the less stringent approach involved keeping phosphopeptides that were identified in at least three out of the five replicates for at least one condition (supplement Figure 3.1.1 B). Each sample yielded between 3,000 and 4,000 phosphopeptides (supplement Figure 3.1.2). Normalization

had a substantial effect on the data, leading to a more uniform distribution of the samples (supplement Figure 3.1.3). Supplement Figure 3.1.4 shows a random distribution of missing values across the dataset. No apparent biased pattern of missing values was observed under specific conditions. The occurrence of missing values in this study appears to be influenced by random factors rather than any specific treatment. As one of the biggest challenges in label-free quantification of the proteome, missing values often occur [109], and can be attributed to various factors, including missed cleavages resulting from protease digestion, incomplete fragmentation of proteins, values falling below the limit of detection, or limitations during the database searching process [93,110]. An intensity density distribution and cumulative fractions were plotted to examine the relationship between missing values and phosphopeptide intensities. Supplement Figure 3.1.5 illustrates the contrasting density distribution between non-missing values and missing values, with the latter predominantly exhibiting low-intensity values. This finding compellingly demonstrates a discernible pattern and prevalence of lower intensity values among the missing values in the dataset. It has been suggested that there is no universally superior imputation method that can be applied to all situations, instead, the choice of the most appropriate imputation method should be guided by the specific context and characteristics of the data being dealt with [93]. Different imputation methods have been recommended, taking into account the patterns of missing values [110,111]. In this study, the globally observed minimum value in the dataset was employed to fill in the missing values. This approach was chosen due to the observation that the missing values had low intensity in this study and it is simple and intuitive [112].

3.1.2 Microgravity-induced phosphoprotein changes

After the completion of data preprocessing, a total of 4266 phosphosites were identified in 1983 phosphoproteins. The analysis of the phosphorylation pattern revealed that 91% of peptides were singly phosphorylated (Figure 3.1.2 A). In addition, the distribution of phosphorylated residues analysis found that serine, threonine, and tyrosine phosphorylation accounted for 88%, 11%, and 1%, respectively, which is consistent with previous studies (Figure 3.1.2 B) [113,114]. Subsequent principal component analysis revealed that changes in gravity intensity, whether increased or decreased, result in distinct alterations in protein phosphorylation patterns (Figure 3.1.2 C).

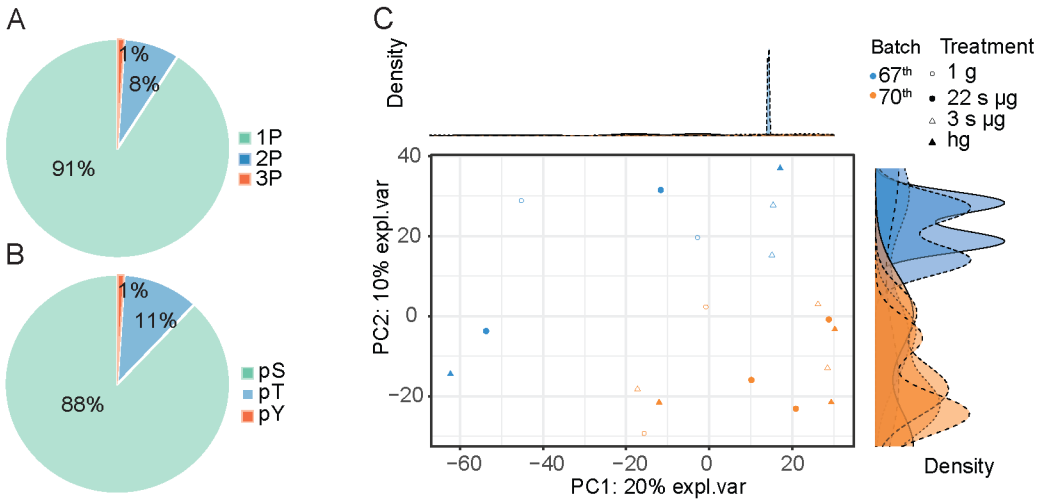

Figure 3.1.2 Distribution of phosphosites and phosphorylated amino acids and principle component analysis. (A) Phosphosites per peptide; (B) Distribution of phosphorylated amino acids; (C) Principle component analysis of identified phosphopeptides across the four conditions. The experimental conditions consisted of a 1 g control condition, 3 s microgravity stimulation, 22 s microgravity stimulation, and a hypergravity treatment denoted by 1.8 g gravity force.

3.1.3 Robust phosphorylation changes

Statistical analysis of variance (ANOVA) was used to evaluate the differentially phosphorylated peptides (significant threshold: $p < 0.05$). While false discovery rate correction is commonly used in large-scale omics studies to control for false positives, the significance threshold was set at $p < 0.05$ without applying an FDR correction for the following reasons. Firstly, in phosphoproteomics studies, the sample sizes are typically small [115], and the magnitude of phosphorylation changes is relatively small compared to transcriptomics studies [116]. If a false discovery rate correction is applied, only a limited number of phosphorylation changes would be significant in this study. Furthermore, considering the exploratory nature of this research, the objective was to capture a comprehensive range of potentially significant phosphorylation events.

In this study, we identified 428 significantly differentially phosphorylated (SDP) peptides in the 3 s microgravity treatment group compared to the 1 g control, corresponding to 355 unique phosphoproteins. Similarly, the 22 s treatment group exhibited 295 SDP peptides representing 256 phosphoproteins. Furthermore, the hyper-g group showed significant differential phosphorylation with 307 peptides (260 proteins) compared to the 1 g control.

Among the SDP peptides in the hypergravity treatment, 3 s microgravity treatment, and 22 s microgravity treatment, a total of 85 peptides were found to be shared by all three groups. Moreover, a total of 138 peptides were found to be shared between the hypergravity treatment and the 3 s microgravity treatment, as well as between the hypergravity treatment and the 22

s microgravity treatment. And 130 peptides were shared between the 3 s and 22 s microgravity treatments (Figure 3.1.3 A). These findings indicate a shared response among these experimental conditions, highlighting potential common regulatory mechanisms involved in the phosphorylation dynamics.

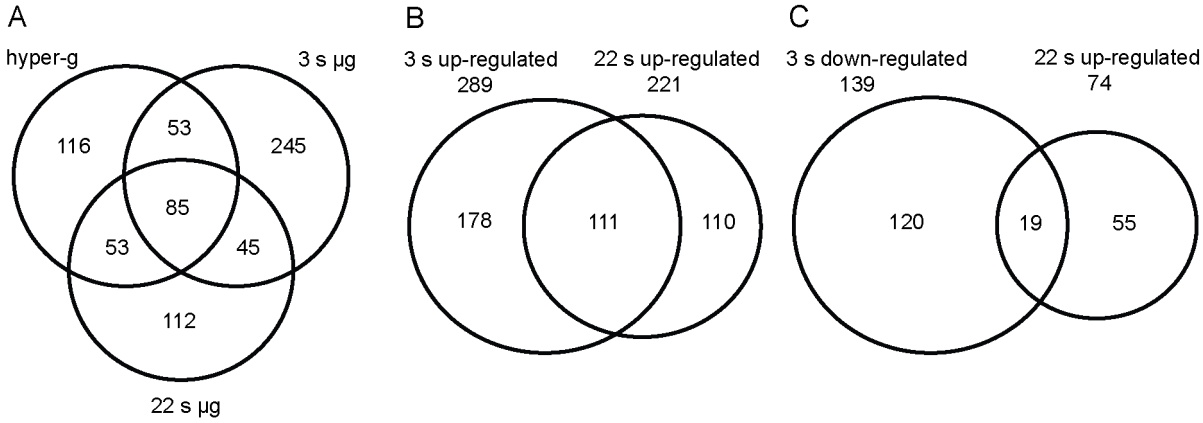

Figure 3.1.3 Venn diagram analysis of significantly differentially phosphorylated peptides across different treatments. (A) Shared significantly differentially phosphorylated peptides among hypergravity treatment, 3 s, and 22 s microgravity treatments; (B) The up-regulated significantly changed phosphopeptides, 3 s versus 22 s. (C) The down-regulated significantly changed phosphopeptides, 3 s versus 22 s.

Among the significantly differentially phosphorylated peptides in the 3 s and 22 s microgravity treatments, 289 and 221 exhibited increased phosphorylation level, respectively. Notably, 111 phosphopeptides were common to both groups, indicating sustained phosphorylation changes. In contrast, the 3 s microgravity treatment exhibited a higher number of dephosphorylation events compared to the 22 s microgravity treatment. Specifically, 139 and 74 phosphopeptides displayed decreased phosphorylation levels, with only 19 phosphopeptides shared between the two groups (Figure 3.1.3 B & C). The analysis of differentially phosphorylation changes in response to 3 s and 22 s microgravity treatment revealed a notable distinction. This study observed a higher total number of robust phosphorylation changes, encompassing both up-regulated and down-regulated phosphopeptides, in the 3 s microgravity treatment compared to the 22 s treatment. This disparity suggests that the phosphorylation pattern varies significantly between the 3 s and 22 s microgravity treatment.

3.1.4 Gene Ontology (GO) enrichment analysis

Furthermore, the majority of the phosphorylation changes occurred after the 3 s microgravity treatment, indicating a transient nature of the phosphorylation events in response to microgravity stimulation. This finding suggests that the plant's response to microgravity involves rapid and dynamic alterations in phosphorylation levels, which may be crucial in initiating and regulating the cellular response to altered gravity conditions.

This research conducted a Gene Ontology (GO) enrichment analysis using the significantly changed phosphoproteins induced by the 3 s and 22 s microgravity treatments. The analysis produced the GO terms "signal transduction", "microtubule cytoskeleton organization" and "phosphatidylinositol binding" which were enriched in the phosphoproteins affected by the 3 s microgravity treatment (Figure 3.1.4). Consistent with previous studies, alterations in microtubule dynamics were also observed in microgravity-treated Arabidopsis seedlings [117]. In addition, the GO terms "cellular response to hormone stimulus" and "cellular development process" exhibited a high level of enrichment in the phosphoproteins affected by the 22 s microgravity treatment (Figure 3.1.4). It has been shown that hormone synthesis, stabilization, and transport play crucial roles in enabling a differential growth response upon gravistimulation [118].

In addition, this study observed a significant increase in phosphorylation levels for several components of the ESCRT (Endosomal Sorting Complex Required for Transport) machinery during the 3 s microgravity treatment compared to the 1 g control. These components including TOM-LIKE 1 (TOL1, S363), TOM-LIKE 2 (TOL2, S378), TOM-LIKE 3 (TOL3, S455), TOM-LIKE 5 (TOL5, S182), TOM-LIKE 6 (TOL6, S319) and TOM-LIKE 9 (TOL9, T149 and S282). Notably, TOL6 exhibited an increased phosphorylation change at Ser319 during the 3-second microgravity treatment, and an increased phosphorylation change at Ser326 during the 22-second microgravity treatmen. A previous study has already established the significance of TOL proteins in root gravitropism of Arabidopsis, as demonstrated by the root gravitropism defects observed in the *tol2-1tol3-1tol5-1tol6-1tol9-1* quintuple mutant (*tolQ*) [53]. Building upon this knowledge, the novel finding of changes in phosphorylation levels of the TOL proteins in response to microgravity stimulation suggests their potential responsiveness to altered gravity conditions and modulation of their phosphorylation states.

Furthermore, this study made an interesting discovery regarding the phosphorylation of the MICROTUBULE-ASSOCIATED PROTEIN 65-1 (MAP65-1). It was found that MAP65-1 exhibited significant differential phosphorylation at the same site (Thr4) across the hypergravity condition, as well as the 3 s and 22 s microgravity treatments. However, the centered intensity of MAP65-1 only exhibited slight changes in the hypergravity condition compared to the 1 g control. In contrast, during the 3-second and 22-second microgravity treatments, significant and dramatic changes in the centered intensity values were observed. In addition to its known role in hypergravity response, this study provides valuable insights into the potential phosphorylation changes occurring at Thr4 of MAP65-1 in response to microgravity stimulation.

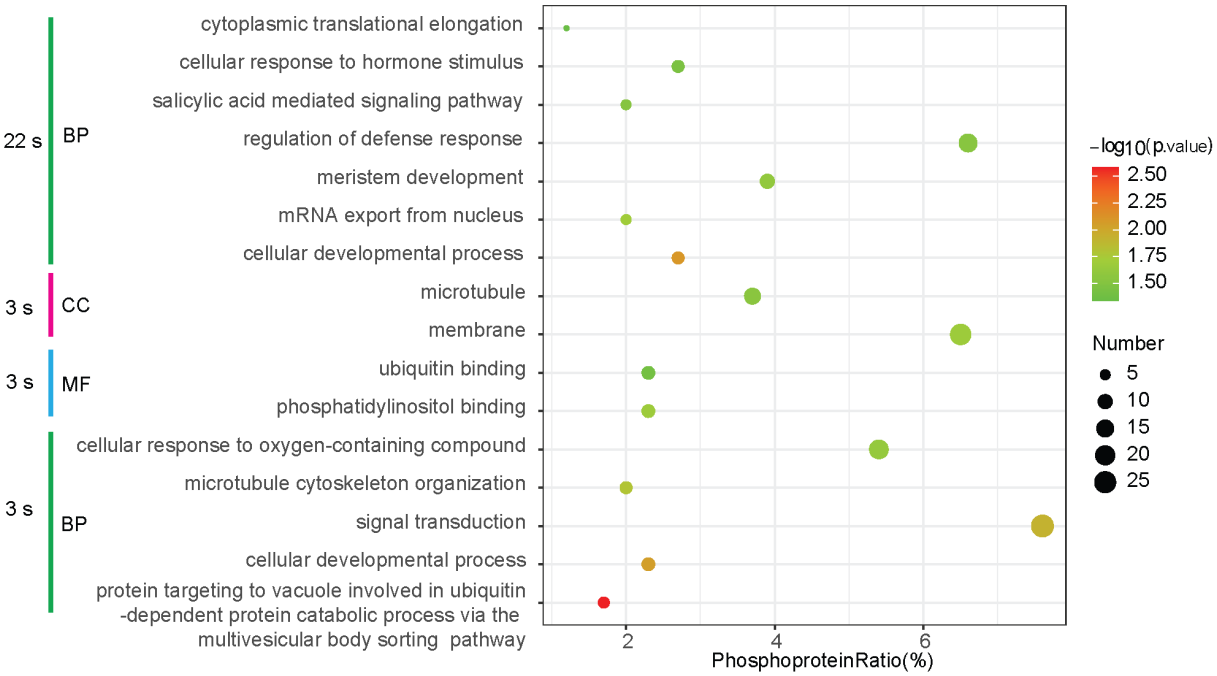

Figure 3.1.4 Enriched GO terms for significantly differentially phosphorylated protein. CC represents cellular component, MF represents molecular function, and BP represents biological process. The phosphoprotein ratio quantifies the proportion of phosphoproteins enriched with GO terms compared to all the proteins that show significant differential phosphorylation between the 1 g and 22 s microgravity treatments. The size of the black circle indicates the number of phosphoproteins, and each color represents a different p-value.

3.1.5 Microgravity-induced protein changes

Microgravity treatments have been shown to induce significant changes in protein abundance. [119,120]. To distinguish between changes in protein abundance and protein phosphorylation, this research performed LC-MS/MS analyses on the remaining total proteins that were not enriched through TiO_2 enrichment. Consistent with expectations, the study identified 234, 215, and 314 unique proteins with significant changes ($p < 0.05$) in the 3 s, 22 s, and hypergravity phases, respectively, compared to the 1 g control. A Venn diagram was used to visually illustrate the overlap between the significantly differentially enriched total proteins and phosphorylated proteins. Interestingly, the diagram demonstrates that only a tiny fraction of proteins occupy the overlapping region (Figure 3.1.5 A-C). This observation indicates that the changes in phosphorylation and protein abundance in this study can be distinguished. A direct comparison was made based on the log2-transformed intensity of the overlap between the total identified proteins and phosphorylated proteins. As shown in Figure 3.1.5 B, among all the overlapped proteins, which include 13 proteins in the 3 s microgravity treatment versus 1 g, 6 proteins in the 22 s microgravity treatment versus 1 g, and 14 proteins in the hyper-g treatment versus 1 g, only 4 out of 33 proteins at the protein level showed a log2 intensity higher than 2. This indicates that the majority of proteins have undergone changes at the

phosphorylation level.

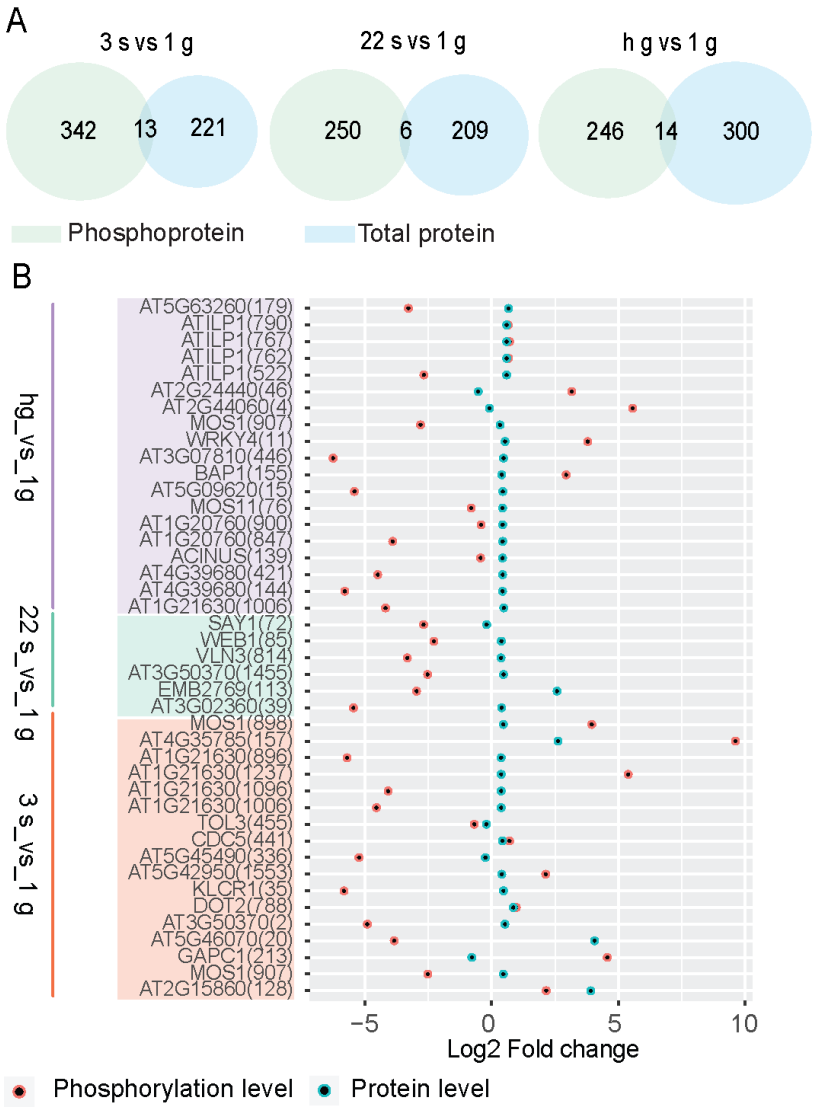

Figure 3.1.5 Comparison of TiO_2 non-enriched total protein and TiO_2 enriched phosphoprotein under microgravity treatment. (A) Overlap between the number of significantly differentially phosphorylated proteins and the number of abundance significantly changed proteins, including 3 s compared to 1 g, 22 s compared to 1 g and hyper-g compared to 1 g; (B) Comparison of log2 fold change for overlapped phosphoproteins and total proteins in different conditions: 3 s microgravity vs 1 g, 22 s microgravity vs 1 g, and hypergraviy vs 1 g. The phosphorylation level and protein level are represented by a red dot and a green dot, respectively.

3.1.6 Classification of phosphopeptides in response to microgravity

A classification analysis of significantly differentially phosphorylated peptides can aid in understanding the change of phosphorylation levels across different microgravity treatments, thus facilitating the identification of treatment-specific phosphorylation events. By using the

silhouette method [121], the data clustered in two distinct groups (Figure 3.1.6 A).

After microgravity treatment, a distinct difference in phosphorylation patterns was observed through comparative classification analysis. The temporal pattern analysis revealed two clusters (Figure 3.1.6 B) depicting the dynamics of phosphorylation changes under different gravitational condition. The cluster 1 phosphopeptides initially exhibited low phosphorylation level under normal gravity (1 g) conditions. However, their phosphorylation increased during the hyper-g phase and then increased slightly during the 3 s and decreased slightly during 22 s microgravity phases. In contrast, the phosphopeptides within the second cluster exhibited an initial high phosphorylation level, which progressively declined during the hyper-g phase. Subsequently, a further decrease was observed during the 3 s microgravity phase, followed by a increase during the 22 s microgravity treatment phase. These findings provide valuable insights into the temporal dynamics of phosphorylation events in response to gravitational changes. The distinct patterns observed in different groups highlight the complexity and specificity of the regulatory mechanisms underlying protein phosphorylation in the context of gravitational stimuli.

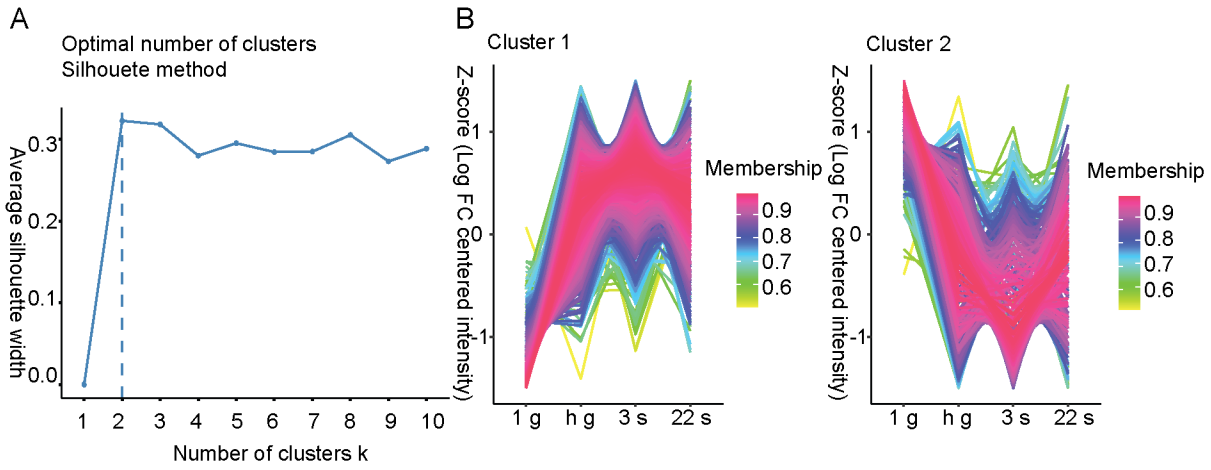

Figure 3.1.6 Phosphorylation pattern analysis of all the significantly differentially phosphorylated phosphopeptides. (A) Comparison of k-means Partitions: A higher average silhouette width indicates that the data points are well-clustered; (B) Analysis of phosphorylation event patterns: Z-score transformed centered log2-fold change of intensity for each treatment. Membership values indicate the degree of data point belonging to each cluster. Labels: 1 g (1 g control), hg (hypergravity treatment), 3 s (3 s microgravity treatment), 22 s (22 s microgravity treatment).

3.1.7 Functional enrichment analysis of clustered phosphopeptides

To comprehensively assess the functional characteristics of the phosphoproteins, this study performed a Gene Ontology (GO) analysis to identify the GO terms enriched in each cluster (significance: $p < 0.05$). In Figure 3.1.7, it can be observed that phosphoproteins belonging to

cluster 1 exhibite enrichment in several biological processes, including "protein targeting to vacuole involved in ubiquitin-dependent protein catabolic process via the multivesicular body sorting pathway," which contains phosphoproteins TOM-LIKEs (TOLs) (Figure 3.1.7). In addition, the processes of "signal transduction" and "cellular response to hormone stimulus" are enriched. In the molecular function category, there is an overrepresentation of the "GTP binding" function. Notably, the presence of TOC120 was identified, which has been suggested to be involved in Altered response to gravity 1 (ARG1)-mediated gravitropism signaling [43]. In cluster 2 of the phosphoproteins (Figure 3.1.7), the "microtubule" GO term under the cellular components category is significantly enriched. This observation holds significance as microtubule proteins have been shown to play a role in gravitropism signaling. Microtubule proteins are a part of the cytoskeleton family which is a network of filamentous proteins that provides structural support, facilitates cellular movement, and plays a role in various cellular processes. The cytoskeleton is composed of three main components: microfilaments (actin filaments), intermediate filaments, and microtubules [122]. The role of the cytoskeleton in gravitropism has been demonstrated in Arabidopsis. For example, ARG1 is a key protein involved in gravitropism, and it has been confirmed that ARG1 physically interacts with actin *in vivo* [123]. These results indicate that protein phosphorylation might be involved in the interplay between the cytoskeleton and gravitropism.

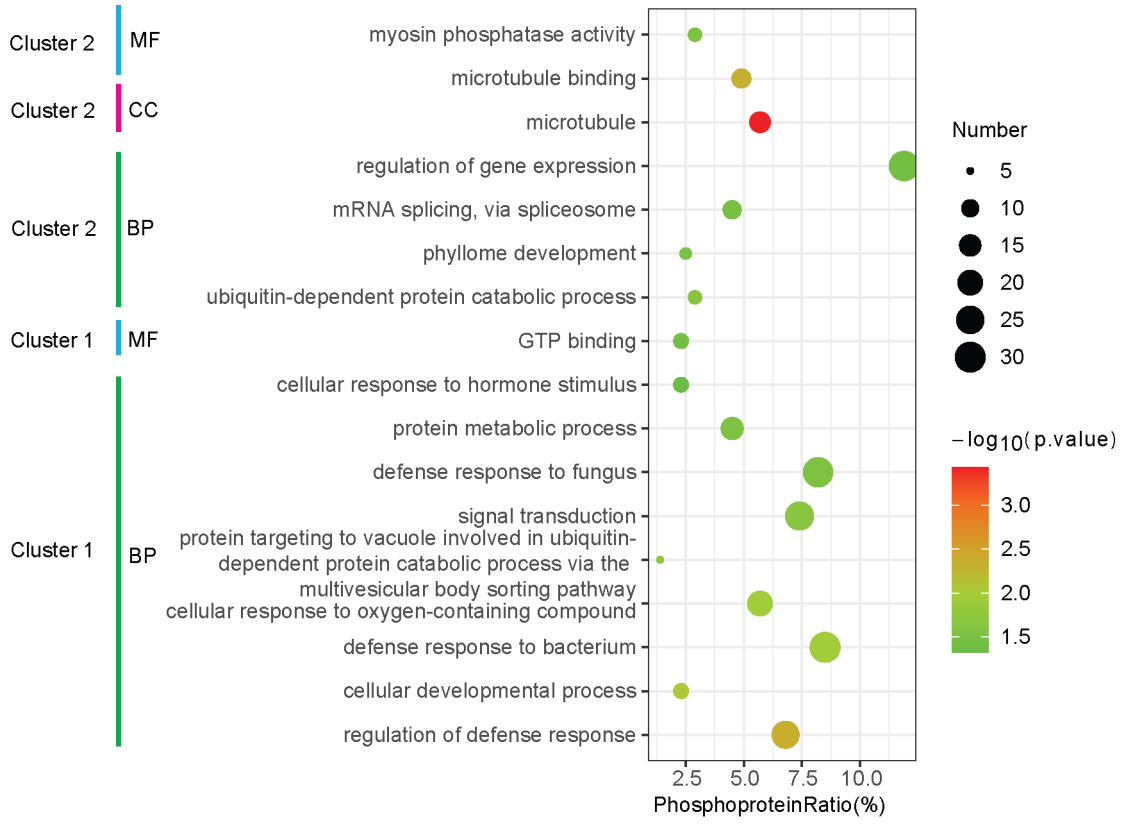

Figure 3.1.7 Scatter plot of the enriched GO terms in cluster 2 phosphoproteins. CC =

cellular component, MF = molecular function, and BP = biological process. The phosphoprotein ratio quantifies the proportion of phosphoproteins enriched with GO terms compared to all the phosphoproteins in either cluster 1 or cluster 2. The size of the black circle indicates the number of phosphoproteins, and each color represents a different p-value.

3.1.8 Kinases involved in the microgravity-induced phosphosignaling events

To gain insights into the kinase preferences for specific protein motifs, the analysis in this study tried to identify enriched motifs among the significantly differentially phosphorylated peptides. By examining both the up-regulated and down-regulated phosphopeptides, this research aimed to uncover patterns and sequences favored by the kinase activity.

In the 3 s microgravity treatment, there is an enrichment of two specific motifs among the up-regulated phosphopeptides: the basophilic motif [-R-x-x-pS-] and the proline-directed motif [-pS-P-]. These motifs were found to be associated with a higher occurrence of phosphorylation events (Figure 3.1.8). On the other hand, in the 22 s microgravity treatment, only the proline-directed motif [-pS-P-] showed enrichment among the up-regulated phosphopeptides.

Interestingly, the proline-directed motif [-pS-P-] was the most abundant among all the enriched motifs in the up-regulated phosphopeptides, comprising 81.6% of the total (Figure 3.1.8). This suggests a strong preference for the kinase to target this specific motif in response to microgravity stimulation. In contrast, both the 3 s microgravity and 22 s microgravity treated down-regulated phosphopeptides showed enrichment only for the proline-directed motif [-pS-P-]. This further supports the significance of the proline-directed motif in the regulation of phosphorylation events associated with the microgravity response.

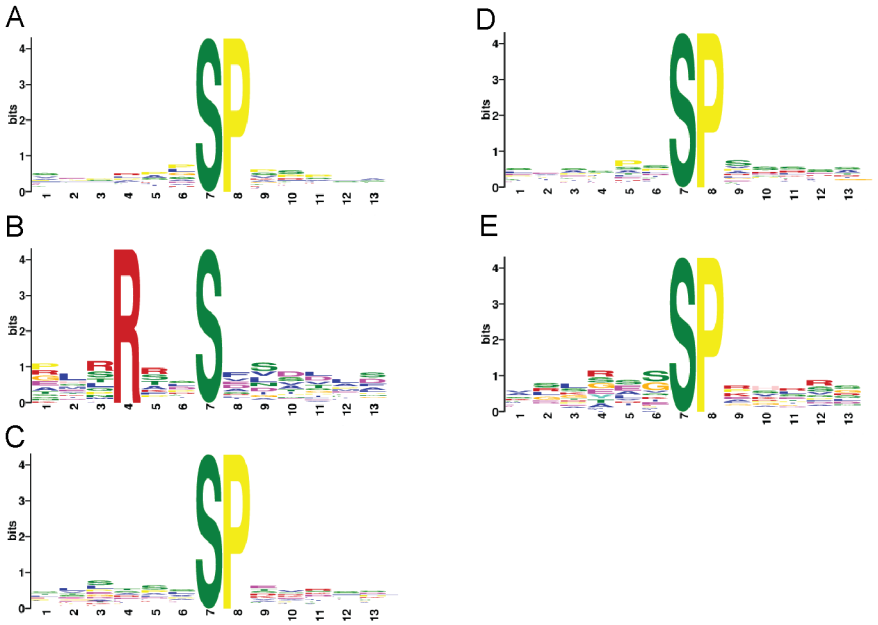

Figure 3.1.8 Enriched up-regulated (A, B, C) and down-regulated (D, E) motifs. (A) Basophilic motif [-R-x-x-pS-] from 3 s versus 1 g sample; (B) Proline-directed motif [-pS-P-] from

3 s versus 1 g sample (C) Proline-directed motif [-pS-P-] from 22 s versus 1 g sample. (D) Proline-directed motif [-pS-P-] from 3 s versus 1 g sample; (E) Proline-directed motif [-pS-P-] from 22 s versus 1 g sample.

3.1.9 Kinase inhibitor assay

Elucidating the intricate relationships between substrates and kinases is pivotal in unraveling complex signal pathways. The precise prediction of the kinase responsible for phosphorylating a specific substrate poses a significant challenge. However, researchers have studied the correlation between phosphorylated motifs and specific groups of kinases based on known kinase-targeted substrate sites. It has been suggested that MITOGEN-ACTIVATED PROTEIN KINASES (MAPKs), CALCIUM-DEPENDENT PROTEIN KINASES (CDPKs), AGC kinases, and LEUCINE-RICH REPEAT RECEPTOR-LIKE KINASE (LRR RLK) recognize an S-P motif [124], moreover, AGC and CDPK kinases exhibit a preference for recognizing and catalyzing the [-R-x-x-pS-] motif [124]. In addition, emerging evidence suggests that the targeting specificity of kinases has remained remarkably conserved across diverse species throughout evolution, as revealed by a kinase specificity model analysis [125].

This study found that the enriched [-pS-P-] motif was indicated as the substrate of kinases, such as CASEIN KINASE II (CK II), SUCROSE NON-FERMENTATION-RELATED PROTEIN KINASE (SnRK), CDPK, CYCLIN-DEPENDENT KINASE (CDK), MAPK, and AGC, whilethe enriched motif [-R-x-x-pS-] was found to be a potential target of AGC and CDPK kinases.. In order to verify the involvement of the selected kinases in gravitropism, a kinase inhibitor assay was performed. The kinase inhibitors used in this study include TTP 22 (CK II inhibitor), and Dinaciclib (CDK1, CDK2, CDK5, and CDK9 inhibitor). The role of inhibitors targeting these two kinases in plant gravitropism has not been previously investigated. Before conducting the gravitropism assay, a high-throughput gravitropism phenotyping platform, called GraviPi, was developed to monitor the gravitropic curvature. Through this platform, this study found thatboth inhibitors blocked Arabidopsis root gravitropism in a dose-dependent manner. When applied at concentrations of 20 μM and 40 μM, TTP 22 exhibited a significant inhibitory effect on root gravitropism (Figure 3.1.9 A). This suggests a dose-dependent response, with a more pronounced impact on root gravitropism at higher concentrations of TTP 22. Similarly, when the concentration of Dinaciclib was 10 nM, this study observed a discernible difference in root gravitropism during the initial stages of root growth compared to the control group. However, as the roots grew beyond a certain threshold (0.4 cm in this study), the curvature became similar to that of non-treated plants. However, when the concentration of Dinaciclib was increased to 100 nM, Dinaciclib not only delayed the curvature but also reduced the overall curvature. (Figure 3.1.9 B). This indicates that the effect of dinaciclib on root gravitropism is also concentration-dependent, with a more pronounced effect observed at higher

concentrations, with the inhibitory effect persistings throughout the entire growth period.

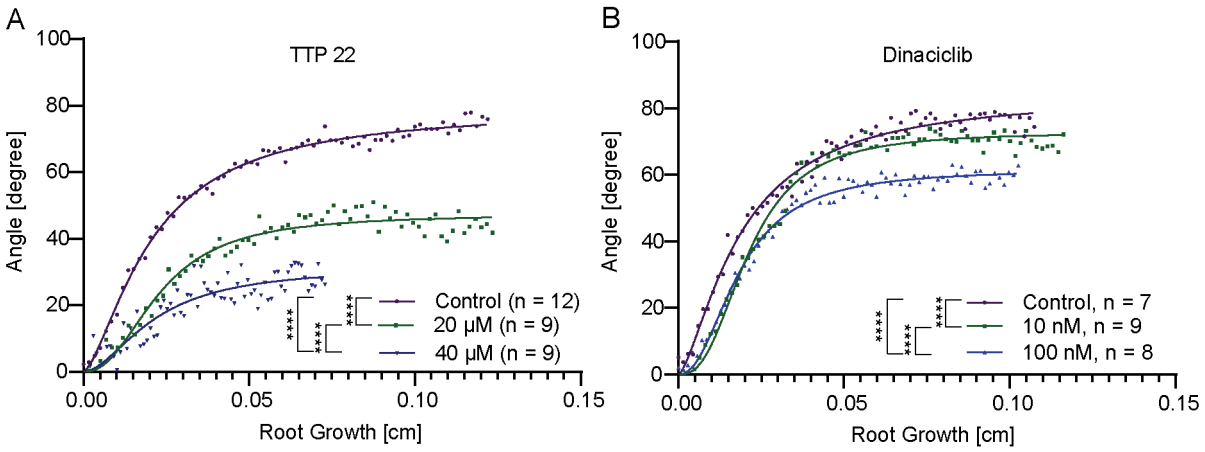

Figure 3.1.9 Root gravitropism assay under treatment of TTP 22 and Dinaciclib. (A) Kinetics of root bending after treatment with TTP 22 at 20 µM, or 40 µM. The control indicates samples treated with DMSO; (B) Kinetics of root bending after treatment with Dinaciclib at 10 nM, or 100 nM. The control indicates samples treated with DMSO. Asterisk (****) represents p-value < 0.0001, p-value represented a paired comparison of fitted nonlinear regression with the extra sum-of-squares F test.

3.1.10 Phosphoprotein network

To elucidate the fundamental biological processes influenced by alterations in phosphorylation patterns under microgravity treatment, a phosphorylation events network analysis was performed with significantly phosphorylated proteins that were enriched in the motif analysis. A comprehensive network was constructed by integrating diverse layers of information, including protein-protein interactions obtained from STRING (https://string-db.org/) and kinase-substrate predictions. In alignment with previous studies, several proteins have been suggested to be involved in the gravitropism response in Arabidopsis, such as BRASSINAZOLE-RESISTANT 1 (BZR1) (Figure 3.1.10 A) and TOC120. BZR1 is a positive mediator of the Brassinosteroid (BR) signaling pathway, and research found that the dominant mutant *bzr1-D*, presents an enhanced gravitropic response under dark conditions [126]. Mutation of *TOC120* was found to enhance the gravitropic defect phenotype of *arg1-2* [43]. The analysis of interaction networks and gene ontology revealed a shared involvement of the identified proteins in various molecular functions, including DNA binding, mRNA binding, and protein binding (Figure 3.1.10 A-D). Notably, the significantly phosphorylated TOL proteins were associated with both ubiquitin-binding and phosphatidylinositol binding, as indicated by the GO analysis (figure 3.1.10 E).

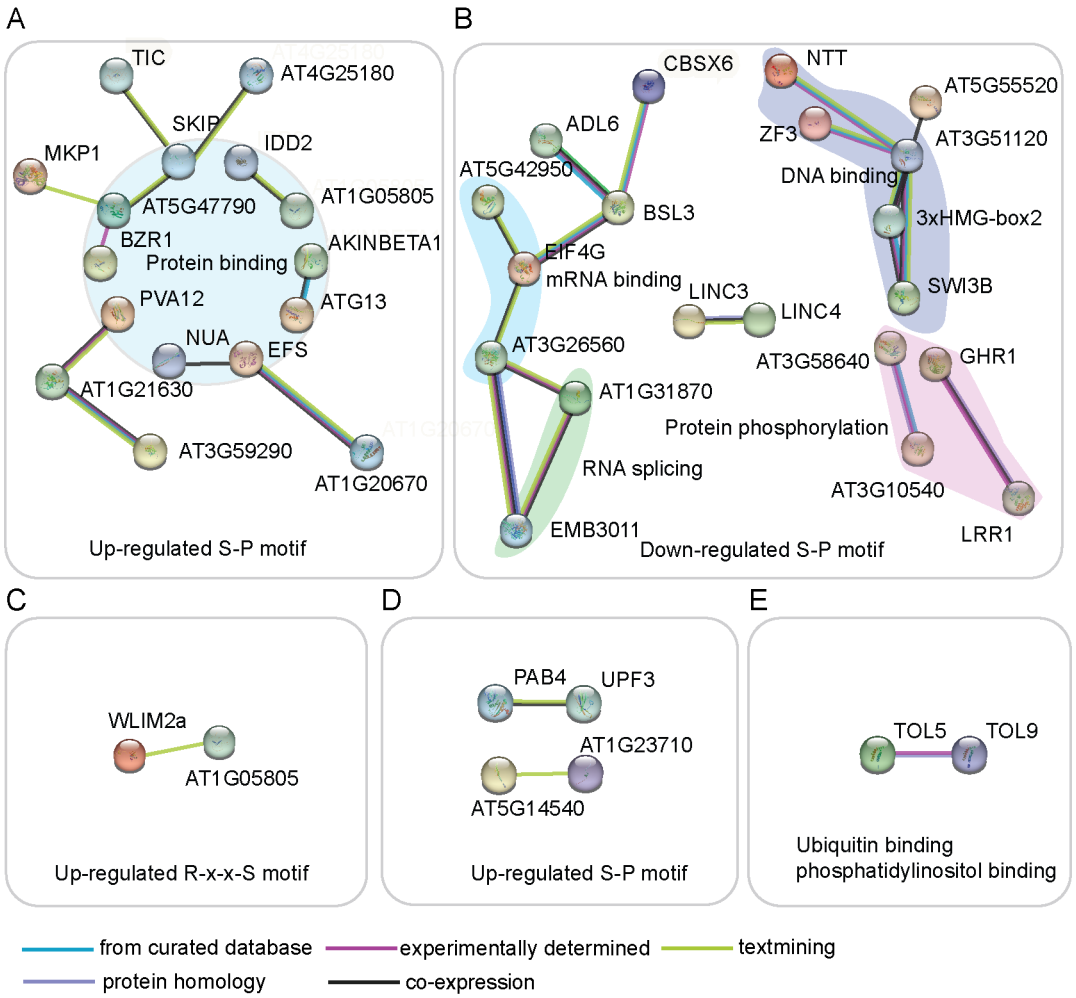

Figure 3.1.10 Microgravity-induced interaction network. (A) The predicted interaction network of significantly phosphorylated proteins from 1 g vs 3 s that harbor the/an up-regulated S-P motif. (B) The predicted interaction network of significantly phosphorylated proteins from 1 g vs 3 s that harbor the/a down-regulated S-P motif. (C) The predicted interaction network of significantly phosphorylated proteins from 1 g vs 3 s significantly that harbor the/an up-regulated R-x-x-S motif. (D) The predicted interaction network of significantly phosphorylated proteins from 1 g vs 22 s that harbor the/an up-regulated S-P motif. (E) The predicted interaction network of significant phosphorylated TOL proteins in this study (TOL1, TOL2, TOL3, TOL5, TOL6 and TOL9). Molecular function is represented by different colors.

3.1.11 Comparison analysis of 3 s phosphorylation changes between two different microgravity platforms

Next, phosphoproteomics data analysis was conducted on the samples obtained from a drop tower campaign [87]. In total, this study identified 1977 phosphopeptides corresponding to 1143 phosphoproteins. Upon performing a paired t-test statistical analysis, 71 phosphopeptides were discovered to be significantly differentially phosphorylated (significance: $p < 0.05$), corresponding to 71 phosphoproteins. In the 3 s microgravity treatment of the

parabolic flight platform, a total of 428 significantly differentially phosphorylated peptides were identified (Figure 3.1.3). Subsequently, this research compared significantly differentially phosphorylated proteins obtained from the drop tower and parabolic flight campaigns. As demonstrated in table 3.1.1, the identification of 12 significantly differentially phosphorylated proteins was achieved using both the drop tower and parabolic flight platforms. However, it is worth noting that out of these 12 proteins, only 7 exhibited shared phosphosites across both experimental platforms. Considering the limited overlap of significantly differentially phosphorylated proteins between the experimental platforms, it is possible that the hypergravity phase in the parabolic flight platform induced phosphorylation changes. These changes might have also been present before the 3 s microgravity treatment in the parabolic flight platform. As a result, it becomes challenging to distinguish whether the higher number of significantly differentially phosphorylated proteins identified in the parabolic flight platform is solely caused by the exact 3 s microgravity treatment or if it includes effects from hypergravity stimulation. To test this hypothesis, this study further removed the 138 shared significantly differentially phosphorylated peptides identified in both the hypergravity stimulation and 3 s microgravity treatment in the parabolic flight platform. Interestingly, among the remaining 290 significantly differentially phosphorylated peptides in the 3 s microgravity treatment of the parabolic flight platform, only 5 overlapped with the 71 significantly differentially phosphorylated peptides in the drop tower platform. This suggests that the observed phosphorylation changes in the 3 s microgravity treatment of the parabolic flight platform may be influenced by the preceding hypergravity treatment.

Table 3.1.1 Overlapping significantly changed phosphoproteins from the drop tower platform and parabolic flight platform.

IDs	Description	Drop tower	Parabolic flight
AT1G20760	CALCIUM-BINDING EF-HAND FAMILY PROTEIN	pS778	pS900, pS988
AT4G32330	TPX2 (TARGETING PROTEIN FOR XKLP2) PROTEIN FAMILY	pT178	pS208
AT2G41840	RIBOSOMAL PROTEIN S5 FAMILY PROTEIN	pS273	pS256, pS273
AT1G28330	DORMANCY-ASSOCIATED PROTEIN-LIKE 1	pT52, pT67	pS50, pT52, pS58
AT5G47790	SMAD/FHA DOMAIN-CONTAINING PROTEIN	pS34	pS34
AT3G54620	BASIC LEUCINE ZIPPER 25	pS62	pS45, pS71
AT5G59210	MYOSIN HEAVY CHAIN-LIKE PROTEIN	pS51	pS30
AT3G20410	CALMODULIN-DOMAIN PROTEIN KINASE 9	pT37	pT37, pS255
AT5G18230	TRANSCRIPTION REGULATOR NOT2/NOT3/NOT5 FAMILY PROTEIN	pS454	pS489, pS502
AT5G64430	OCTICOSAPEPTIDE/PHOX/BEM1P FAMILY PROTEIN	pS159	pS159
AT5G66800	MEMBRANE-ASSOCIATED KINASE REGULATOR-LIKE PROTEIN	pS22	pS22
AT2G25620	DNA-BINDING PROTEIN PHOSPHATASE 1	pS374	pS374

3.1.12 The distribution of quantified phosphopeptides

A volcano plot was made to visualize the distribution of phosphopeptides that were quantified in this phosphoproteomics study (Figures 3.1.11). Based on the significant alterations in phosphorylation levels and the relevant gene ontology annotations, the following candidates were selected for downstream physiological experiments: 'SHUTTLE' IN CHINESE (SUO), PATELLIN 2 (PATL2), PHOSPHOENOLPYRUVATE CARBOXYKINASE 1 (PCK1), MEDIATOR 26C (MED26C), VILLIN3, SMALL ORGAN 4 (SMO4), HYALURONAN, MICROTUBULE-ASSOCIATED PROTEINS 65-1 (MAP65-1), NAI2-INTERACTING PROTEIN 1 (NAIP1), TARGETING PROTEIN FOR XKLP2 (TPX2), TANDEM ZINC FINGER 3 (TZF3), and TOC120.

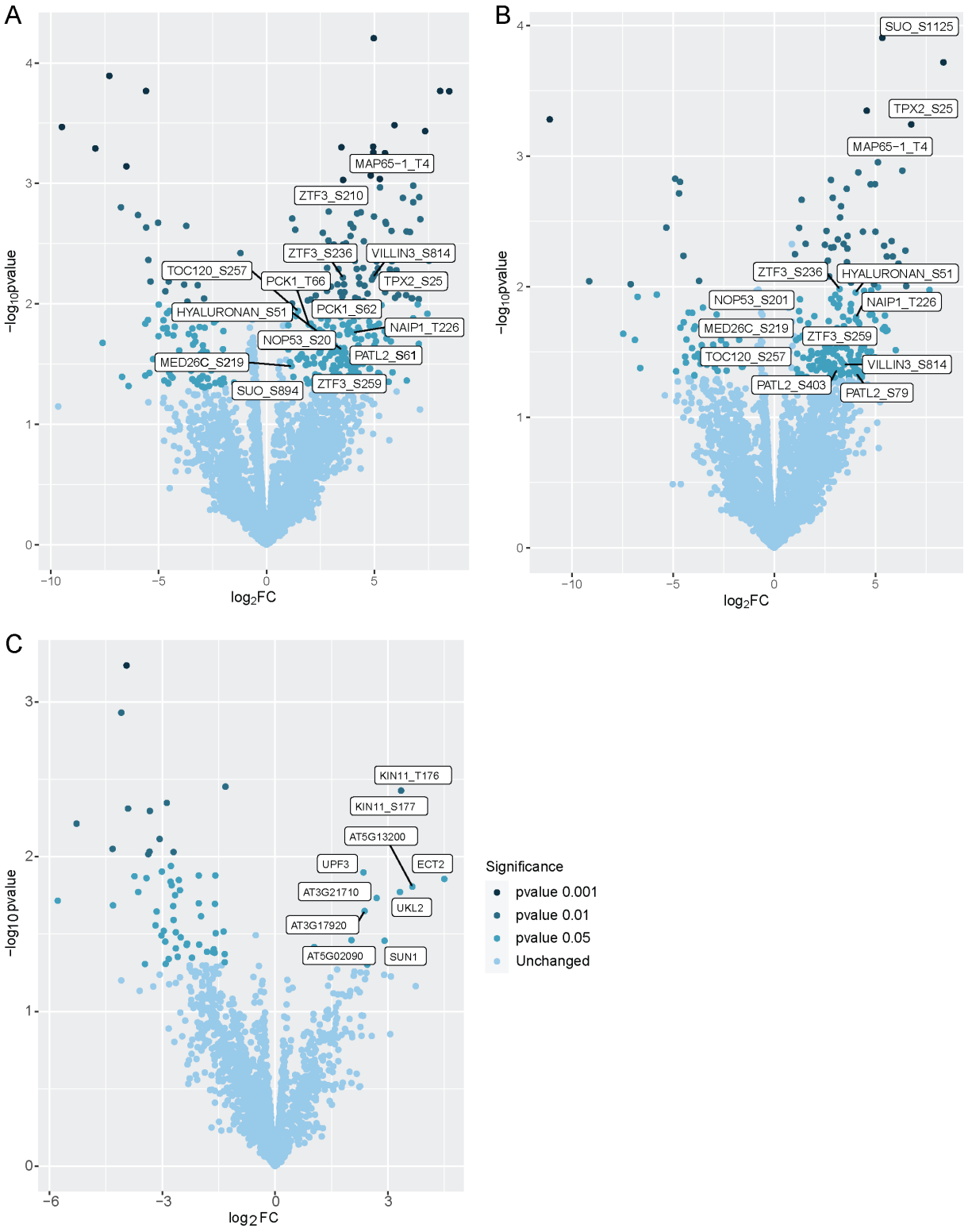

Figure 3.1.11 Comparison of the distribution of quantified phosphopeptides. (A) parabolic flight campaign: 3 s microgravity treatment versus 1 g control condition; (B) parabolic flight campaign: 22 s microgravity treatment versus 1 g control condition; (C) drop tower campaign: 3 s microgravity treatment versus 1 g control condition. The Log2FC = log2 fold change of centered intensity. Peptides with a log2 fold change < 1 and p-value > 0.05 are considered unchanged.

The p-value is determined from an ANOVA (parabolic flight samples) or paired t-test (drop tower samples). The labeled candidates are those used for downstream physiological experiments in the parabolic flight experiment.

3.1.13 Root gravitropism assay for selected candidates

To further investigate the functional roles of the selected candidates in gravitropism, this study conducted a root gravitropism assay using corresponding mutants and the GraviPi platform (specifically designed for high-throughput gravitropism assays). In the experimental setup, this study opted for a normalized approach to assess root bending angles. Rather than measuring the absolute bending angle over time, this study normalized the bending angle with the average growth of the root. It has been pointed out that normalization of the root bending angle with time can yield ambiguous results, such as certain time points exhibiting significant differences, while others may not show a similar distinction [102]. While root gravitropic curvature and root growth response are separate processes, they are interconnected. The curvature of the root is a result of the growth response to the gravitational stimulus. As the root grows, it exhibits differential elongation on the upper and lower sides, leading to bending and curvature. Therefore, changes in the root growth response can affect the magnitude and direction of the gravitropic curvature.

In this study, an allosteric sigmoidal equation was utilized to fit the curve for each dataset. Next, the evaluation focused on whether the fitted nonlinear regression curve exhibited significant differences between the WT Col-0 curve and the corresponding mutant curve. To perform this analysis, several parameters were selected for comparison using an extra-sum-of-squares F test, employing a significance level of $p < 0.05$. These parameters included the maximum root curvature angle (Vmax), the length of root growth that resulted in half-maximal root curvature (Khalf), and the hill slope (h). The hill slope (h) serves as an empirical measure of the curve's steepness and provides insights into the presence of cooperativity. As shown in Figures 3.1.12 and 3.1.13, except for *map65-1*, *hyaluronan* and *villin3*, the other mutants, such as *patl2*, *pck1*, *med26c*, *smo4-2*, *naip1*, *tpx2*, *suo-1, toc120,* and *tzf3* exhibited distinct kinetics in gravitropic bending compared to WT ($p < 0.05$). Mutants such as *patl2-1*, *med26c*, *naip1*, *tpx2*, and *tzf3* exhibited a lag phase in the beginning of curvature compared to wild-type plants. On the other hand, mutants *suo-1* and *pck1* showed a faster initial bending response compared to Col-0. In addition, *toc120* exhibited a significant difference during the middle of the curvature phase. Interestingly, a previous study has demonstrated that Arabidopsis PATELLINS (PATLS) function redundantly to mediate root development, and higher order mutants in *patls* showed a defect in gravitropism under 2,4-dichlorophenoxyacetic acid (2,4D) treatment, a synthetic auxin analog [127]. Here, this study found that the single *patl2-1* exhibited a defect in response to gravity stimulation. *PCK1* encodes a phosphoenolpyruvate carboxykinase. It has been

suggested that *PCK1* plays a role in malate metabolism in stomatal closure [128]. Another interesting mutant is *tpx2*. According to the GO annotation, it has a molecular function in microtubule binding and is involved in microtubule cytoskeleton organization. The altered gravitropism kinetics of *tpx2* might indicate its involvement in gravitropism. Although a previous study suggested that the *toc120* mutant has a normal root gravitropism response similar to the wild type [43], it is important to note that the previous study only measured the overall curvature angle after a certain time without examining the root gravitropism kinetics over time. In contrast, this study demonstrated that while the maximum root curvature of the *toc120* mutant may not be significantly different from WT at the later-stage response, there could be differences observed during the middle phase. These findings are consistent with the previous study's conclusion but highlight the importance of analyzing the root gravitropism kinetics in detail to fully understand the mutant phenotype.

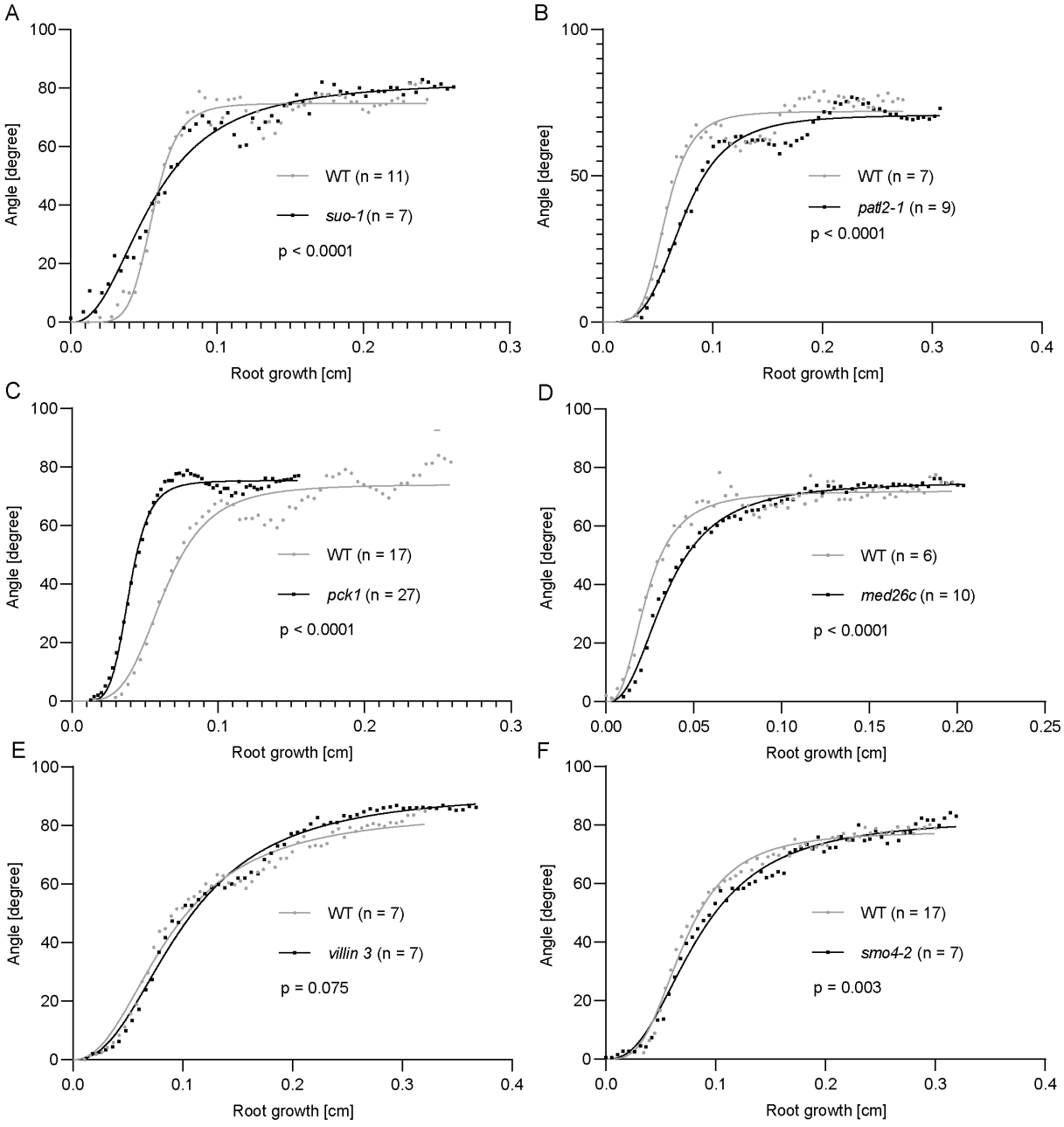

Figure 3.1.12 Root gravitropism assay. Kinetics of root gravitropism in *suo-1*, *patl2*, *pck1*, *med26c*, *villin3*, and *smo4-2* Mutants, with Wild Type (WT) as Control. The root gravitropism kinetics were assessed by measuring the bending angle and root growth towards gravity. The angle indicated the degree of curvature of the roots, while the root growth represented the length of the roots. P-values were calculated by comparing the fitted nonlinear regression using the extra sum-of-squares F test.

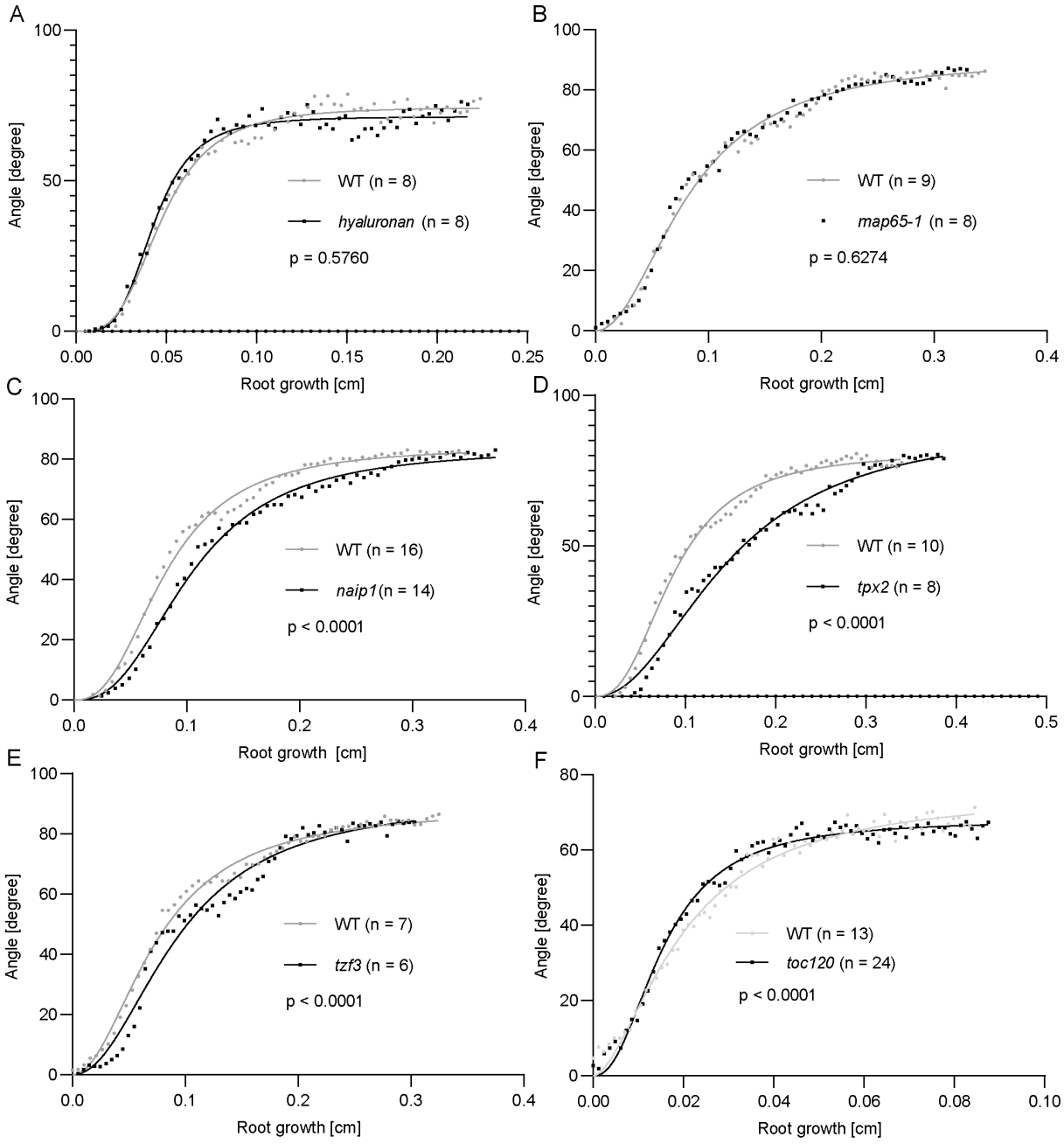

Figure 3.1.13 Root gravitropism assay. Kinetics of root gravitropism in *hyaluronan*, *map65-1*, *naip1*, *tpx2*, *tzf3 and toc120* Mutants, with Wild Type (WT) as Control. The root gravitropism kinetics were assessed by measuring the bending angle and root growth. The angle indicated the degree of curvature of the roots, while the root growth represented the length of the roots. P-

values were calculated by comparing the fitted nonlinear regression using the extra sum-of-squares F test.

3.1.14 Overlap of TOR-regulated phosphosites and microgravity-induced phosphosites

As one of the most conserved serine/threonine kinases, TOR is essential in mediating plant growth, nutrition uptake, and abiotic stress response [129]. A large-scale phosphoproteomics and interactomics study has been performed to map TOR signalling events in Arabidopsis and found 111 potential phosphosites dependent on TOR, corresponding to 83 phosphoproteins [130]. Concerning the critical role of TOR in gravitropism signaling, this study further checked the overlap between our microgravity-induced phosphosites with the previously identified TOR-regulated phosphosites. This study found 14 (3.93%) and 12 (4.07%) significantly phosphorylated proteins under 3 s microgravity treatment and 22 s microgravity treatment that are also targets of TOR (Table 3.1.2). Among them, seven proteins shared the same phosphosites with TOR-dependent phosphosites. These proteins include ATS40-7(pS147, pS214), ATTOPHAGY-RELATED PROTEIN 13 (pS404, pS558), HYPOTHETICAL PROTEIN (AT3G50370, pS302), HISTONE DEACETYLASE (pS416), NAGB/RPIA/COA TRANSFERASE-LIKE PROTEIN (pS88), EUKARYOTIC TRANSLATION INITIATION FACTOR 4B1 (pS486), and CBS/OCTICOSAPEPTIDE/PHOX/BEMP1 (PBI) DOMAINS-CONTAINING PROTEIN (pS12).

Table 3.1.2 Overlapping significantly differentially phosphorylated proteins among 3 s, 22 s microgravity treatment, and TOR signaling.

ID	Description	3 s	22 s	TOR [130]
AT3G21100	RNA-BINDING FAMILY PROTEIN	pS230, pS567	pS487,pS567	pS297
AT4G25880	PUMILIO 6	pS83	NA	pS154
AT4G01290	CONSERVED BINDING OF EIF4E 1	pS602	NA	pS359, pS704
AT4G15545	NAI2-INTERACTING PROTEIN 1	pT226	pT226	pS240
AT2G40620	BASIC LEUCINE-ZIPPER 18	pS120	NA	pS39
AT3G15040	ATS40-7	pS147, pS214	NA	pS147, pS157, pS204, pS214
AT5G14540	FLOE2	pS474	pS474	pS101, pS104
AT3G49590	AUTOPHAGY-RELATED PROTEIN 13	pS404, pS466	pS404, 466, 558	pS248,268,404,406,407,558,pT 251
AT3G50370	HYPOTHETICAL PROTEIN	pS302	pS1445	pS302
AT4G38130	HISTONE DEACETYLASE 1	pS416	NA	pS416
AT5G60170	NOT4A	pS974	NA	pS886
AT1G29400	MEI2-LIKE PROTEIN 5	pS653, pS596	pS53	pS384, 390
AT5G38640	NAGB/RPIA/COA TRANSFERASE-LIKE PROTEIN	pS88	pS88	pS88, pS127
AT2G43680	IQ-DOMAIN 14	pT271	pS157	pT592

AT1G78880	SHOU4	NA	pS163	pS171
	EUKARYOTIC TRANSLATION INITIATION			
AT3G26400	FACTOR4B1	NA	pS486	pS486
AT5G61960	MEI2-LIKE PROTEIN_1	NA	pS534	pS433, 541, 681
	CBS / OCTICOSAPEPTIDE/PHOX/BEMP1 (PB1) DOMAINS-			
AT5G63490	CONTAINING PROTEIN	NA	pS12	pS12

3.2 GraviPi: A high-throughput tropism phenotyping and angle measurement tool

3.2.1 The GraviPi setup

GraviPi is a high-throughput tropism phenotyping platform that integrates cost-saving hardware, including Raspberry Pi, Arduino, Raspberry Pi camera, rotation stage (provided by Prof. Dr. Maik Böhmer), programmable LED light (obtained from Sven Plath), and an angle measuring software, called PLANgleT.py (developed by Freya Arthe). The plant seedling plates can be easily assembled onto the plate holders located on the rotation stage. Images can be captured by the camera at desired intervals using Raspberry Pi's operating system, ensuring fixed properties such as white balance and auto-exposure. After image collection, the angle measuring software can directly measure the angles of selected seedlings in each image and save the measurements to a file.

The development of GraviPi was crucial for this study as it provided a high-throughput, cost-effective, time-saving, and highly precise platform for downstream physiological experiments. These experiments included the gravitropism assay for kinase inhibitors and the selection of large-scale candidate mutants identified through the phosphoproteomics study.

3.2.2 The GraviPi works for different species

Having demonstrated its effectiveness in the physiological gravitropism assay in the previous chapter, this study aims to extend the capabilities of the GraviPi platform to other species. One challenge encountered in studying root gravitropism across different species is the variation in root width. For instance, *Arabidopsis thaliana* has a root width of approximately 0.04 cm, while soybean (*Glycine max*) ranges from 0.1 to 0.2 cm. To assess the versatility of the GraviPi in measuring root tip angles across different species, this study conducted experiments involving various species with root widths ranging from less than 0.05 cm to 0.2 cm. As depicted in Figure 3.2.1, the root width of different species was evaluated using the PLANgleT.py software. In addition, a supplementary Table 3.2.2 was created, which includes the line widths specifically designed for each species. In addition, if a particular species was not specifically tested in this study, users can easily measure the width of that species using Fiji or similar tools.

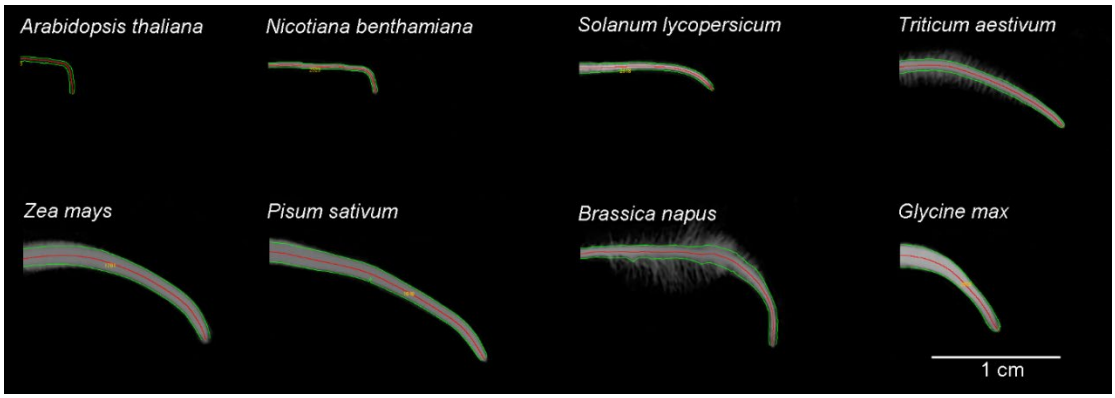

Figure 3.2.1 The root width of different species. Species including *Arabidopsis thaliana*, *Nicotiana benthamiana*, *Solanum lycopersicum*, *Triticum aestivum*, *Zea Mays*, *Pisum sativum*, *Brassica napus*, and *Glycine max*, were quantified using the PLANgleT.py software in the gravitropism assay. These species were subjected to gravitropic stimulation, and their root widths were subsequently measured using the PLANgleT.py software.

Furthermore, the root gravitropism assay was conducted for eight different species from four families (Figure 3.2.2 A), and the bending kinetics of their roots were compared (Figure 3.2.2 B). In this study, notable differences in gravitropic curvature were observed among various species. *Nicotiana benthamiana*, *Arabidopsis thaliana*, and *Brassica napus* exhibited a larger final curvature angle compared to the other species after 600 minutes of gravitropic stimulation (Figure 3.2.2 B). As members of the Brassicaceae family, *Brassica napus* exhibited faster curvature kinetics than *Arabidopsis thaliana* over time. However, in the case of the Solanaceae family, both *Nicotiana benthamiana* and *Solanum lycopersicum* displayed distinct patterns. Before 100 minutes gravitropic stimulation, *Solanum lycopersicum* exhibited a faster curvature than *Nicotiana benthamiana*. However, after 100 minutes, a reverse pattern emerged, with *Nicotiana benthamiana* displaying faster curvature compared to *Solanum lycopersicum*. In addition, all tested species showed clear two-phase curvature. The first phase occurred within the first 100-120 minutes after gravitropic stimulation for species such as *Arabidopsis thaliana*, *Nicotiana benthamiana*, and *Brassica napus*, with bending angles around 40°. The observed two-phase root gravitropic curvature is consistent with a previous study, which suggested that in *Arabidopsis thaliana*, a curvature angle of 40° might indicate the tipping point for amyloplasts to perceive gravitropic stimulation and reposition themselves [131]. Once the roots bend to 40°, the distribution of auxin asymmetry starts to diminish, resulting in a slower rate of root bending [131]. For *Zea mays, Triticum aestivum* and *Solanum lycopersicum*, the faster phase occurred also within 100 minutes after gravitropic stimulation, resulting in roots bending to around 25°. Overall, the observations in this study indicate that the gravitropism curvature kinetics pattern is species-dependent, and a two-phase curvature pattern appears to exist in the tested species.

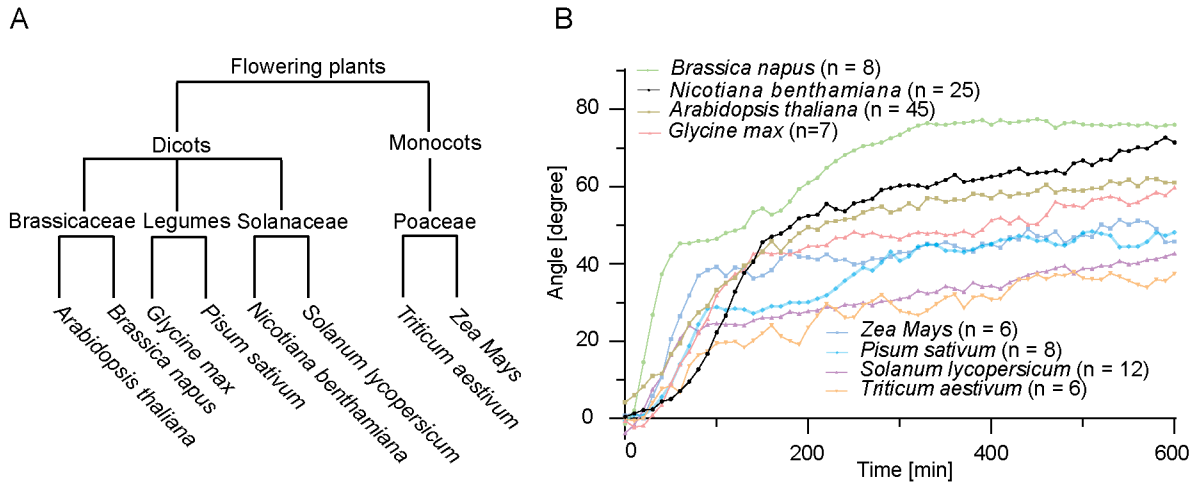

Figure 3.2.2 Kinetics of root gravitropism in eight species. (A) Species from different plant lineages included in the analysis (from left to right) were: Brassicaceae (*Arabidopsis thaliana*, *Brassica napus*), Legumes (*Glycine max*, *Pisum sativum*), Solanaceae (*Nicotiana benthamiana*, *Solanum lycopersicum*), and Poaceae (*Triticum aestivum*, *Zea mays*); (B) The root gravitropism kinetics of eight species were assessed with a time interval of 10 minutes for imaging.

3.2.3 The GraviPi performance in hydrotropism, hypocotyl and coleoptiles

To test the effectiveness of PLANgleT.py for different tropisms beyond sole gravitropism, a hydrotropism assay was conducted using WT (Col-0) plants. In brief, 7-day-old Arabidopsis seedlings at the normal growth stage were transferred to a split half-strength MS agar plate. The top section of the plate contained a normal half-strength MS medium, at the same time, 400mM sorbitol was supplied at the bottom of the medium as an osmolyte (Figure 3.2.3 A). This created a high-water potential at the top of the normal half-strength MS plate, causing the Arabidopsis root tips to bend towards the water potential. The acquired images were rotated 90 degrees to align with the measurement orientation of the script. The PLANgleT.py algorithm effectively recognized the roots of the seedlings and accurately recorded the angles of root tip bending (Figure 3.2.3 B). The successful application of the GraviPi in quantifying root tip bending angles in the hydrotropism assay demonstrates its versatility beyond gravitropism analysis. This capability enables researchers to explore various tropisms using a standardized and efficient approach.

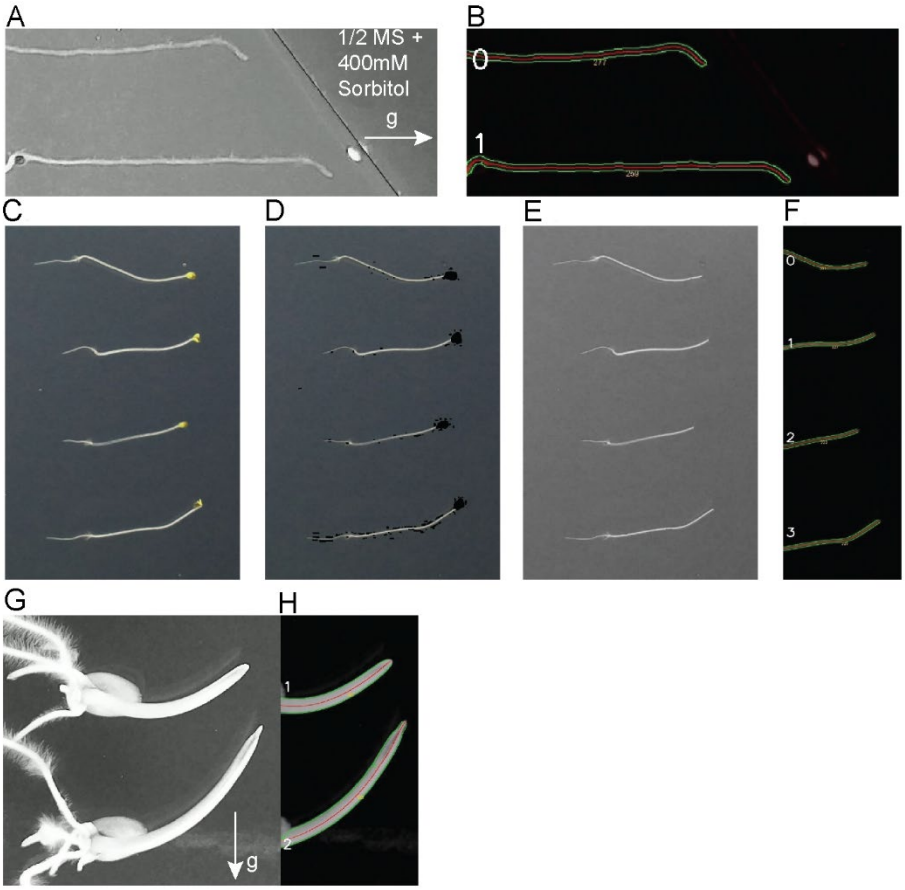

Figure 3.2.3 Detection of *Arabidopsis thaliana* root hydrotropism, hypocotyl and wheat coleoptiles. (A) Wild-type Arabidopsis thaliana subjected to the hydrotropism assay in the presence of 400mM Sorbitol; (B) GraviPi-detected hydrotropism of wild-type Arabidopsis thaliana roots; (C) Raw image of Arabidopsis thaliana hypocotyl captured by GraviPi; (D & E) Removal of cotyledon mask and background from the image; (F) Detection of hypocotyl using GraviPi, with identification markings (IDs); (G) & (H) GraviPi-detected wheat coleoptiles.

Opposite to roots, the hypocotyl of Arabidopsis exhibits negative gravitropism, where it bends away from the gravitational pull. Normally, researchers have relied on manual measurements to quantify the bending angle of the hypocotyl. However, this approach can be time-consuming and subjective, leading to variations in the obtained results [51,132]. The software was initially developed to measure changes in root tip angles. However, during the investigation of dark-grown Arabidopsis hypocotyls using GraviPi, it became evident that with proper image pre-treatment, the GraviPi could also be applied to measure hypocotyl angles. By effectively removing the cotyledon parts of Arabidopsis seedlings through a pre-processing step, this study was able to distinguish between the yellowish cotyledons and the white hypocotyls. The cotyledons were masked out, and the hypocotyls were refined using morphological erosion, resulting in improved angle detection accuracy. In addition, the parameters in the Fiji macro were fine-tuned to eliminate noise before applying ridge detection techniques, as depicted in Figure 3.2.3 C-F.

To assess the applicability of the PLANgleT.py in measuring the bending angle of coleoptiles, which are unique to monocot plants and play a crucial role in breaking soil obstacles during germination, this study conducted a wheat coleoptiles gravitropism assay.

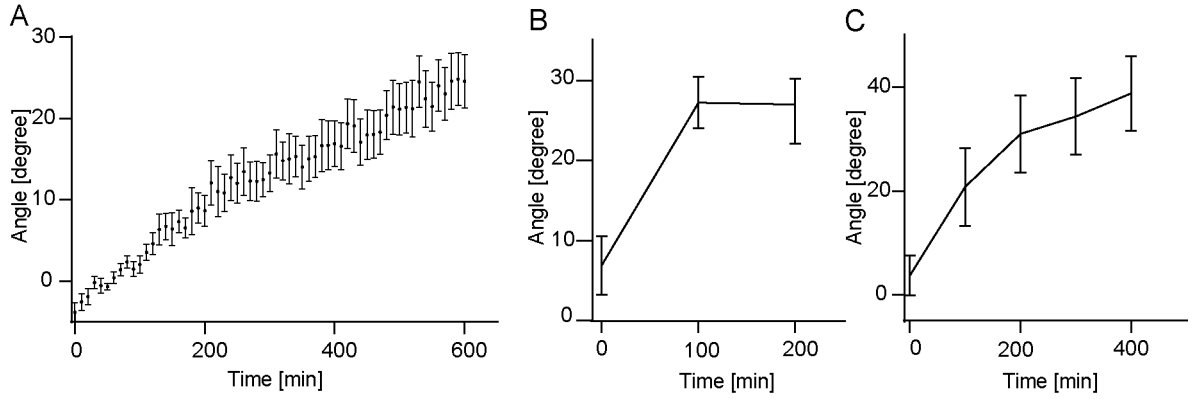

Figure 3.2.4 Kinetics of hydrotropism, hypocotyl curvature, and coleoptile curvature. (A) Kinetics of hydrotropism curvature in Arabidopsis WT Col-0; (B) Kinetics of hypocotyl curvature in Arabidopsis WT Col-0; (C) Kinetics of gravitropism curvature in wheat coleoptiles. The error bar stands for the standard error.

The results clearly demonstrate that the software effectively measures the bending angle of coleoptiles, as illustrated in Figure 3.2.3 G & H and Figure 3.2.4 C . This finding highlights the versatility and utility of the system in studying various plant structures and their responses to gravitropic stimulation.

3.2.4 Comparison of the GraviPi with available angle measuring software

The field of measuring root bending angles has seen the emergence of several software applications. These tools aim to meet the requirements of efficient measurement time and accurate results. The GraviPi has been specifically designed to address the need for high-throughput measurements of plant organ tropic bending angles. To evaluate the performance of the software in terms of both speed and accuracy, a comparative analysis with two recently developed software programs was conducted: BRAT and Acorba.

BRAT software adopts a method that measures the angle between the root vector and the vertical axis of the image [75]. However, this approach may hinder the accuracy of measuring the natural root bending angle, as the curvature occurs at the elongation zone of the root tip [1]. Acorba is a software developed using a machine learning approach and is specifically tailored for analyzing root bending angles from scanned images and microscope images [77]. To compare the measurement capabilities of GraviPi and Acorba, this study utilized raw images obtained from Acorba's attached files. Both the Acorba software and our GraviPi system were used in this study to measure the bending angle of wild-type Arabidopsis roots. In addition, Fiji was included as a manual measurement tool for comparison in this study. The angles detected by PLANgleT.py and Fiji manual measurement were found to be similar, with no significant

difference. However, there were significant differences in the results obtained by Acorba, which utilizes deep machine learning methods, compared to the results observed from PLANgleT.py and the Fiji manual measurements, particularly at the time points of 150 minutes and 210 minutes. The PLANgleT.py showed curvature angles of 48.18 ± 3.43 degrees and 65.19 ± 5.81 degrees, which were similar to Fiji's results of 47.24 ± 4.39 degrees and 62.26 ± 4.50 degrees. In contrast, Acorba exhibited lower accuracy at these time points, with angles of only 37.32 ± 4.61 degrees and 51.88 ± 5.03 degrees (Figure 3.2.5 A). In addition, the PLANgleT.py completed the measurements in 2 minutes, while Acorba took 3 minutes. Furthermore, the GraviPi software demonstrated notable efficiency, completing the measurements in just 2 minutes, whereas Acorba required 3 minutes. These findings indicate that the software developed for this study not only achieves accurate results, but also offers a significant advantage in terms of measurement speed compared to Acorba.

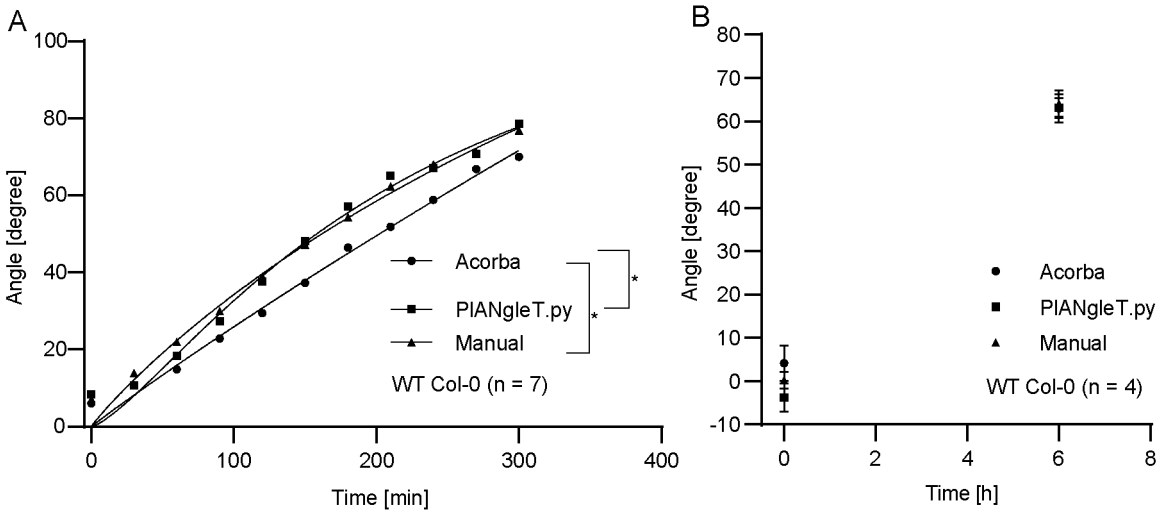

Figure 3.2.5 Comparison of Arabidopsis thaliana (WT Col-0) root gravitropism curvature using different tools. (A) Root bending angle measurement using images from Acorba; (B) Root bending angle measurement using images from this study (Scanned image). The values shown represent the mean bending angle, and the error bars indicate the standard error. The p-values presented in both cases indicate a paired comparison of fitted nonlinear regression using the extra sum-of-squares F test. An asterisk (*) indicates $p < 0.05$.

To conduct a comprehensive comparison of measurement capabilities between the GraviPi system and the Acorba software, scanned images of wild-type Arabidopsis root gravitropism were used. As illustrated in Figure 3.2.5 B, both the GraviPi and Acorba exhibited highly consistent results, demonstrating their effectiveness in accurately quantifying root gravitropism. Notably, a significant disparity was observed in the processing time required by each tool. The GraviPi system achieved remarkable efficiency, completing the measurement task within 18 seconds, while Acorba took approximately 37 seconds to accomplish the same task. These findings emphasize the exceptional speed and accuracy offered by the GraviPi software,

enabling rapid and precise measurements of root gravitropism.

The substantial time advantage provided by the GraviPi system not only accelerates data analysis but also enhances overall workflow productivity. The comparable performance in terms of measurement accuracy between our GraviPi and Acorba, coupled with the significantly reduced processing time of our script, positions it as a valuable tool for high-throughput analysis of root gravitropism and other related phenotypic assessments.

3.2.5 Arabidopsis root gravitropism kinetics in varying sucrose concentrations

Extensive research has revealed a significant correlation between sucrose treatment and gravitropic bending in Arabidopsis. Specifically, it has been found that adding 1% sucrose enhances the gravitropic curvature and elongation length of the roots [133]. Moreover, a dose-dependent positive relationship has been observed between sucrose concentration (ranging from 0% to 2%), root length, and gravitropic responsiveness [134]. However, the previous investigation conducted by the mentioned researchers focused on the final curvature after a specific duration of gravitropic stimulation, and the effect of different sucrose concentrations on the kinetics of root bending in response to gravitropic stimulation remains unclear. Furthermore, a recent study has introduced an innovative approach to normalization in the context of root bending analysis, departing from the conventional practice of using time as the normalization factor [102]. Instead, this novel method employs the root growth as a more robust and accurate normalization parameter, enhancing the accuracy and reliability of root bending measurements.This alternative approach has demonstrated its efficacy in distinguishing between root bending and root growth more accurately. When analyzing kinetics across multiple time points, employing this new normalization method proves beneficial. By incorporating the fitted curve parameters, it becomes easier to determine the significance of observed differences.

To investigate the impact of sucrose concentration on the kinetics of root bending in Arabidopsis seedlings, an experiment using different sucrose treatments was performed. Specifically, seedlings were grown in half-strength MS medium supplemented with either 1% sucrose, 3% sucrose, or no sucrose (as a control), imaging every 10 min for 24 hours.

Consistent with previous studies, this study revealed a significant effect of sucrose on root tip curvature. Analysis of the root bending angle over time demonstrated that seedlings treated with 1% sucrose exhibited a noticeable increase in root tip curvature compared to those grown without sucrose. This difference became apparent after approximately 40 minutes of exposure to gravitropic stimuli, as depicted in Figure 3.2.6 A. Interestingly, seedlings grown in the 3% sucrose medium displayed a slower response, taking approximately 12.8 hours to surpass the root bending angle observed in the control group. This suggests that higher sucrose concentrations may lead to a delayed gravitropic response in Arabidopsis seedlings.

However, when applied the normalization method of root bending measurements in relation to root growth, this study observed opposite patterns before the root length reached approximately 0.15 cm. Notably, at a root length of 0.1 cm, the control group exhibited a faster rate of root curvature (66 degrees) compared to the 1% sucrose-treated group (60 degrees) and the 3% sucrose-treated group (50 degrees). The 3% sucrose-treated group exhibited the slowest rate of root curvature among the three groups.

As the root length progressed beyond 0.15 cm, this study observed distinct behaviors among the different treatment groups. In the control group, the root bending and growth appeared to have reached a plateau with minimal further curvature (this is the end of imaging, 24 hours). In contrast, both the 1% and 3% sucrose-treated groups exhibited continued growth and bending even as the root length reached 0.35 cm. Intriguingly, at this stage, the 3% sucrose-treated samples surpassed the 1% sucrose-treated samples in terms of bending angle. It can be inferred that prior to reaching a certain length, sucrose concentrations, particularly at 1% and 3%, may exert a negative influence on the bending angle of roots following gravitropic stimulation. On the other hand, as sucrose provides energy for plants, it is important to note that in the absence of sucrose, plants grown in the dark cannot generate sufficient energy through photosynthesis. This observation might explain why the control group plants exhibited slow growth. In constrast, both the 1% and 3% sucrose-treated plants had sufficient energy reserves to support growth and bending.

Furthermore, normalizing the root bending angle with respect to root growth provides a valuable modification to the analysis. This normalization method allows for a more accurate assessment of the relationship between root bending and growth, offering insights into the dynamic interplay between these two processes. The use of this normalization approach enhances our understanding of how sucrose concentrations impact root growth and gravitropic responses.

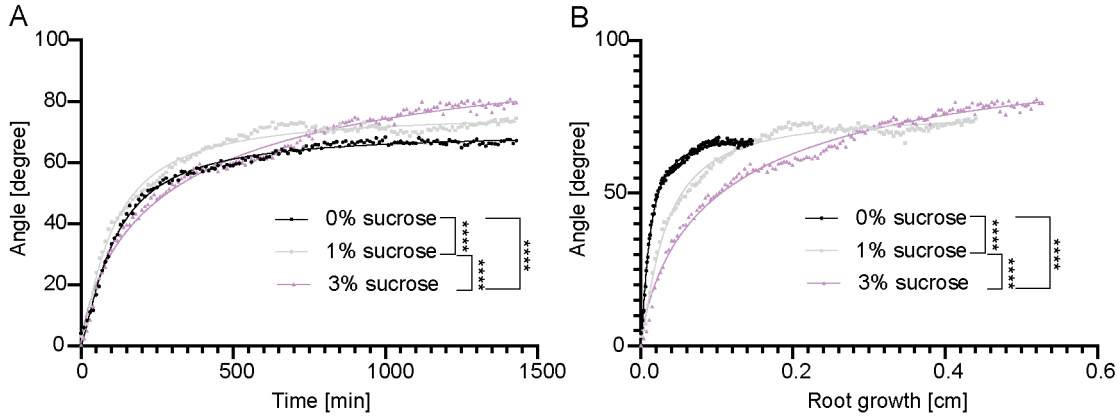

Figure 3.2.6 Kinetics of root curvature in different sucrose concentrations with time or normalized root growth. (A) Normalized kinetics of gravitropic curvature with time (B) Normalized kinetics of gravitropic curvature with root growth. Seedlings grown in sucrose-free

medium, 1% and 3% sucrose medium. WT no-sucrose: n = 45, WT 1% sucrose: n = 45, WT 3% sucrose: n = 46. Values mean bending angle. Asterisk (****) represents p-value < 0.0001, p-value represented a paired comparison of fitted nonlinear regression with the extra sum-of-squares F test.

3.3 ARG1 interacts with ARL1 and HSP70-1 to control initial gravitropism signaling in *Arabidopsis thaliana*

3.3.1 Pre-test to verify the pull-down process

Transgenic plants (*arg1-3* background) expressing *ARG1-YFP* were generated, where the coding DNA sequence (CDS) of *ARG1* was fused with a yellow fluorescent protein (YFP) at the C-terminus. The expression of *ARG1-YFP* was driven by a constitutive Cauliflower Mosaic Virus 35S promoter (CaMV 35S). Homozygous *ARG1-YFP OE* lines were selected in the T3 generation. Before proceeding with the IP-MS experiment, a preliminary experiments was conducted to validate the complementation of ARG1 in the *arg1-3* mutant using *ARG1-YFP* transgenic plants. A root gravitropism assay comparing the *arg1-3* mutant with two independent lines of transgenic plants (*ARG1-YFP OE #1* and *ARG1-YFP OE #2*) was performed. Both transgenic lines exhibited restored root gravitropism, indicating that the introduction of ARG1-YFP successfully rescued the gravitropism defect in the *arg1-3* mutant. This observation confirms the functional capability of ARG1-YFP in complementing the root gravitropism deficiency in the *arg1-3* mutant. The *ARG1-YFP OE #1* line was chosen for subsequent downstream experiments.

Furthermore, before embarking on the mass spectrometry analysis, a pre-test pull-down experiment was conducted using GFP-trap agarose beads to evaluate the specificity and efficiency of ARG1-YFP enrichment. As depicted in Figure 3.3.1, the elution lane displayed specific detection of ARG1-YFP, indicating successful enrichment using this strategy. These results provide confidence in the effectiveness of our approach for subsequent mass spectrometry analysis.

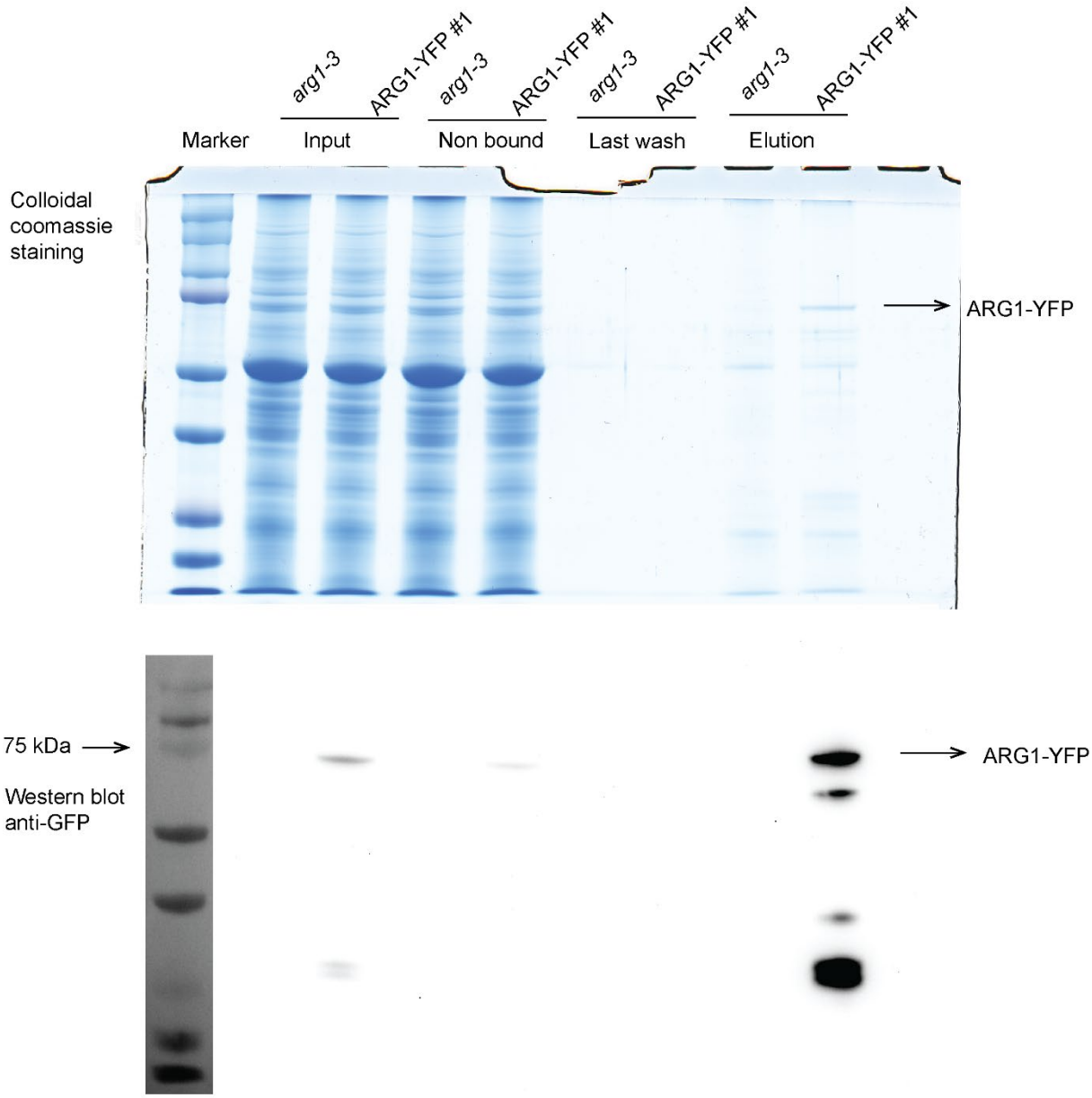

Figure 3.3.1 Pre-test to verify the pull-down process. The top shows the colloidal coomassie staining. ARG1-YFP was pulled-down by GFP-Trap agarose beads (GFP-Trap, Agarose, gta-20, ChromoTek), here the *arg1-3* was used as a negative control. The ARG1-YFP was specifically shown in the elution lane, but not in the background control. Western blot was done using an anti-GFP antibody to further confirm the presence of ARG1-YFP (shown at the bottom gel).

3.3.2 IP-MS workflow

Three-week-old *arg1-3* and *ARG1-YFP OE #1* plants were harvested, and proteins were isolated under native conditions. Subsequently, GFP-trap agarose beads were utilized to capture ARG1-YFP and its potential interaction partners. The pulled-down proteins were then subjected to quantitative mass spectrometry analysis (Figure 3.3.2).

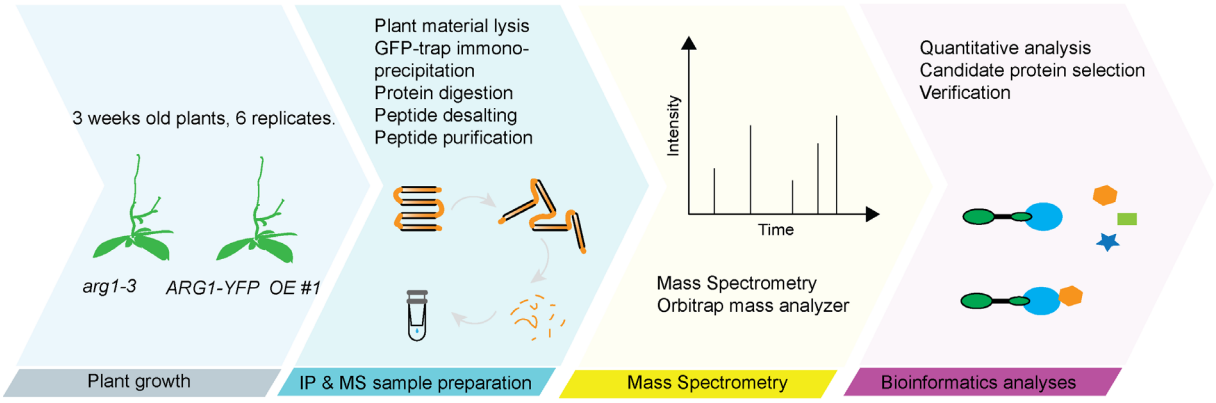

Figure 3.3.2 Workflow of the IP-MS experiment. Plant materials at three weeks old were harvested and used for immunoprecipitation and mass spectrometry sample preparation. Subsequently, the samples were subjected to mass spectrometry analysis, followed by data analysis and selection of candidates.

3.3.3 Bioinformatics analysis of IP-MS samples

To increase the likelihood of identifying true binding partners of ARG1, this study performed a differential enrichment analysis using a paired t-test. This analysis allowed us to compare the protein enrichment in the IP group samples with that in the control group samples. By excluding proteins that showed significant enrichment in the control samples, this study identified 83 potential candidates that exhibited specific enrichment in the ARG1 IP samples (supplement Table 3.3.1). These candidates represent a narrowed-down list of proteins that are likely to interact with ARG1 and could potentially be its faithful binding partners.To assess the functional relevance of the proteins identified in the pull-down samples and their potential involvement in gravitropism, a Gene Ontology (GO) annotation analysis for the selected 83 candidate proteins was conducted (Figure 3.3.3).

Figure 3.3.3 Scatter plot of selected 83 proteins in the ARG1-YFP pull-down samples. CC = cellular component, MF = molecular function, BP = biological process. The protein ratio represents the proportion of enriched proteins to all the 83 proteins being used. The size of the black circle indicates the protein number. Each color indicates a different p-value.

In alignment with the putative chaperone property of ARG1, the protein binding involved in protein folding term are enriched, as chaperone protein is supposed to assist in protein binding. This might indicate that these proteins could form a co-chaperone system involved in protein binding in Arabidopsis gravitropism. It has been suggested that ARG1 might localize at endomembrane systems, including the plasma membrane, endoplasmic reticulum, and Golgi [36]. Here the cellular component terms revealed that the pulled-down proteins not only have endomembrane system localization but also have cytosol and inner membrane localization. At the biological process level, protein responsible for folding and refolding are highly enriched candidate proteins, including HSP70 proteins, such as HSP70-1, HSP70-2, HSP70-3, and HSP70-4. This might suggest that ARG1 can interact with proteins involved in protein folding. In a previous study, it was discovered that ARG1 has physical interactions with HSP70s [123]. However, the specific HSP70 proteins involved in these interactions remain unclear, as Arabidopsis chromosomes contain 14 *HSP70s* [135], further experiments are required to elucidate the precise interactions between ARG1 and specific HSP70 proteins. This study identified HSP70-1, HSP70-2, HSP70-3, HSP70-4, and chloroplast heat shock protein 70-1 (cpHSP70-1) as potential candidates for interaction with ARG1. Furthermore, ARL1 was identified exclusively in the immunoprecipitation (IP) samples. ARL1 is a paralogue protein of ARG1 [31]. Interestingly, it has been shown that an mRNA-null mutant of *arl1-4* did not show

any agravitropic phenotype, and the *arg1-2arl1-4* or *arl2-1arl1-4* double mutant has the same phenotype as *arg1-2* or *arl2-1* [136].

3.3.4 ARG1 interact with HSP70-1 and ARL1

A co-immunoprecipitation assay (co-ip) was performed to investigate the potential interaction between ARG1 and HSP70s. This study selected HSP70-1 as a candidate because ARG1 is a periphery membrane protein, the carboxyl terminus might expose to the cytosol to interact with substrate proteins, and the HSP70-1 might be the suitable chaperone protein to help the proper activity of the substrate proteins. This study did a co-ip assay in *N. benthamiana*. As shown in Figure 3.3.4 A, ARG1 can interact with HSP70-1 but not the free GFP. This result suggests that HSP70-1 might interact with ARG1 *in vivo*. Although a T-DNA insertion *hsp70-1* mutant test did not show any gravitropism defection in roots or hypocotyl, this might be caused by the functional redundancy among the paralogue HSP70s.

ARG1 has two paralogues in Arabidopsis, ARL1 and ARL2. It has been suggested that ARL2 shares the same gravitropism pathway with ARG1, and ARG1 can directly interact with ARL2 *in vivo* [123], and *arl2* has the same gravitropism phenotype as *arg1* [37]. Notably, no related phenotype was found in *arl1*, while the IP-MS data showed a specific intensity signal of ARL1 only in IP samples. This phenomenon encourages us to test whether an interaction exists between ARL1 and ARG1. A co-ip was done based on a transient expression assay in *N. benthamiana*, and the result clearly shows that ARG1 can interact with ARL1 *in vivo* (Figure 3.3.4 B). Deletion of the ARG1 coiled-coil domain abolished the interaction between ARG1 and ARL1 (Figure 3.3.4 C), this indicates that the interaction sites located at the coiled-coil region of ARG1.

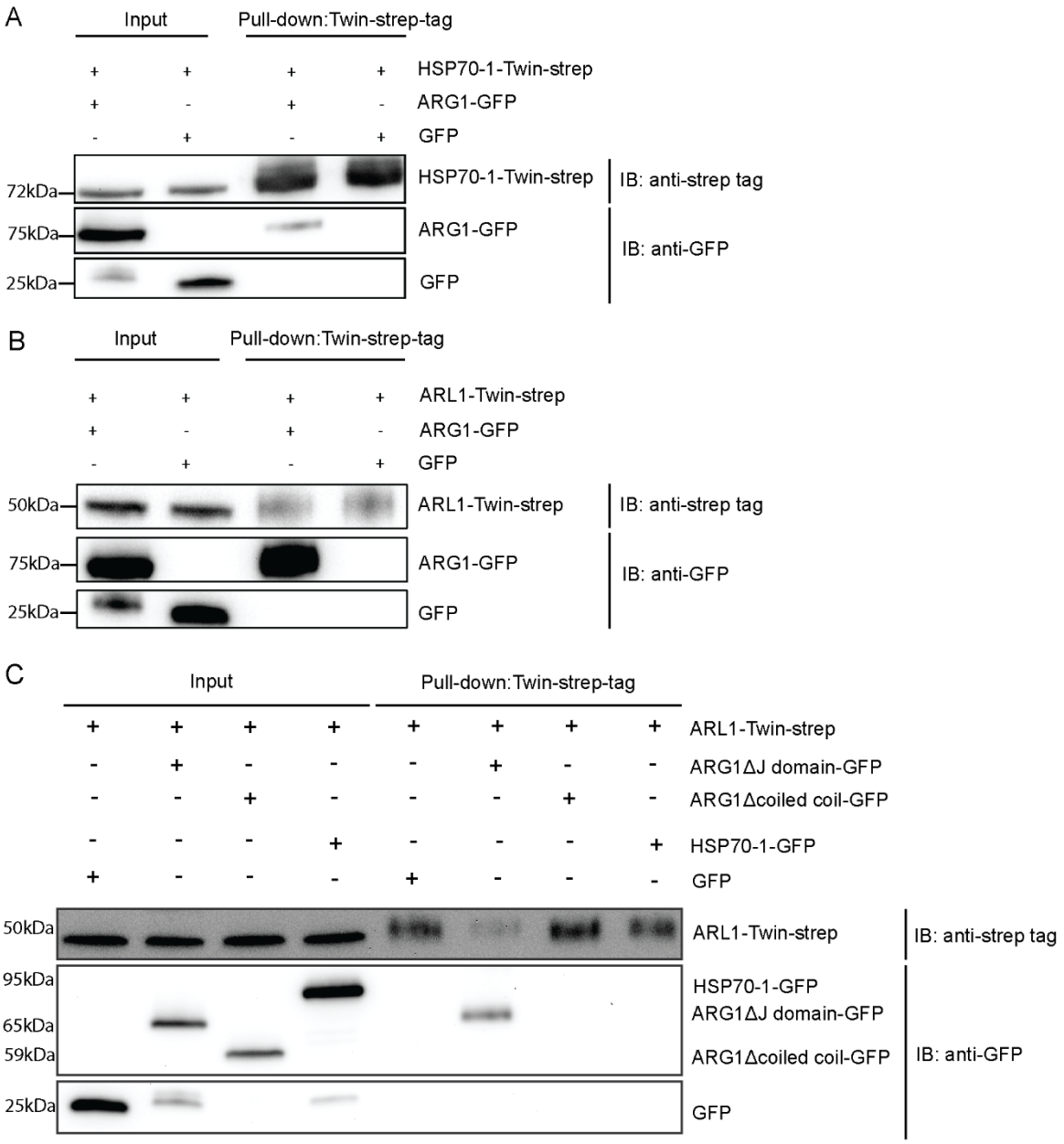

Figure 3.3.4 Co-ip assay. (A) ARG1 interacts with HSP70-1; (B) ARG1 interacts with ARL1; (C) ARG1 interacts with ARL1 through coiled coil domain, and ARL1 does not interact with HSP70-1. HSP70-1-Twin-strep and ARL1-Twin-strep were detected with Strep-Tactin AP-conjugated antibody (IBA Lifesciences), ARG1-GFP, HSP70-1-GFP and GFP were detected via GFP antibody.

3.3.5 ARL1 physically interacts with ARG1 at the nucleus in protoplast

To further confirm the interaction between ARG1 and ARL1, a bimolecular fluorescence complementation (BiFC) experiment was conducted. ARG1 and ARL1 were fused with the N-terminal fragment of yellow fluorescent protein (YN) or the C-terminal fragment of yellow fluorescent protein (YC), respectively. These fusion constructs were expressed in Col-0

protoplasts under the control of the CaMV 35S promoter. Protoplasts co-expressing ARG1-YC/YN and YFPc/YFPn, as well as ARL1-YC/YN and YFPc/YFPn combinations, did not exhibit a yellow fluorescence signal. However, yellow fluorescence signals were observed in the nuclei of protoplasts expressing ARG1-YN in combination with ARL1-YC or ARG1-YC in combination with ARL1-YN. Neither ARG1-GFP nor ARL1-GFP showed any signal indicating localization within the nuclei. These results provide strong evidence for a physical interaction between ARG1-YN/ARL1-YC and ARG1-YC/ARL1-YN within the nucleus (Figure 3.3.5).

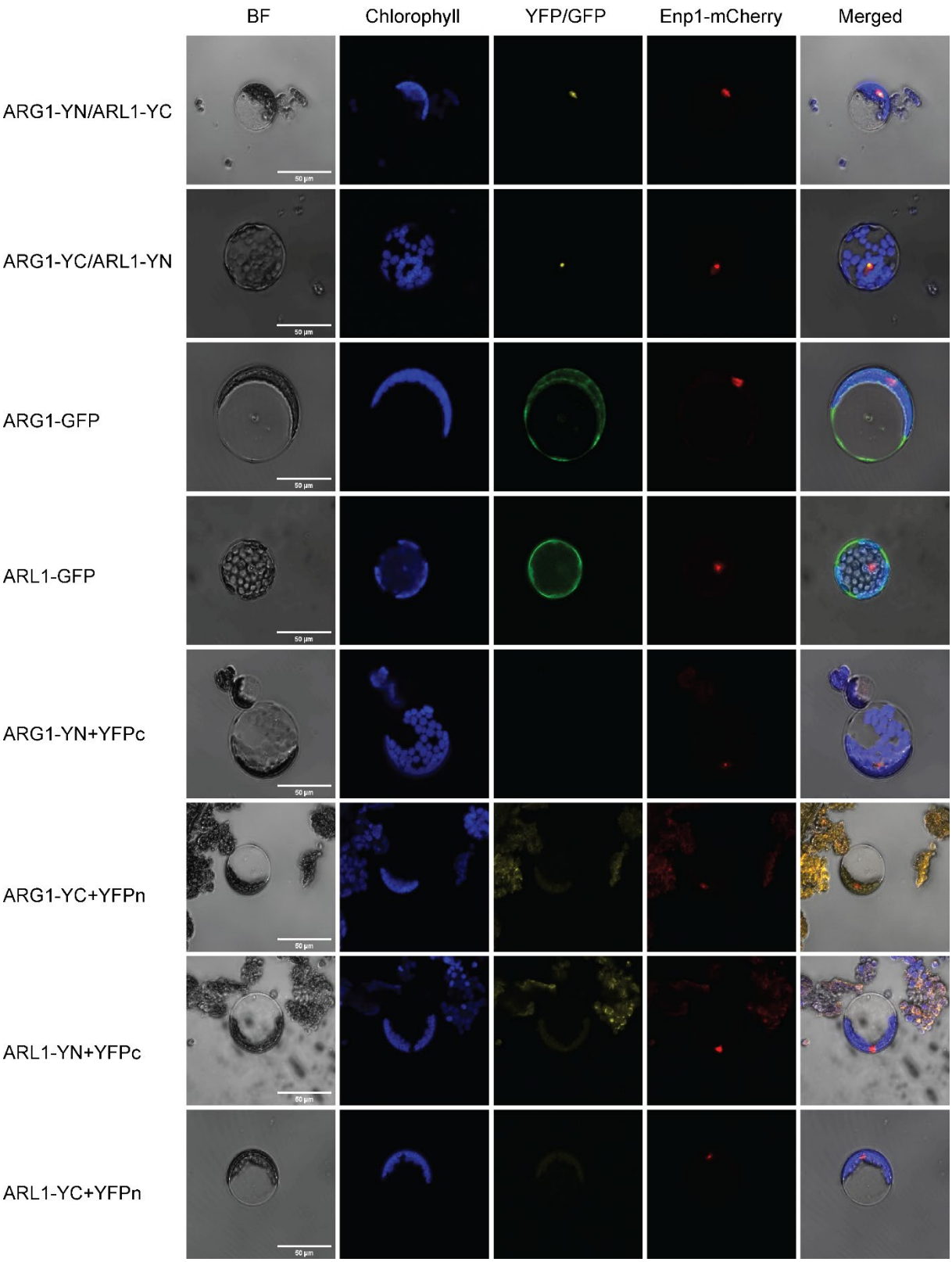
BF
Chlorophyll
YFP/GFP
Enp1-mCherry
Merged
ARG1-YN/ARL1-YC
ARG1-YC/ARL1-YN
ARG1-GFP
ARL1-GFP
ARG1-YN+YFPc
ARG1-YC+YFPn
ARL1-YN+YFPc
ARL1-YC+YFPn

Figure 3.3.5 Analysis of ARG1 associations with ARL1 proteins in Arabidopsis Col-0 protoplasts. Bimolecular fluorescence complementation assays were conducted using protoplasts co-expressing ARG1-GFP, ARL1-GFP with Enp1-mcherry, ARG1-YN/ARL1-YC/Enp1-mcherry, ARG1-YC/ARL1-YN/Enp1-mcherry or co-expressing YFPc and YFPn alone with ARG1-YN/ARG1/YC, ARL1-YN/ARL1-YC. Imaging was performed using a Zeiss LSM 780 confocal microscope with settings for YFP (Ex: 514 nm, Em: 517–553 nm), GFP (Ex: 488 nm, Em: 510 nm), and mCherry (Ex: 587 nm, Em: 610 nm). Bright-field images (BF) and merged images are also presented. Scale bars represent 50 μm.

3.4 Discussion

3.4.1 Phosphoproteomics analysis is a powerful strategy in the study of gravitropism

Extensive research efforts have been dedicated to unraveling the molecular mechanisms underlying plant gravitropism, leading to the identification of several essential proteins involved in this process. Among these, ARG1 has emerged as a critical player in gravitropism [31,36]. Despite several promising hypotheses regarding gravitropism perception, such as the starch statolith and tensegrity models, none have yet been confirmed [137]. The starch statolith model proposes that gravity sensing in plants is mediated by starch-filled amyloplasts, known as statoliths, which sediment in response to gravity and transmit the gravitational signal to downstream signaling pathways [2,3].

While this model provides an intriguing framework for understanding how plants perceive gravity, additional experimental evidence is required to validate the precise mechanisms of gravitropism. Understanding the mechanisms of gravitropism poses significant challenges, primarily due to the presence of elusive pathways and molecules intricately involved in this process. Despite significant progress being made in unraveling the molecular and cellular aspects of gravitropism, key components, and signaling pathways remain elusive and, thus, require further investigation. Investigating the early signal transduction events in response to microgravity stress represents a critical avenue for advancing our understanding of how plants perceive and respond to changes in gravity. By studying these initial signaling events, we can gain valuable insights into the molecular mechanisms underlying gravitropism in plants.

Phosphorylation plays a pivotal role in regulating plant gravitropism, as it serves as a critical mechanism for transmitting and modulating signals involved in this fundamental biological process [130]. Multiple kinases, including PID, D6PK and TOR, have been identified as potential key factors in mediating the gravitropic response in plants. The *pid-9* exhibits a defect in root gravitropism, as do the *d6pkd6pkl1d6pkl2*, and *TOR RNAi* plants [54,59,65,72,138]. In addition, the gravitropism response is initiated rapidly, typically occurring within seconds of

gravitropic stimulation [139]. For example, real-time observations have revealed that gravistimulation (within 20 seconds) triggers the occurrence of Ca2+ sparks in the root cap, particularly in the lower side of the lateral root cap [21].

In order to gain deeper insights into the molecular events occurring during the initial seconds of microgravity exposure, this study embarked on a phosphoproteomics study of Arabidopsis seedlings. By focusing on this early time frame, this research aimed to capture the dynamic phosphorylation events that play a crucial role in the plant's response to altered gravity conditions.

This study employed two well-established platforms: the drop tower and the parabolic flight platforms, facilitated by the Center of Applied Space Technology And Microgravity (ZARM) in Bremen and Novespace in Bordeaux, France. The comprehensive analysis in this study yielded a total of 4,266 phosphosites. The phosphorylation pattern and residue ratios observed in this study were consistent with previous Arabidopsis phosphoproteomics studies, affirming the reliability and reproducibility of the findings [115,141,142].

3.4.2 Robust phosphorylation changes

The analysis of significantly differentially phosphorylated peptides in the hypergravity treatment, 3 s and 22 s microgravity treatments revealed interesting patterns of overlap. A total of 85 peptides were found to be shared among all three experimental groups, indicating a common response across these conditions. In addition, except for the shared 85 peptides among all the three groups, 53 peptides were found to be present in both the hypergravity treatment and the 3 s microgravity treatment, whilst another 53 peptides were found to be shared between the hypergravity treatment and the 22 s microgravity treatment. Moreover, 130 peptides were shared between the 3 s and 22 s microgravity treatments. These findings indicate that certain proteins exhibit consistent changes in their phosphorylation states across different durations of microgravity and hypergravity exposures, suggesting a shared response and potential regulatory mechanisms in response to gravity force changes.

The enriched Gene Ontology (GO) terms for the significantly differentially phosphorylated proteins in the 3 s microgravity treatment included "signal transduction", "microtubule cytoskeleton organization" and "protein targeting to vacuole involved in ubiquitin-dependent protein catabolic process via the multivesicular body sorting pathway". These findings highlight the rapid activation of signaling pathways and the involvement of cytoskeletal and lipid signaling proteins in the early stages of the gravitropism response.

In contrast, the 22 s microgravity treatment showed enrichment only in biological processing terms, particularly in the cellular response to hormone stimuli and salicylic acid-mediated signaling pathways. This indicates that longer-duration microgravity exposure may trigger specific biological processes related to hormone responses and signaling.

3.4.3 Clustering analysis revealed distinct phosphorylation patterns

Phosphorylation pattern analysis across different treatments provides valuable information, especially on the dynamic regulation of protein phosphorylation in response to specific experimental conditions. By comparing the phosphorylation profiles of proteins in different treatment groups, researchers can gain insights into the signaling pathways and cellular processes involved in the observed responses. By utilizing clustering analysis, this study classified the identified significantly differentially phosphorylated peptides into two distinct clusters, each exhibiting unique phosphorylation patterns (Figure 3.1.6). Importantly, at the biological process level, intriguing preferences were observed within these clusters. Specifically, Figure 3.1.7 highlights the enrichment of cluster 1 phosphoproteins in the biological process of "protein targeting to vacuole involved in ubiquitin-dependent protein catabolic process via the multivesicular body sorting pathway", which includes TOM-LIKE (TOL) phosphoproteins. Previous research has already established the involvement of TOL proteins in gravitropism [53], while this thesis has In addition uncovered intriguing changes in their phosphorylation levels. This suggests that phosphorylation may play a regulatory role in the gravitropism pathway of TOL proteins. In contrast, the enrichment of cluster 2 phosphoproteins in the biological process of "regulation of gene expression" suggests their role in modulating gene activity in response to the microgravity stimulation. This finding implies that changes in protein phosphorylation patterns may influence the expression of specific genes, thereby affecting cellular responses to microgravity. In addition, the cluster 2 phosphoproteins (Figure 3.1.7) also exhibited enrichment in the cellular components category, specifically the "microtubule" Gene Ontology (GO) term. Microtubules are an integral component of the cytoskeleton, a network of filamentous proteins that provides structural support, facilitates cellular movement, and participates in various cellular processes [142]. The role of the cytoskeleton in gravitropism has been well-established in Arabidopsis. One notable example is the use of Latrunculin B (Lat B), a depolymerizing agent that specifically targets the microfilament cytoskeleton [143]. Studies have demonstrated that the application of Lat B facilitates the curvature response of Arabidopsis roots by inhibiting cell elongation [144]. In addition, one of the key proteins involved in gravitropism is ARG1. Intriguingly, it has been demonstrated that ARG1 physically interacts with actin *in vivo* [123]. The enrichment of microtubule-associated proteins within the identified clusters suggests their potential roles in regulating microtubule dynamics and organization, both of which are crucial for various cellular processes including cytoskeletal rearrangement and directional growth in response to gravitropic stimuli.

3.4.4 Motif enrichment and kinase-substrate analysis

Protein sequence motifs serve as distinctive features of protein families and are valuable tools for predicting protein function [145]. In this study, the enriched motifs of the significantly differentially phosphorylated proteins identified in the 3 s and 22 s microgravity treatments were analyzed. Two enriched motifs were discovered, namely [-R-x-x-pS-] and [-pS-P-], within the significantly up-regulated phosphorylated peptides. However, it is important to note that only the [-R-x-x-pS-] motif was present in the up-regulated 3 s microgravity treatment samples. This finding aligns with a recent study that treated Arabidopsis briefly with 120 s changes in the direction of gravity. They identified three types of motifs: acidophilic motif (p[S/T][D/E] or p[S/T]xx[D/E]), basophilic motif (Rxxp[S/T]) and a proline-directed motif (p[S/T]P) [140]. Consistent with their findings, this research also revealed the presence of the [-R-x-x-pS-] and [-pS-P-] motifs. The absence of the acidophilic motif in this research could be attributed to the differences in experimental conditions. While this research conducted microgravity treatments for 3 seconds and 22 seconds, the above study utilized a longer duration of 120 seconds although it focused solely on changing the direction of gravity in a ground-based setting.

To elucidate further the phosphorylation events, a phosphorylation event network based on the kinase-substrate relationship was constructed. Interestingly, several proteins have been suggested to be involved in the gravitropism in Arabidopsis, such as BZR1 and TOC120. Previous studies have suggested the involvement of *TOC120* in gravitropism, particularly in the context of mutated *ARG1* [43]. Given the plastid localization of TOC120, the phosphorylation of TOC120 could potentially play a role in rapidly inducing gravitropic signaling through the movement of amyloplasts. While the exact mechanism of gravitropic stimulation perception remains unknown, it is plausible that the sedimentation of amyloplasts triggers kinase activation and subsequent phosphorylation signaling mediated by TOC120.

One potential kinase that may be involved in this process is the kinase at the outer chloroplast membrane 1 (KOC1), which has been suggested to phosphorylate TOC120 in vitro and is a crucial component of the plastid import process [146]. Investigating whether KOC1 exhibits defects in a gravitropism assay could provide valuable insights into its potential role in mediating gravitropic responses.

The motif-based kinase-substrate analysis uncovered several kinase families that could potentially be involved in gravitropism, notably CK II and CDK. To investigate the involvement of these kinases in gravitropism, kinase-inhibitor assays were conducted using TTP 22 as a CK II inhibitor and dinaciclib as a CDK inhibitor. The results showed that the impact on root gravitropism varied depending on the concentration of the inhibitors. When TTP 22 was applied at concentrations of 20 μM and 40 μM, a significant inhibitory effect on root gravitropism was observed, indicating a dose-dependent response. Higher concentrations of TTP 22 resulted in a more pronounced effect on root gravitropism. Furthermore, the two inhibitors exhibited

distinct impact patterns. Treatment with TTP 22 at 20 μM or 40 μM led to a reduction in the total curvature of the roots. However, at a concentration of 10 nM, dinaciclib was found to reduce significantly root curvature during the early stages of root growth when the length was less than 0.4 cm. In the later stages, the inhibitory effect of dinaciclib was not as pronounced and the root curvature became similar to that of non-treated plants. However, when the concentration of dinaciclib was increased to 100 nM, a more drastic inhibitory effect on root curvature was observed, indicating a partial blockage of the overall curvature response. CK II has been proposed to play a critical role in transcriptional regulation in plants [147], while cyclin-dependent kinases (CDKs) are central to the regulation of the cell cycle [148]. The use of TTP 22 and dinaciclib in this study may have inhibited the transcriptional and cell cycle activities involved in the root gravitropic response. This supports the notion that CDK and CK II kinases play crucial roles in regulating the gravitropic response, and their inhibition has observable effects on the directional growth of plant roots.

3.4.5 Comparison of the significantly differentially phosphorylated changes across different platforms

Several studies have extensively demonstrated the effectiveness of short-term microgravity stimulation assays using various research platforms such as drop towers, parabolic flights, and sounding rockets [149,150]. This thesis took advantage of these platforms to investigate the effect of different platforms on phosphoproteomics analysis and found that fewer phosphopeptides were observed in the drop tower samples than in those of the parabolic flight platform. Furthermore, the drop tower platform resulted in a decrease in the number of significantly differentially phosphoralated peptides identified. These differences can be attributed to technical variations in conducting the 3-second microgravity induction experiments on different platforms. Indeed, upon removing the peptides that had already shown significant differential phosphorylation in the hypergravity phase of the parabolic flight platform, it was observed that only five of the remaining significantly differentially phosphorylated peptides in the 3 s microgravity treatment overlapped with the 71 peptides identified by using the drop tower platform. Furthermore, the classification analysis depicted in Figure 3.1.6 B also demonstrated that hypergravity treatment had a distinct impact on protein phosphorylation prior to the 3 s microgravity treatment. These findings collectively suggest that the observed phosphorylation changes in the 3 s microgravity treatment when using the parabolic flight platform may be influenced by the prior exposure to hypergravity conditions.
Despite these platform-related variations, this research identified 12 phosphoproteins that showed significant overlap across both platforms. The presence of these proteins and their corresponding phosphosites suggests a robust and consistent involvement of phosphorylation during microgravity treatment.

3.4.6 Root gravitropism assay of selected candidates

Several mutant candidates were selected for the gravitropism assay, including *suo-1*, *patl2*, *pck1*, *med26c*, *villin3*, *smo4-2*, *hyaluronan*, *map65-1*, naip1, *tpx2*, *toc120* and *tzf3*. The results, illustrated in Figures 3.1.12 and 3.1.13, revealed distinct kinetics in gravitropic bending for various mutants compared to the WT ($p < 0.05$), except for *map65-1*, *hyaluronan* and *villin3*. Mutants such as *patl2-1*, *med26c*, *naip1*, *tpx2*, and *tzf3* displayed a lag phase at the beginning of the curvature, while the mutants *suo-1* and *pck1* exhibited a faster initial bending response. Notably, *toc120* exhibited a significant difference during the middle curvature phase.

PATL2, belonging to the PATL protein family, has previously been implicated in auxin-mediated PIN1 relocation [127]. Given the crucial role of auxin in the gravitropic stimulation response, the observed phosphorylation changes in PATL2 suggest that it may respond to gravity changes through post-translational modification.

TPX2, known for its involvement in microtubule cytoskeleton organization [151], aligns with the growing evidence highlighting the importance of the cytoskeleton-mediated gravitropism perception or response [34]. The phosphorylation alterations observed in TPX2 under microgravity stimulation further emphasize the potential significance of phosphorylation in the TPX2-mediated gravitropism response. However, to determine the impact of phosphorylation on these proteins, it is necessary to perform additional experiments, such as generating phosphomimic (amino acid substitutions that mimic a phosphorylation statute of protein, such as serine to aspartic acid) or phospho-dead (amino acid substitutions that mimic a nonphosphorylation statute of protein, such as serine to alanine) versions of these proteins through mutagenesis PCR.

It is worth noting that although MAP65-1 exhibited significant phosphorylation alterations compared to the 1 g control under this 3 s and 22 s microgravity treatments, there were no significant differences between the mutant and wild-type plants regarding root curvature despite MAP65-1 having being implicated in cell proliferation and axial growth in Arabidopsis roots [152]. However, the lack of discernible effects on root curvature in the mutant could be attributed to protein redundancy or functional overlap between MAP65-1 and its paralog.

Further investigations are needed to unravel the precise functional implications of phosphorylation events and the specific roles played by these candidate proteins in the intricate process of gravitropism.

3.4.7 Phosphorylation changes revealed TOR signaling

This thesis identified intriguing indications of TOR signaling through a phosphoproteomic study. Specifically, this research observed that 14 phosphoproteins in the 3s microgravity-treated samples and 12 phosphoproteins in the 22s microgravity-treated samples were also known targets of TOR. This finding strongly suggests the involvement of TOR signaling in the

microgravity-induced phosphorylation changes observed in Arabidopsis.
The identification of overlapping phosphoproteins targeted by TOR reinforces the notion that TOR signaling plays a crucial role in modulating the phosphorylation events triggered by microgravity in Arabidopsis. The TOR pathway is well-known for its regulatory functions in various cellular processes, including growth, metabolism, and stress responses [63–65,153]. Its involvement in the context of microgravity-induced phosphorylation changes adds another layer of complexity to our understanding of how plants perceive and respond to gravity alterations. Further investigations are needed for the specific mechanisms and downstream effects of TOR signaling in microgravity. Elucidating the intricate interplay between TOR signaling and phosphorylation events will contribute to a more comprehensive understanding of the molecular mechanisms underlying plant gravitropism and its modulation in response to microgravity conditions.

3.4.8 GraviPi is a powerful gravitropism curvature-measuring tool

Phenotyping is a critical aspect of plant tropism research, and this study further recognized the need for an accessible and reliable phenotyping tool. To fulfill this requirement, this research developed GraviPi, a novel platform comprising imaging hardware and measuring software (PlANgle.py, developed by Freya Arthen). The aim was to provide a cost-effective alternative to expensive devices and manual measurement tools (e.g., ImageJ) while ensuring stability and accuracy. Through rigorous testing and validation, this study confirmed the hardware's robustness and the software's precision. GraviPi demonstrated consistent performance and reliable data collection in measuring plant tropism responses. With its user-friendly interface and automated analysis capabilities, GraviPi has the potential to streamline and to enhance experimental workflows in the field of plant tropism research. By offering a cost-effective and accessible solution, GraviPi opens up opportunities for a broader range of researchers to investigate plant tropism phenomena without the limitations imposed by expensive equipment or time-consuming manual measurements. Furthermore, the ease of use and reliable performance of the GraviPi make it a valuable tool for both small-scale experiments and large-scale phenotyping studies.

3.4.9 GraviPi is a cost-saving and reliable imaging tool

The cost of imaging systems is primarily attributed to the devices used. Traditional hardware, including digital cameras and scanners, often incur costs of several hundred euros (Supplement Table 3.2.1). However, Raspberry Pi and related devices serve as relatively affordable alternatives that have been proven to be effective for plant phenotyping [154]. This study further investigated the potential ability of using Raspberry Pi to control a high-quality camera for capturing fixed property images, including white balance, auto exposure, and time

interval. The affordability and accessibility of Raspberry Pi-based imaging systems make them particularly advantageous for researchers with budget constraints or for those seeking more cost-effective alternatives. In addition, the flexibility and versatility of Raspberry Pi devices allow for customization and integration with other software and hardware components, further enhancing their suitability for plant phenotyping applications.

In the context of imaging plant tropisms, particularly gravitropism, the presence of a controllable light source is crucial. It has been well documented that illumination plays a significant role in auxin signaling and auxin-mediated root gravitropism [70]. Therefore, it is essential to control the lighting conditions carefully to minimize the impact of light on the observed tropic responses. The GraviPi, developed in this study, incorporates a controllable green LED light source (modified by Sven Plath) specifically designed for transient lighting during imaging sessions. This innovative feature allows researchers to regulate and manipulate the lighting conditions, creating a dark environment that is optimal for studying plant gravitropism. By utilizing a green LED light source, the GraviPi minimizes the potential interference of light on auxin signaling pathways and the subsequent gravitropic response. The controllable nature of the LED light source further enhances the experimental versatility of the GraviPi. Researchers can precisely adjust the intensity and duration of the green light exposure to suit their specific experimental requirements, ensuring accurate and reproducible measurements of plant tropic responses.

Furthermore, the GraviPi system not only incorporates a controllable light source but also expands the imaging capabilities through the integration of a rotation stage and a user-friendly control system, including a graphical user interface (GUI). These advancements empower the users to perform high-throughput phenotyping by effortlessly measuring dozens of plates simultaneously. The incorporation of a rotation stage within the GraviPi system revolutionizes the imaging process by allowing automated imaging of multiple plates, containing dozens of plants at once. This feature enhances experimental efficiency and significantly reduces the time and effort required for data acquisition. With the ability to rotate and capture images from different angles, researchers can obtain comprehensive and detailed information about plant tropism responses. The control system, along with the intuitive graphical user interface, provides users with a seamless and user-friendly experience. The GUI enables easy navigation and the control of various imaging parameters, such as image acquisition timing, lighting conditions and rotation angles. Researchers can effortlessly customize the imaging settings according to their experimental requirements, further enhancing the flexibility and versatility of the system.

The ability to measure multiple plates simultaneously has several significant advantages. Firstly, it enables researchers to obtain a higher number of biological replicates, leading to more robust and reliable experimental results. Increased replicates enhance the statistical

power and allow for a more comprehensive analysis of the data. In addition, the high-throughput nature of the GraviPi system facilitates the monitoring of larger plant populations, making it particularly valuable for mutant selection in downstream omics experiments. By providing the capability to measure dozens of plates at once, the GraviPi system streamlines the experimental workflow and maximizes efficiency. This scalability opens up new opportunities for conducting large-scale studies and accelerates the pace of research in plant tropism and related fields.

3.4.10 GraviPi provides a reliable measuring software

This study tested advanced angle measurement software (developed by Freya Arthen) and found that the software offers higher accuracy compared to existing tools such as Acorba and BRAT. One key advantage of the pipeline is its ability to achieve precise measurements of bending angles. This software incorporates adjustable parameters that allow researchers to optimize background reduction, resulting in more accurate and reliable angle measurements and is particularly beneficial considering the variations in image quality that researchers may encounter. By adjusting the parameters, users can effectively remove unwanted backgrounds and non-targeted regions, such as leaves, when quantifying root bending angles. This level of customization ensures that measurements are focused on the regions of interest, leading to more precise and meaningful results.

3.4.11 GraviPi can measure the Arabidopsis hypocotyl bending angle and other species' gravitropism angles

The GraviPi pipeline represents a novel approach as the first semi-automated method for quantifying Arabidopsis hypocotyl bending angles. By leveraging color-based filtration and morphological erosion techniques, this study has successfully eliminated leaf interference, allowing researchers to focus solely on the hypocotyl region. Subsequently, the developed software can efficiently and accurately measure the bending angle of the hypocotyl. This automated process not only saves time and effort but also enhances the consistency and reliability of the measurements.

Furthermore, the pipeline extends its detection capabilities beyond the Arabidopsis root and hypocotyl bending. This study has successfully adapted the methodology to investigate other tropisms and the gravitropism in different plant species. For instance, this study has applied the pipeline to measure the bending angles of wheat coleoptiles; these exhibit negative gravitropism and present challenges due to their elusive movement patterns and non-repeatable tracks between the tip and the node. Through the implementation of position filters and matching algorithms, the software successfully identifieds and tracked these intricate movement patterns, enabling the accurate measurement of coleoptile bending angles. This

breakthrough expands the scope of the pipeline and demonstrates its versatility in studying tropisms across various plant species.

3.4.12 Effects of sucrose treatment on root gravitropism

A comprehensive understanding of the kinetics of Arabidopsis root gravitropism in relation to the root growth rate under varying sucrose conditions is lacking in the current literature. This study aimed to fill this gap and provide a precise depiction of these dynamics. When the root curvature was normalized with respect to root growth, this study revealed a significant negative correlation between sucrose-promoted root growth and root curvature. Specifically, before the root length reaches approximately 0.15 cm, this study observed that seedlings treated with sucrose exhibited a slower bending angle compared to seedlings without sucrose treatment. Root bending towards gravity is driven by the uneven distribution of auxin, a hormone that can be modulated by sucrose. Recent studies have confirmed AUXIN-BINDING PROTEIN 1 (ABP1) as an auxin receptor [155], further supporting the intricate relationship between auxin signaling and root tropism. Interestingly, a previous investigation reported that increased glucose concentration up-regulated the expression of *ABP1* and *PIN-FORMED 1* (*PIN1*), both of which are involved in auxin signaling and transport, while, in contrast, another auxin receptor, *TRANSPORT-INHIBITOR-RESISTANT1* (*TIR1)*, exhibited reduced expression levels following induction by a higher glucose concentration [156]. These findings suggest that variations in sucrose concentration can potentially affect root curvature by influencing the activities of auxin receptors and transporters. Taken together, this study highlights the negative correlation between sucrose-promoted root growth and root curvature, with higher sucrose concentrations leading to decreased curvature. The intricate interplay between sugar and auxin signaling, involving receptors such as ABP1, PIN1 and TIR1, likely contributes to these observed effects.

3.4.13 ARG1 interacts with ARL1 and HSP70-1

ARG1, a DnaJ-like protein, has been implicated in signal transduction during changes in the gravity vector, along with its paralog ARL2 [123,136]. Previous studies have suggested that the ARG1/ARL2 complex, based on its chaperone-like characteristics, may recruit cytosolic HSC70 to a membrane, and thus act as a membrane-associated pattern for gravitropism signaling [123]. Alternatively, it could recruit HSC70 to modulate actin dynamics in response to gravitropic stimulation. It is also possible that the activity of the ARG1/ARL2 complex is independent of HSC70 and the cytoskeleton. However, the lack of information regarding novel interaction partners for ARG1 has impeded the further understanding of its mechanism in gravitropism signal transduction.

This study identified ARL1 and HSP70-1 as interacting partners of ARG1 and, thus this raises the question of whether ARL1 and HSP70-1 are involved in the same gravitropism signaling

pathway as ARG1. The HSP70 proteins in Arabidopsis exhibit a high degree of functional redundancy, as evidenced by the presence of 14 additional HSP70 proteins in the Arabidopsis genome [135]. In the immunoprecipitation-mass spectrometry (IP-MS) data, this study observed the significant enrichment of five HSP70 proteins. In order to gain further insights, it is essential to investigate the interaction between ARG1 and other HSP70 proteins, including those identified in our IP-MS analysis.

Surprisingly, this study also discovered and verified the interaction between ARL1 and ARG1. While ARL1, as a paralog of ARG1, has been well-characterized, it appears not to be directly involved in gravitropism. Single-gene knockout mutants of *arl1*-1 did not exhibit an agravitropic phenotype, and even higher order mutants combining *arg1-2*/*arl2-1* or triple mutants (*arg1-2*/*arl1-1*/*arl2-1*) did not show an enhanced agravitropic phenotype [37]. Instead, it has been suggested that ARL1 may have roles in other aspects of plant growth and stress responses [37]. Unexpectedly, the BIFC assay conducted in this study using Arabidopsis revealed a nuclear interaction between ARG1-YN/ARL1-YC or ARG1-YC/ARL1-YN. This is intriguing since it is widely accepted that ARG1 is primarily involved in facilitating the translocation of transducer proteins to the plastid or membrane and, thus, plays a role in gravitropism signaling. The nuclear localization observed in this study suggests a new direction for the function of ARG1. It is possible that ARL1 and ARG1 interact within the nucleus to regulate transcription or even degradation processes (e.g., ubiquitin-mediated protein degradation), however, further experiments are required to validate this hypothesis. In addition, another important protein implicated in gravitropism signaling, known as LAZY1, has been found to localize to both the plasma membrane and the nucleus, although its precise function remains unknown [157].

ARG1 has long been recognized as a key player in gravitropism signal transduction and, therefore, its discovery has significantly contributed to our understanding of this intricate mechanism. The recent identification of genetic connections between *ARG1* and components of the TOC complex, particularly *TOC75-III*, *TOC120* and *TOC132*, has provided further support for an intriguing ligand interaction model [39]. According to this model, ARG1, or its paralog ARL2, facilitates the translocation of an unidentified protein to the plasma membrane or endoplasmic reticulum through vesicle trafficking [39]. Simultaneously, TOC132 mediates the import of plastid-associated proteins into plastids where they subsequently localize to the outer membrane. The interaction between the ARG1/ARL2-associated protein and the TOC132-associated protein is proposed to facilitate signal transduction [39]. While this model shows promise, the specific proteins involved in these processes have yet to be identified.

ARG1 has been implicated in various cellular compartments involved in protein trafficking [36]. The IP-MS results have revealed several exciting candidates that might be involved in ARG1-mediated gravitropism signal transduction. Among these candidates (supplement Table 3.3.1), MEMBRANE STEROID BINDING PROTEIN 1 (MSBP1), PHOSPHOLIPASE D DELTA

(PLDDELTA) and PATELLIN 2 (PATL2) have been previously implicated in vesicle trafficking, making them particularly intriguing [127,158,159]. It is feasible that the ARG1/HSP70-1 complex plays a role in facilitating the trafficking of an unknown protein through the vesicle trafficking pathway. Potential candidate proteins that could be involved in this process include MSBP1, PLDDELTA, and PATL2. Further investigation is necessary to validate their involvement and to elucidate the precise mechanisms by which the ARG1/HSP70-1 complex mediates its trafficking.

Furthermore, in this study, the interaction between ARL1 and ARG1 has been successfully verified to occur within the nucleus. However, the specific function of this localization remains unknown. It is speculated that this nuclear localization of the ARL1/ARG1 complex could potentially be involved in processes such as degradation or transcription. Further experiments and investigations are needed to determine the exact role and significance of this interaction within the nucleus and its implications for cellular processes such as protein degradation and gene transcription.

Moreover, there are ongoing efforts focused on confirming the involvement of other potential partners of ARG1, including MSBP1, phospholipase D delta, HSP70-2, HSP70-3, HSP70-4 and cpHSP70-1. By unraveling the interactions and roles of these proteins, this future study aims to gain a comprehensive understanding of ARG1-mediated gravitropism signal transduction and shed light on the molecular mechanisms that underlie this essential plant response.

3.5 Conclusion

3.5.1 Microgravity-induced phosphoproteomics study

The objective of the phosphoproteomics study was to uncover the phosphorylation events and signaling pathways that are modulated in response to microgravity stimulation. In conclusion, this comprehensive phosphoproteomics study has shed light on the intricate phosphorylation changes that occur in response to microgravity stimulation in Arabidopsis. A total of 4,266 phosphosites corresponding to 1,983 phosphoproteins were identified. Gene Ontology (GO) enrichment analysis provided insights into the biological processes affected by microgravity-induced phosphorylation changes. The 3 s microgravity treatment influenced processes such as signal transduction, microtubule cytoskeleton organization and phosphatidylinositol binding. On the other hand, the 22 s microgravity treatment showed enrichments in processes related to cellular responses to hormone stimuli and cellular development.

The study also discovered specific phosphorylation motifs and kinase-substrate relationships that may be involved in gravitropic signaling, such as CK II and CDK. The subsequent kinase-inhibitor assay further supported the involvement of CDK and casein kinase in root gravitropism. To validate the functional significance of the identified phosphoproteins, this study conducted mutant gravitropism assays. Among the selected mutants, *suo-1*, *patl2*, *pck1*, *med26c*, *smo4-2*, naip1, *tpx2*, *toc120*, and *tzf3* exhibited altered bending kinetics compared to the wild type, indicating their involvement in the gravitropic response. Interestingly, mutant *map65-1* did not result in distinguishable curvature kinetics, suggesting the potential redundancy or alternative mechanisms in these cases. These findings provide valuable genetic evidence supporting the functional relevance of the identified phosphoproteins in gravitropism.

Furthermore, this study explored the influence of different platforms on phosphorylation changes. By comparing the phosphoproteomics data from drop towers and parabolic flight platforms, this study observed variations in the number and significance of the detected phosphopeptides. Further comparison analysis revealed the potential impact of hypergravity treatment in the parabolic flight platform. These findings highlight the importance of considering hypergravity phase impact when conducting microgravity studies. In addition, this study uncovered the involvement of TOR signaling in microgravity-induced phosphorylation changes, expanding our understanding of the intricate signaling networks underlying plant gravitropism responses.

3.5.2 GraviPi is a high throughput tropism phenotyping and angle measurement tool

The GraviPi system represents a novel and cost-effective pipeline for phenotyping plant tropisms, with a particular focus on measuring plant gravitropism bending angles. The objective

of the GraviPi project was to develop an automated approach that integrates non-expensive hardware and angle measurement software to streamline the processes of acquiring high-resolution images and accurately measuring bending angles. By implementing color-based filtration and morphological erosion techniques, GraviPi successfully removes unwanted background elements and isolates the Arabidopsis hypocotyl for precise angle measurement. In addition, the GraviPi's expanded capabilities extend beyond Arabidopsis to enable the detection of other tropisms and the measurement of bending angles in different plant species, such as wheat coleoptiles. Thus, the GraviPi system, with its user-friendly GUI and high-throughput capacity, offers researchers a valuable tool for efficiently studying plant tropisms and conducting downstream omics experiments.

3.5.3 ARL1 is a new partner of ARG1

The objective of the third part of this study was to explore new interaction partners of ARG1, a protein of interest. By utilizing immunoprecipitation coupled with mass spectrometry (IP-MS) analysis, novel interaction partners of ARG1 were successfully identified. To validate the interaction between ARG1 and ARL1, *in vivo* co-immunoprecipitation (co-IP) assays and bimolecular fluorescence complementation (BiFC) assays were conducted. These experiments confirmed the physical interaction between ARG1 and ARL1. Furthermore, it was discovered that the interaction between ARG1 and ARL1 occurred within the nucleus of protoplasts, providing insights into the subcellular localization of this interaction. These findings shed light on the molecular mechanisms underlying gravitropism and open up new ways to further investigate the specific functions and interactions of ARG1, ARL1 and HSP70-1 within this signaling pathway.

3.6 Outlook

This thesis has focused on expanding our understanding of Arabidopsis gravitropism by identifying novel proteins and investigating their roles in the signaling pathways. The first objective was accomplished through a comprehensive phosphoproteomics study, which revealed several attractive candidates, including PTAL2 and TPX2. In terms of future work, further verification studies are necessary to confirm the functional impact of phosphorylation on the identified candidates. This can involve generating phosphomimic and phosphodead versions of PATL2 and TPX2 through mutagenesis PCR.

To facilitate the study of plant gravitropism, a custom platform called GraviPi was developed and utilized for gravitropism imaging and measurements. This platform provides a user-friendly interface and offers the potential for high-throughput analysis of multiple samples simultaneously. Future improvements can include the development of a graphical user interface for the GraviPi software, enhancing the user experience and facilitating data analysis.

Moreover, the study successfully identified and verified the interaction between ARL1 and ARG1, indicating that ARL1 may be involved in the same gravitropism response pathway as ARG1. To deepen our understanding of their relationship, it is imperative to investigate the interactions of ARL1 and ARG1 in transgenic Arabidopsis plants. This can be accomplished by co-transforming ARL1 and ARG1 with different fluorescence tags into the double mutants of *arg1-3arl1-1*, allowing for the examination of their localization. In addition, it is important to investigate the interaction of ARG1 with other candidate proteins to gain a comprehensive understanding of its functional network in gravitropism. In conclusion, the future directions of this study encompass the validation of phosphorylation-dependent functional changes, enhancement of the GraviPi platform, and exploration of the interactions between other candidates and ARG1. By pursuing these ways, we can unravel the intricate mechanisms underlying Arabidopsis gravitropism and shed light on the molecular processes governing plant responses to gravity.

4 Acknowledgment

I would like to say many thanks to all those lovely people who have supported me throughout my whole Ph.D. time. This thesis would not have been done without the help of my supervisor, Prof. Dr. Maik Böhmer. I want to thank him for providing such an excellent chance to study in his lab. His lab is a place full of new ideas and innovations. I appreciate all the support, guidance, and feedback of Prof. Dr. Maik Böhmer throughout my research journey at Frankfurt University.

I want to thank the committee members for their precious suggestions on my thesis.

I would like to thank all the plant cell biology lab members in the Biological Science Department at Frankfurt University for providing competitive, collaborative, and supportive surroundings. Especially Dario, Andi, Alexandra, also Dr. Uwe, Dr. Akis, Theresa, Philippe, Nicole, and Dr. Thiru, for providing me with the opportunities to expand my knowledge and skills in genetics and biochemical, as well as bioinformatics studies.

I would like to say thanks to Dr. Oliver Schüler, and Dr. Ella Nukarinen for the development of the hardware for the parabolic flight and drop tower campaign used in this study and Mass Spectrometry sample preparation. I want to thank Volkan Cevik for joining me in preparing and conducting a parabolic flight campaign. In addition, I want to say thanks to Prof. Dr. Stefan Simm for sharing methods for phosphoproteomics data analysis.

I want to thank the China Scholarship Council and the GRADE for funding my study.

I want to thank Maik for providing the rotation stage, Sven for providing the programmable LED, and Freya Arthen for developing the software.

I want to thank Theresa for helping prepare MS samples and Georg Tascher for measuring MS samples. I want to thank Holger Schranz and Susanne Pietsch for providing seeds.

I want to say great thanks to my girlfriend Yang Wang (王阳), for her understanding, love, and support. I also want to say thanks to my family for their support.

5 Supplemental files

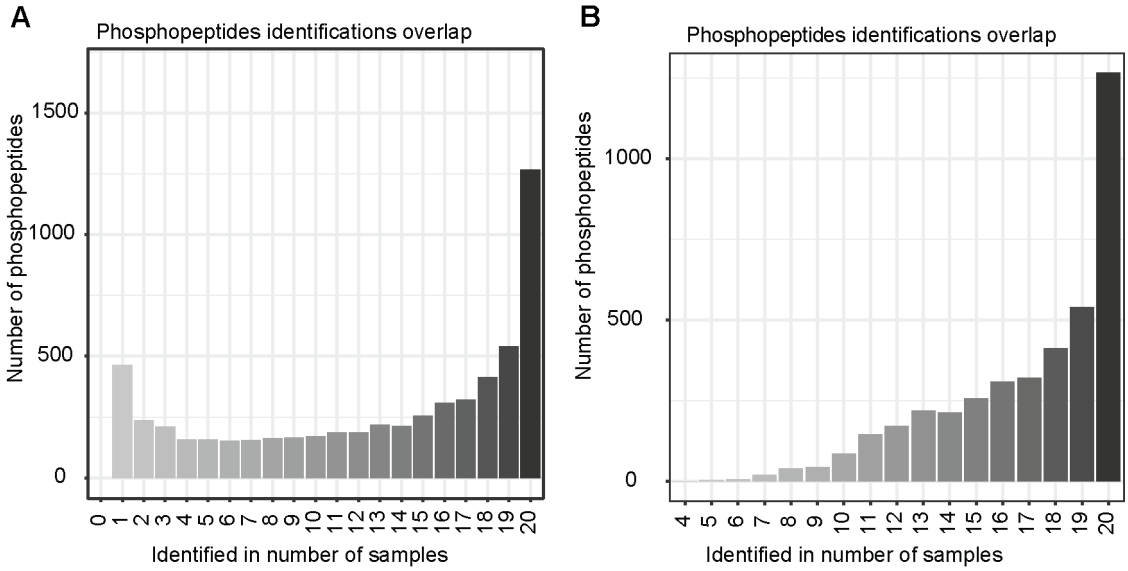

Supplemental Figure 3.1.1 The overlap of phosphopeptides identifications. (A) before filtering. (B) after filtering.

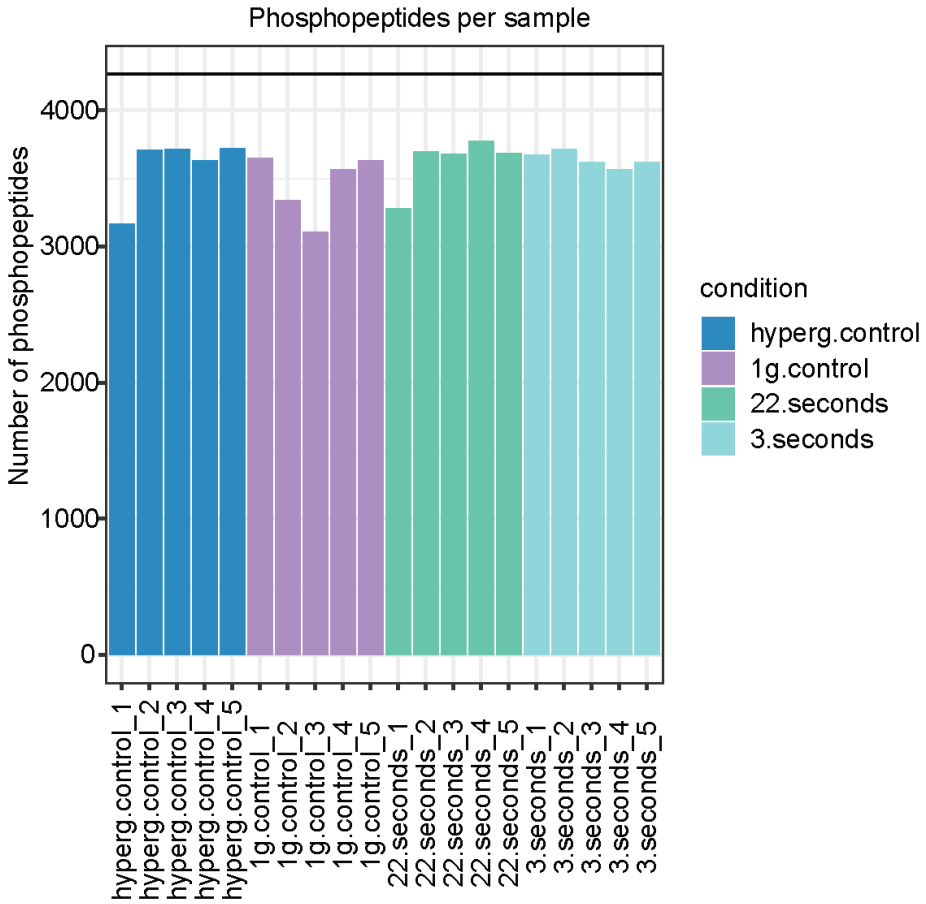

Supplemental Figure 3.1.2 The numbers of identified phosphopeptides per sample.

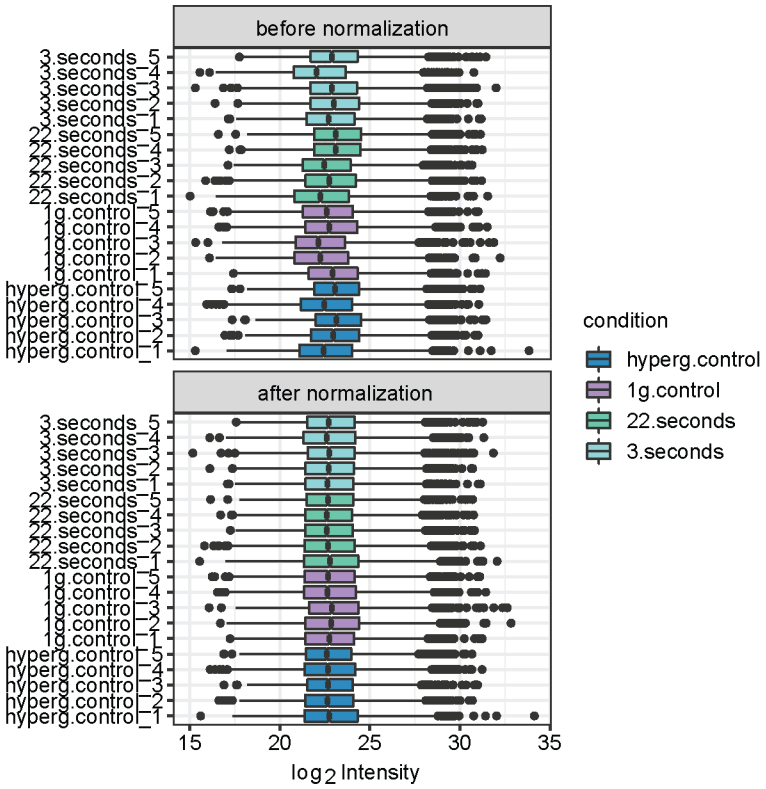

Supplemental Figure 3.1.3 Sample distribution before and after normalization.

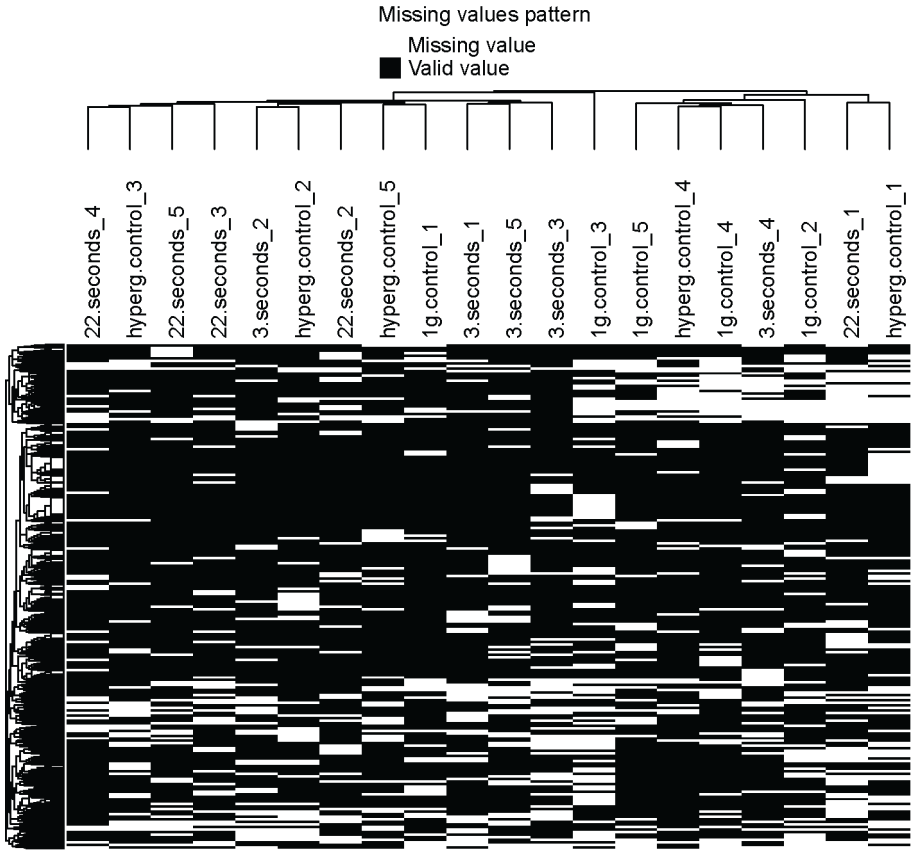

Supplemental Figure 3.1.4 Missing values pattern. Missed values are indicated by white color, while valid values are represented by black color.

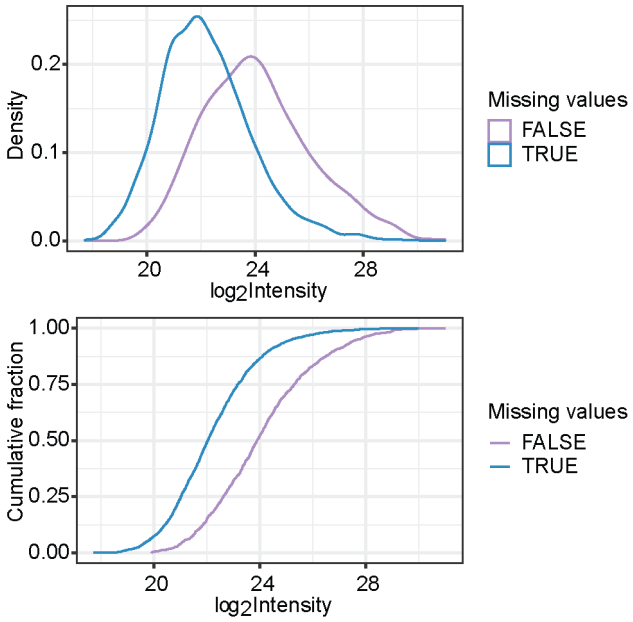

Supplemental Figure 3.1.5 Phosphopeptides density distribution and cumulative fractions. Missing values are indicated by blue (with), or red (without) color.

Supplemental Table 3.2.1 Comparison of often used phenotyping equipment cost.

Equipment	Cost	Reference
Epson Perfection (v370, v600, v700)	~400 €	[77]
Spot RT-slider CCD camera	7000 $	[39]
digital Nikon D7100	1,800 €	[160]
Raspberry Pi high-quality camera	~750 €	This study

Supplemental Table 3.2.2 Parameters used for different species.

Species	Line width	Sigma	Lower _Threshold	Upper_Threshold
Glycine max	20	6.27	0	0.34
Pisum Sativum	20	6.27	0	0.34
Zea Mays	20	6.27	0	0.34
Brassica napus	20	6.27	0	0.34
Solanum Lycopersicum	15	4.83	0.17	0.51
Triticum aestivum	15	4.83	0.17	0.51
Nicotiana benthamiana	10	3.39	0.51	1.19
Arabidopsis thaliana	10	3.39	0.51	1.19

Supplemental Table 3.3.1 The candidate proteins from the IP-MS.

ID	Description	p.adj	Fold change	Coverage
ARG1-YFP	ARG1-YFP	1.47E-14	13.3	77.3
AT1G24120.1	ARG1-LIKE 1	1.47E-14	6.77	42.7
AT1G30380.1	PHOTOSYSTEM I SUBUNIT K	4.33E-05	5.82	14.6
AT1G78630.1	RIBOSOMAL PROTEIN L13 FAMILY PROTEIN	0.00975	5.33	20.7
AT1G18660.3	ZINC FINGER (C3HC4-TYPE RING FINGER) FAMILY PROTEIN	1.47E-14	4.88	12.6
AT3G12580.1	HEAT SHOCK PROTEIN 70	1.74E-09	4.51	36.9
AT2G30930.1	HYPOTHETICAL PROTEIN	5.08E-06	4.47	72
AT3G09440.4	HEAT SHOCK PROTEIN 70 (HSP 70) FAMILY PROTEIN	0.00163	4.14	45.5
AT5G14220.2	FLAVIN CONTAINING AMINE OXIDOREDUCTASE FAMILY	1.56E-09	4.11	13
AT5G16660.2	LOW-DENSITY RECEPTOR-LIKE PROTEIN	6.14E-06	4.1	24.7
AT5G48810.1	CYTOCHROME B5 ISOFORM D	0.00331	4.04	39.3
AT1G06690.1	NAD(P)-LINKED OXIDOREDUCTASE SUPERFAMILY PROTEIN	0.00128	3.97	25.7
AT1G77490.2	THYLAKOIDAL ASCORBATE PEROXIDASE	0.00169	3.81	16.9
AT4G29410.2	RIBOSOMAL L28E PROTEIN FAMILY	0.000265	3.8	25.2
AT1G75500.2	WALLS ARE THIN 1	1.47E-14	3.79	5.4
AT2G30490.1	CINNAMATE-4-HYDROXYLASE	0.000221	3.61	8.1
AT5G52240.1	MEMBRANE STEROID BINDING PROTEIN 1	5.51E-07	3.58	26.8
AT4G33510.1	3-DEOXY-D-ARABINO-HEPTULOSONATE 7-PHOSPHATE SYNTHASE	1.47E-14	3.52	11
AT5G03880.1	THIOREDOXIN FAMILY PROTEIN	0.00387	3.51	23.9
AT4G18430.1	RAB GTPASE HOMOLOG A1E	0.000831	3.42	10.6
AT4G28025.2	HYPOTHETICAL PROTEIN	0.00824	3.35	15.5
AT4G35860.1	GTP-BINDING 2	6.80E-05	3.34	37.9
AT1G22530.2	PATELLIN 2	5.39E-13	3.27	13.7
AT1G79340.1	METACASPASE 4	0.00628	3.13	8.1
AT3G47520.1	MALATE DEHYDROGENASE	0.0244	3.13	23.8
AT5G02490.1	HEAT SHOCK PROTEIN 70 (HSP 70) FAMILY PROTEIN	5.41E-08	3.13	35.8
AT4G03560.1	TWO-PORE CHANNEL 1	0.0029	3.1	3.3
AT4G02080.1	SECRETION-ASSOCIATED RAS SUPER FAMILY 2	0.000942	3.08	15.5
AT1G45201.2	TRIACYLGLYCEROL LIPASE-LIKE 1	0.0124	3.06	13.2
AT4G28510.1	PROHIBITIN 1	0.0142	3.03	12.8
AT2G20890.1	PHOTOSYSTEM II REACTION CENTER PSB29 PROTEIN	0.0174	3.02	17.7
AT1G73110.1	P-LOOP CONTAINING NUCLEOSIDE TRIPHOSPHATE HYDROLASES SUPERFAMILY PROTEIN	0.00106	3.01	35.9
AT4G25080.4	MAGNESIUM-PROTOPORPHYRIN IX METHYLTRANSFERASE	0.0154	3.01	26.9
AT5G58270.1	ABC TRANSPORTER OF THE MITOCHONDRION 3	2.94E-05	3.01	8.2
AT5G08060.1	FURRY	0.0124	2.94	22.1
AT2G17695.1	OUTER ENVELOPE PROTEIN	0.0329	2.93	18.5
AT1G56500.1	HALOACID DEHALOGENASE-LIKE HYDROLASE FAMILY PROTEIN	2.08E-09	2.88	10.3
AT1G22700.3	TETRATRICOPEPTIDE REPEAT (TPR)-LIKE SUPERFAMILY PROTEIN	0.00127	2.86	18.5
AT5G51010.1	RUBREDOXIN-LIKE SUPERFAMILY PROTEIN	0.046	2.84	18.2

AT4G14210.3	PHYTOENE DESATURASE 3	0.00499	2.78	5.7
AT4G35450.3	ANKYRIN REPEAT-CONTAINING PROTEIN 2	0.0251	2.77	20.5
AT1G15980.1	NDH-DEPENDENT CYCLIC ELECTRON FLOW 1	4.73E-06	2.72	4.6
AT1G68830.1	SERINE/THREONINE KINASE DOMAIN PROTEIN	0.0204	2.72	4.4
AT3G23400.4	PLASTID-LIPID ASSOCIATED PROTEIN PAP / FIBRILLIN FAMILY PROTEIN	0.02	2.65	28.1
AT5G13120.2	CYCLOPHILIN 20-2	0.00216	2.65	8.6
AT1G70410.3	BETA CARBONIC ANHYDRASE 4	0.0212	2.62	22.9
AT5G02500.1	HEAT SHOCK COGNATE PROTEIN 70-1	1.97E-05	2.61	49
AT4G23430.3	NAD(P)-BINDING ROSSMANN-FOLD SUPERFAMILY PROTEIN	0.0159	2.55	13.5
AT4G35790.1	PHOSPHOLIPASE D DELTA	0.000399	2.55	5.8
AT1G64770.1	NDH-DEPENDENT CYCLIC ELECTRON FLOW 1	0.015	2.51	10.3
AT2G30390.1	FERROCHELATASE 2	0.0242	2.46	10.5
AT5G20140.1	SOUL HEME-BINDING FAMILY PROTEIN	0.000589	2.38	10.1
AT5G01460.1	LMBR1-LIKE MEMBRANE PROTEIN	0.0185	2.37	5.3
AT3G59780.1	RHODANESE/CELL CYCLE CONTROL PHOSPHATASE SUPERFAMILY PROTEIN	0.0312	2.35	17.5
AT5G67030.1	ZEAXANTHIN EPOXIDASE (ZEP) (ABA1)	0.0238	2.32	6.4
AT4G04020.1	FIBRILLIN	0.0214	2.31	48.1
AT3G44890.1	RIBOSOMAL PROTEIN L9	0.031	2.29	23.9
AT5G42765.1	PLASMA MEMBRANE FUSION PROTEIN	5.32E-08	2.26	22.7
AT4G13010.1	OXIDOREDUCTASE%2C ZINC-BINDING DEHYDROGENASE FAMILY PROTEIN	0.016	2.22	21.9
AT5G16840.3	BINDING PARTNER OF ACD11 1	0.0284	2.22	23
AT1G79010.1	ALPHA-HELICAL FERREDOXIN	0.0292	2.12	27
AT1G25490.1	ARM REPEAT SUPERFAMILY PROTEIN	0.0294	1.98	8.5
AT2G42220.1	RHODANESE/CELL CYCLE CONTROL PHOSPHATASE SUPERFAMILY PROTEIN	2.89E-05	1.93	36.8
AT3G27850.1	RIBOSOMAL PROTEIN L12-C	0.0141	1.85	15
AT1G16880.1	URIDYLYLTRANSFERASE-LIKE PROTEIN	0.000391	1.67	11.7
AT5G19940.2	PLASTID-LIPID ASSOCIATED PROTEIN PAP / FIBRILLIN FAMILY PROTEIN	0.0391	1.6	33.6
AT2G34460.1	NAD(P)-BINDING ROSSMANN-FOLD SUPERFAMILY PROTEIN	0.00371	1.5	10.4
AT5G62670.1	H[+]-ATPASE 11	0.0196	1.45	13.3
AT1G72150.1	PATELLIN 1	0.0362	1.43	27.4
AT3G61260.1	REMORIN FAMILY PROTEIN	0.022	1.39	28.3
AT4G20260.5	PLASMA-MEMBRANE ASSOCIATED CATION-BINDING PROTEIN 1	0.0312	1.35	59.9
AT1G74470.1	PYRIDINE NUCLEOTIDE-DISULFIDE OXIDOREDUCTASE FAMILY PROTEIN	0.0171	1.29	42.8
AT5G14105.1	HYPOTHETICAL PROTEIN	0.0473	1.25	17.1
AT1G20020.1	FERREDOXIN-NADP[+]-OXIDOREDUCTASE 2	0.04	1.2	17.9
AT1G44575.1	CHLOROPHYLL A-B BINDING FAMILY PROTEIN	0.0377	1.18	27.5
AT5G40770.1	PROHIBITIN 3	0.0207	1.08	46.9
AT3G18890.1	NAD(P)-BINDING ROSSMANN-FOLD SUPERFAMILY PROTEIN	0.0456	1.05	23.1
AT4G01050.1	THYLAKOID RHODANESE-LIKE PROTEIN	0.0114	1	22.1
ATCG00710.1	PHOTOSYSTEM II REACTION CENTER PROTEIN H	0.0281	0.998	34.2

AT4G24280.1	CHLOROPLAST HEAT SHOCK PROTEIN 70-1	0.0229	0.947	30.9
AT5G64040.1	PHOTOSYSTEM I REACTION CENTER SUBUNIT PSI-N%2C CHLOROPLAST%2C PUTATIVE / PSI-N%2C PUTATIVE (PSAN)	0.0491	0.934	26.9
ATCG00280.1	PHOTOSYSTEM II REACTION CENTER PROTEIN C	0.0255	0.879	26
AT2G28900.1	OUTER PLASTID ENVELOPE PROTEIN 16-1	0.0283	0.836	26.4
ATCG00680.1	PHOTOSYSTEM II REACTION CENTER PROTEIN B	0.0296	0.823	42.5

6 References

[1] S.-H. Su, N.M. Gibbs, A.L. Jancewicz, P.H. Masson, Molecular Mechanisms of Root Gravitropism, Curr Biol. 27 (2017) 964–972. https://doi.org/10.1016/j.cub.2017.07.015.

[2] T.A. Knight, XXI. On the direction of the radicle and germen during the vegetation of seeds. In a Letter to the Right Hon. Sir J oseph B anks , K.B. P.R.S, The Philosophical Magazine. 25 (1806) 122–130. https://doi.org/10.1080/14786440608563422.

[3] R. Chen, E. Rosen, P.H. Masson, Gravitropism in Higher Plants, Plant Physiology. 120 (1999) 343–350. https://doi.org/10.1104/pp.120.2.343.

[4] G.K. Kirschner, S. Rosignoli, L. Guo, I. Vardanega, J. Imani, J. Altmüller, S.G. Milner, R. Balzano, K.A. Nagel, D. Pflugfelder, C. Forestan, R. Bovina, R. Koller, T.G. Stöcker, M. Mascher, J. Simmonds, C. Uauy, H. Schoof, R. Tuberosa, S. Salvi, F. Hochholdinger, ENHANCED GRAVITROPISM 2 encodes a STERILE ALPHA MOTIF-containing protein that controls root growth angle in barley and wheat, Proc Natl Acad Sci U S A. 118 (2021). https://doi.org/10.1073/pnas.2101526118.

[5] O. Monje, G.W. Stutte, G.D. Goins, D.M. Porterfield, G.E. Bingham, Farming in space: Environmental and biophysical concerns, Advances in Space Research. 31 (2003) 151–167. https://doi.org/10.1016/S0273-1177(02)00751-2.

[6] G. Haberlandt, Über die Perception des geotropischen Reizes, Borntraeger, 1900.

[7] M.T. Morita, M. Tasaka, Gravity sensing and signaling, Curr Opin Plant Biol. 7 (2004) 712–8. https://doi.org/10.1016/j.pbi.2004.09.001.

[8] E.B. Blancaflor, J.M. Fasano, S. Gilroy, Mapping the functional roles of cap cells in the response of Arabidopsis primary roots to gravity, Plant Physiol. 116 (1998) 213–22. https://doi.org/10.1104/pp.116.1.213.

[9] T. Caspar, B.G. Pickard, Gravitropism in a starchless mutant of Arabidopsis : Implications for the starch-statolith theory of gravity sensing, Planta. 177 (1989) 185–197. https://doi.org/10.1007/BF00392807.

[10] S. Vitha, M. Yang, F.D. Sack, J.Z. Kiss, Gravitropism in the starch excess mutant of Arabidopsis thaliana, Am J Bot. 94 (2007) 590–598. https://doi.org/10.3732/ajb.94.4.590.

[11] C. Limbach, J. Hauslage, C. Schäfer, M. Braun, How to activate a plant gravireceptor. Early mechanisms of gravity sensing studied in characean rhizoids during parabolic flights, Plant Physiol. 139 (2005) 1030–40. https://doi.org/10.1104/pp.105.068106.

[12] C. Schimek, P. Eibel, T. Horie, P. Galland, T. Ootaki, Protein crystals in Phycomyces sporangiophores are involved in graviperception, Adv Space Res. 24 (1999) 687–96. https://doi.org/10.1016/s0273-1177(99)00400-7.

[13] Y. Zhang, G. Xiao, X. Wang, X. Zhang, J. Friml, Evolution of fast root gravitropism in seed plants, Nat Commun. 10 (2019) 3480. https://doi.org/10.1038/s41467-019-11471-8.

[14] H.Q. Zheng, L.A. Staehelin, Nodal Endoplasmic Reticulum, a Specialized Form of

Endoplasmic Reticulum Found in Gravity-Sensing Root Tip Columella Cells, Plant Physiology. 125 (2001) 252–265. https://doi.org/10.1104/pp.125.1.252.

[15] C. Plieth, A.J. Trewavas, Reorientation of Seedlings in the Earth's Gravitational Field Induces Cytosolic Calcium Transients, Plant Physiology. 129 (2002) 786–796. https://doi.org/10.1104/pp.011007.

[16] H. Tatsumi, M. Toyota, T. Furuichi, M. Sokabe, Calcium mobilizations in response to changes in the gravity vector in *Arabidopsis* seedlings: Possible cellular mechanisms, Plant Signaling & Behavior. 9 (2014) e29099. https://doi.org/10.4161/psb.29099.

[17] M. Toyota, T. Furuichi, H. Tatsumi, M. Sokabe, Critical consideration on the relationship between auxin transport and calcium transients in gravity perception of Arabidopsis seedlings, Plant Signaling & Behavior. 3 (2008) 521–524. https://doi.org/10.4161/psb.3.8.6339.

[18] S. Daye, R.L. Biro, S.J. Roux, Inhibition of gravitropism in oat coleoptiles by the calcium chelator, ethyleneglycol-bis-(beta-aminoethyl ether)-N,N'-tetraacetic acid, Physiol Plant. 61 (1984) 449–54. https://doi.org/10.1111/j.1399-3054.1984.tb06354.x.

[19] D.C. Urbina, H. Silva, L.A. Meisel, The Ca2+ pump inhibitor, thapsigargin, inhibits root gravitropism in Arabidopsis thaliana, Biol Res. 39 (2006) 289–96. https://doi.org/10.4067/s0716-97602006000200011.

[20] N.F. Keinath, R. Waadt, R. Brugman, J.I. Schroeder, G. Grossmann, K. Schumacher, M. Krebs, Live Cell Imaging with R-GECO1 Sheds Light on flg22- and Chitin-Induced Transient [Ca 2+] cyt Patterns in Arabidopsis, Molecular Plant. 8 (2015) 1188–1200. https://doi.org/10.1016/j.molp.2015.05.006.

[21] R. Zhao, Z. Liu, Z. Li, S. Xu, X. Sheng, Gravity induces asymmetric Ca2+ spikes in the root cap in the early stage of gravitropism, Plant Signal Behav. 17 (2022) 2025325. https://doi.org/10.1080/15592324.2021.2025325.

[22] I.Y. Perera, I. Heilmann, S.C. Chang, W.F. Boss, P.B. Kaufman, A role for inositol 1,4,5-trisphosphate in gravitropic signaling and the retention of cold-perceived gravistimulation of oat shoot pulvini, Plant Physiol. 125 (2001) 1499–507. https://doi.org/10.1104/pp.125.3.1499.

[23] I.Y. Perera, C.-Y. Hung, S. Brady, G.K. Muday, W.F. Boss, A universal role for inositol 1,4,5-trisphosphate-mediated signaling in plant gravitropism, Plant Physiol. 140 (2006) 746–60. https://doi.org/10.1104/pp.105.075119.

[24] I.Y. Perera, I. Heilmann, W.F. Boss, Transient and sustained increases in inositol 1,4,5-trisphosphate precede the differential growth response in gravistimulated maize pulvini, Proc Natl Acad Sci U S A. 96 (1999) 5838–43. https://doi.org/10.1073/pnas.96.10.5838.

[25] U. Ali, S. Lu, T. Fadlalla, S. Iqbal, H. Yue, B. Yang, Y. Hong, X. Wang, L. Guo, The functions of phospholipases and their hydrolysis products in plant growth, development

and stress responses, Progress in Lipid Research. 86 (2022) 101158. https://doi.org/10.1016/j.plipres.2022.101158.

[26] R.-H. Tang, S. Han, H. Zheng, C.W. Cook, C.S. Choi, T.E. Woerner, R.B. Jackson, Z.-M. Pei, Coupling Diurnal Cytosolic Ca^{2+} Oscillations to the CAS-IP_3 Pathway in *Arabidopsis*, Science. 315 (2007) 1423–1426. https://doi.org/10.1126/science.1134457.

[27] H. Lee, A. Ganguly, S. Baik, H.-T. Cho, Calcium-dependent protein kinase 29 modulates PIN-FORMED polarity and *Arabidopsis* development via its own phosphorylation code, The Plant Cell. 33 (2021) 3513–3531. https://doi.org/10.1093/plcell/koab207.

[28] X. Tan, L.I.A. Calderon-Villalobos, M. Sharon, C. Zheng, C.V. Robinson, M. Estelle, N. Zheng, Mechanism of auxin perception by the TIR1 ubiquitin ligase, Nature. 446 (2007) 640–645. https://doi.org/10.1038/nature05731.

[29] N. Dharmasiri, S. Dharmasiri, M. Estelle, The F-box protein TIR1 is an auxin receptor, Nature. 435 (2005) 441–445. https://doi.org/10.1038/nature03543.

[30] J.C. Sedbrook, R. Chen, P.H. Masson, ARG1 (altered response to gravity) encodes a DnaJ-like protein that potentially interacts with the cytoskeleton, Proc Natl Acad Sci U S A. 96 (1999) 1140–5. https://doi.org/10.1073/pnas.96.3.1140.

[31] J.C. Sedbrook, R. Chen, P.H. Masson, ARG1 (altered response to gravity) encodes a DnaJ-like protein that potentially interacts with the cytoskeleton, Proc Natl Acad Sci U S A. 96 (1999) 1140–1145. https://doi.org/10.1073/pnas.96.3.1140.

[32] R. Rosenzweig, N.B. Nillegoda, M.P. Mayer, B. Bukau, The Hsp70 chaperone network, Nat Rev Mol Cell Biol. 20 (2019) 665–680. https://doi.org/10.1038/s41580-019-0133-3.

[33] D. Menzel, Chasing Coiled Coils: Intermediate Filaments in Plants, Botanica Acta. 106 (1993) 294–300. https://doi.org/10.1111/j.1438-8677.1993.tb00751.x.

[34] F. Baluška, K.H. Hasenstein, Root cytoskeleton: its role in perception of and response to gravity, Planta. 203 (1997) 69–78. https://doi.org/10.1007/PL00008117.

[35] J.-J. Zou, Z.-Y. Zheng, S. Xue, H.-H. Li, Y.-R. Wang, J. Le, The role of Arabidopsis Actin-Related Protein 3 in amyloplast sedimentation and polar auxin transport in root gravitropism, Journal of Experimental Botany. 67 (2016) 5325–5337. https://doi.org/10.1093/jxb/erw294.

[36] K. Boonsirichai, J.C. Sedbrook, R. Chen, S. Gilroy, P.H. Masson, ALTERED RESPONSE TO GRAVITY is a peripheral membrane protein that modulates gravity-induced cytoplasmic alkalinization and lateral auxin transport in plant statocytes, Plant Cell. 15 (2003) 2612–25. https://doi.org/10.1105/tpc.015560.

[37] C. Guan, E.S. Rosen, K. Boonsirichai, K.L. Poff, P.H. Masson, The ARG1-LIKE2 gene of Arabidopsis functions in a gravity signal transduction pathway that is genetically distinct from the PGM pathway, Plant Physiol. 133 (2003) 100–12. https://doi.org/10.1104/pp.103.023358.

[38] B. Harrison, P.H. Masson, ARG1 and ARL2 form an actin-based gravity-signaling chaperone complex in root statocytes?, Plant Signal Behav. 3 (2008) 650–3. https://doi.org/10.4161/psb.3.9.5749.

[39] J.P. Stanga, K. Boonsirichai, J.C. Sedbrook, M.S. Otegui, P.H. Masson, A role for the TOC complex in Arabidopsis root gravitropism, Plant Physiol. 149 (2009) 1896–905. https://doi.org/10.1104/pp.109.135301.

[40] J. Soll, E. Schleiff, Protein import into chloroplasts, Nat Rev Mol Cell Biol. 5 (2004) 198–208. https://doi.org/10.1038/nrm1333.

[41] S. Kubis, R. Patel, J. Combe, J. Bédard, S. Kovacheva, K. Lilley, A. Biehl, D. Leister, G. Ríos, C. Koncz, P. Jarvis, Functional specialization amongst the Arabidopsis Toc159 family of chloroplast protein import receptors, Plant Cell. 16 (2004) 2059–77. https://doi.org/10.1105/tpc.104.023309.

[42] J. Bauer, K. Chen, A. Hiltbunner, E. Wehrli, M. Eugster, D. Schnell, F. Kessler, The major protein import receptor of plastids is essential for chloroplast biogenesis, Nature. 403 (2000) 203–7. https://doi.org/10.1038/35003214.

[43] A.K. Strohm, G.A. Barrett-Wilt, P.H. Masson, A functional TOC complex contributes to gravity signal transduction in Arabidopsis, Front Plant Sci. 5 (2014) 148. https://doi.org/10.3389/fpls.2014.00148.

[44] P. Žádníková, D. Smet, Q. Zhu, D. van der Straeten, E. Benková, Strategies of seedlings to overcome their sessile nature: auxin in mobility control, Front Plant Sci. 6 (2015) 218. https://doi.org/10.3389/fpls.2015.00218.

[45] A. Müller, C. Guan, L. Gälweiler, P. Tänzler, P. Huijser, A. Marchant, G. Parry, M. Bennett, E. Wisman, K. Palme, AtPIN2 defines a locus of Arabidopsis for root gravitropism control, EMBO J. 17 (1998) 6903–11. https://doi.org/10.1093/emboj/17.23.6903.

[46] J. Friml, J. Wiśniewska, E. Benková, K. Mendgen, K. Palme, Lateral relocation of auxin efflux regulator PIN3 mediates tropism in Arabidopsis, Nature. 415 (2002) 806–9. https://doi.org/10.1038/415806a.

[47] M. Ruiz Rosquete, S. Waidmann, J. Kleine-Vehn, PIN7 Auxin Carrier Has a Preferential Role in Terminating Radial Root Expansion in Arabidopsis thaliana, Int J Mol Sci. 19 (2018) 1238. https://doi.org/10.3390/ijms19041238.

[48] J. Friml, E. Benková, I. Blilou, J. Wisniewska, T. Hamann, K. Ljung, S. Woody, G. Sandberg, B. Scheres, G. Jürgens, K. Palme, AtPIN4 mediates sink-driven auxin gradients and root patterning in Arabidopsis, Cell. 108 (2002) 661–73. https://doi.org/10.1016/S0092-8674(02)00656-6.

[49] M.J. Bennett, A. Marchant, H.G. Green, S.T. May, S.P. Ward, P.A. Millner, A.R. Walker, B. Schulz, K.A. Feldmann, Arabidopsis AUX1 gene: a permease-like regulator of root gravitropism, Science. 273 (1996) 948–50. https://doi.org/10.1126/science.273.5277.948.

[50] N. Geldner, J. Friml, Y.D. Stierhof, G. Jürgens, K. Palme, Auxin transport inhibitors block PIN1 cycling and vesicle trafficking, Nature. 413 (2001) 425–8. https://doi.org/10.1038/35096571.

[51] H. Rakusová, J. Gallego-Bartolomé, M. Vanstraelen, H.S. Robert, D. Alabadí, M.A. Blázquez, E. Benková, J. Friml, Polarization of PIN3-dependent auxin transport for hypocotyl gravitropic response in Arabidopsis thaliana, Plant J. 67 (2011) 817–26. https://doi.org/10.1111/j.1365-313X.2011.04636.x.

[52] R. Chen, P.H. Masson, Auxin Transport and Recycling of PIN Proteins in Plants, in: J. Šamaj, F. Baluška, D. Menzel (Eds.), Plant Endocytosis, Springer-Verlag, Berlin/Heidelberg, 2005: pp. 139–157. https://doi.org/10.1007/7089_009.

[53] Arabidopsis TOL Proteins Act as Gatekeepers for Vacuolar Sorting of PIN2 Plasma Membrane Protein, Current Biology. 23 (2013) 2500–2505. https://doi.org/10.1016/j.cub.2013.10.036.

[54] P. Grones, M. Abas, J. Hajný, A. Jones, S. Waidmann, J. Kleine-Vehn, J. Friml, PID/WAG-mediated phosphorylation of the Arabidopsis PIN3 auxin transporter mediates polarity switches during gravitropism, Sci Rep. 8 (2018) 10279. https://doi.org/10.1038/s41598-018-28188-1.

[55] M. Michniewicz, M.K. Zago, L. Abas, D. Weijers, A. Schweighofer, I. Meskiene, M.G. Heisler, C. Ohno, J. Zhang, F. Huang, R. Schwab, D. Weigel, E.M. Meyerowitz, C. Luschnig, R. Offringa, J. Friml, Antagonistic regulation of PIN phosphorylation by PP2A and PINOID directs auxin flux, Cell. 130 (2007) 1044–56. https://doi.org/10.1016/j.cell.2007.07.033.

[56] H.-W. Zhou, C. Nussbaumer, Y. Chao, A. Delong, Disparate roles for the regulatory A subunit isoforms in Arabidopsis protein phosphatase 2A, Plant Cell. 16 (2004) 709–22. https://doi.org/10.1105/tpc.018994.

[57] L. Bögre, Growth signalling pathways in Arabidopsis and the AGC protein kinases, Trends in Plant Science. 8 (2003) 424–431. https://doi.org/10.1016/S1360-1385(03)00188-2.

[58] Y. Xiao, R. Offringa, PDK1 regulates auxin transport and Arabidopsis vascular development through AGC1 kinase PAX, Nat Plants. 6 (2020) 544–555. https://doi.org/10.1038/s41477-020-0650-2.

[59] S. Tan, X. Zhang, W. Kong, X.-L. Yang, G. Molnár, Z. Vondráková, R. Filepová, J. Petrášek, J. Friml, H.-W. Xue, The lipid code-dependent phosphoswitch PDK1-D6PK activates PIN-mediated auxin efflux in Arabidopsis, Nat Plants. 6 (2020) 556–569. https://doi.org/10.1038/s41477-020-0648-9.

[60] M.M. Marquès-Bueno, L. Armengot, L.C. Noack, J. Bareille, L. Rodriguez, M.P. Platre, V. Bayle, M. Liu, D. Opdenacker, S. Vanneste, B.K. Möller, Z.L. Nimchuk, T. Beeckman, A.I. Caño-Delgado, J. Friml, Y. Jaillais, Auxin-Regulated Reversible Inhibition of TMK1

Signaling by MAKR2 Modulates the Dynamics of Root Gravitropism, Curr Biol. 31 (2021) 228–23710. https://doi.org/10.1016/j.cub.2020.10.011.

[61] M.M. Moloney, M.C. Elliott, R.E. Cleland, Acid growth effects in maize roots: Evidence for a link between auxin-economy and proton extrusion in the control of root growth, Planta. 152 (1981) 285–291. https://doi.org/10.1007/BF00388251.

[62] W. Lin, X. Zhou, W. Tang, K. Takahashi, X. Pan, J. Dai, H. Ren, X. Zhu, S. Pan, H. Zheng, W.M. Gray, T. Xu, T. Kinoshita, Z. Yang, TMK-based cell-surface auxin signalling activates cell-wall acidification, Nature. 599 (2021) 278–282. https://doi.org/10.1038/s41586-021-03976-4.

[63] O. Son, S. Kim, D. Kim, Y.-S. Hur, J. Kim, C.-I. Cheon, Involvement of TOR signaling motif in the regulation of plant autophagy, Biochemical and Biophysical Research Communications. 501 (2018) 643–647. https://doi.org/10.1016/j.bbrc.2018.05.027.

[64] M. Schepetilnikov, L.A. Ryabova, Recent Discoveries on the Role of TOR (Target of Rapamycin) Signaling in Translation in Plants, Plant Physiol. 176 (2018) 1095–1105. https://doi.org/10.1104/pp.17.01243.

[65] M. Schepetilnikov, M. Dimitrova, E. Mancera-Martínez, A. Geldreich, M. Keller, L.A. Ryabova, TOR and S6K1 promote translation reinitiation of uORF-containing mRNAs via phosphorylation of eIF3h, EMBO J. 32 (2013) 1087–102. https://doi.org/10.1038/emboj.2013.61.

[66] H. Zhang, L. Guo, Y. Li, D. Zhao, L. Liu, W. Chang, K. Zhang, Y. Zheng, J. Hou, C. Fu, Y. Zhang, B. Zhang, Y. Ma, Y. Niu, K. Zhang, J. Xing, S. Cui, F. Wang, K. Tan, S. Zheng, W. Tang, J. Dong, X. Liu, TOP1α fine-tunes TOR-PLT2 to maintain root tip homeostasis in response to sugars, Nat. Plants. 8 (2022) 792–801. https://doi.org/10.1038/s41477-022-01179-x.

[67] J. Lynch, Root Architecture and Plant Productivity, Plant Physiol. 109 (1995) 7–13. https://doi.org/10.1104/pp.109.1.7.

[68] R. Bastien, O. Guayasamin, S. Douady, B. Moulia, Coupled ultradian growth and curvature oscillations during gravitropic movement in disturbed wheat coleoptiles, PLoS ONE. 13 (2018) e0194893. https://doi.org/10.1371/journal.pone.0194893.

[69] V. Lube, M.A. Noyan, A. Przybysz, K. Salama, I. Blilou, MultipleXLab: A high-throughput portable live-imaging root phenotyping platform using deep learning and computer vision, Plant Methods. 18 (2022) 38. https://doi.org/10.1186/s13007-022-00864-4.

[70] J. Silva-Navas, M.A. Moreno-Risueno, C. Manzano, M. Pallero-Baena, S. Navarro-Neila, B. Téllez-Robledo, J.M. Garcia-Mina, R. Baigorri, F.J. Gallego, J.C. Del Pozo, D-Root: a system for cultivating plants with the roots in darkness or under different light conditions, Plant J. 84 (2015) 244–55. https://doi.org/10.1111/tpj.12998.

[71] M. Furutani, Y. Hirano, T. Nishimura, M. Nakamura, M. Taniguchi, K. Suzuki, R. Oshida,

C. Kondo, S. Sun, K. Kato, Y. Fukao, T. Hakoshima, M.T. Morita, Polar recruitment of RLD by LAZY1-like protein during gravity signaling in root branch angle control, Nat Commun. 11 (2020) 76. https://doi.org/10.1038/s41467-019-13729-7.

[72] P. Sukumar, K.S. Edwards, A. Rahman, A. Delong, G.K. Muday, PINOID kinase regulates root gravitropism through modulation of PIN2-dependent basipetal auxin transport in Arabidopsis, Plant Physiol. 150 (2009) 722–735. https://doi.org/10.1104/pp.108.131607.

[73] J. Chang, X. Li, W. Fu, J. Wang, Y. Yong, H. Shi, Z. Ding, H. Kui, X. Gou, K. He, J. Li, Asymmetric distribution of cytokinins determines root hydrotropism in Arabidopsis thaliana, Cell Res. 29 (2019) 984–993. https://doi.org/10.1038/s41422-019-0239-3.

[74] A. Naeem, A.P. French, D.M. Wells, T.P. Pridmore, High-throughput feature counting and measurement of roots, Bioinformatics. 27 (2011) 1337–8. https://doi.org/10.1093/bioinformatics/btr126.

[75] R. Slovak, C. Göschl, X. Su, K. Shimotani, T. Shiina, W. Busch, A Scalable Open-Source Pipeline for Large-Scale Root Phenotyping of Arabidopsis, Plant Cell. 26 (2014) 2390–2403. https://doi.org/10.1105/tpc.114.124032.

[76] P. Basu, A. Pal, J.P. Lynch, K.M. Brown, A novel image-analysis technique for kinematic study of growth and curvature, Plant Physiol. 145 (2007) 305–16. https://doi.org/10.1104/pp.107.103226.

[77] N.B.C. Serre, M. Fendrych, ACORBA: Automated workflow to measure Arabidopsis thaliana root tip angle dynamics, Quant Plant Bio. 3 (2022). https://doi.org/10.1017/qpb.2022.4.

[78] K. Okada, Y. Shimura, Mutational Analysis of Root Gravitropism and Phototropism of <I>Arabidopsis thaliana</I> Seedlings, Functional Plant Biology. 19 (1992) 439–448. https://doi.org/10.1071/PP9920439.

[79] C.-P. Witte, L.D. Noël, J. Gielbert, J.E. Parker, T. Romeis, Rapid one-step protein purification from plant material using the eight-amino acid StrepII epitope, Plant Mol Biol. 55 (2004) 135–47. https://doi.org/10.1007/s11103-004-0501-y.

[80] T. Nakagawa, T. Suzuki, S. Murata, S. Nakamura, T. Hino, K. Maeo, R. Tabata, T. Kawai, K. Tanaka, Y. Niwa, Y. Watanabe, K. Nakamura, T. Kimura, S. Ishiguro, Improved Gateway binary vectors: high-performance vectors for creation of fusion constructs in transgenic analysis of plants, Biosci Biotechnol Biochem. 71 (2007) 2095–100. https://doi.org/10.1271/bbb.70216.

[81] C. Wang, H. Hu, X. Qin, B. Zeise, D. Xu, W.-J. Rappel, W.F. Boron, J.I. Schroeder, Reconstitution of CO_2 Regulation of SLAC1 Anion Channel and Function of CO_2-Permeable PIP2;1 Aquaporin as CARBONIC ANHYDRASE4 Interactor, Plant Cell. 28 (2016) 568–582. https://doi.org/10.1105/tpc.15.00637.

[82] J. Sambrook, D.W. Russell, J. Sambrook, The condensed protocols from Molecular

cloning: a laboratory manual, Cold Spring Harbor Laboratory Press, Cold Spring Harbor, N.Y, 2006.

[83] D. Weigel, J. Glazebrook, Transformation of agrobacterium using electroporation, CSH Protoc. 2006 (2006). https://doi.org/10.1101/pdb.prot4665.

[84] H. Schägger, Tricine–SDS-PAGE, Nat Protoc. 1 (2006) 16–22. https://doi.org/10.1038/nprot.2006.4.

[85] R. Di Mambro, S. Sabatini, Developmental Analysis of Arabidopsis Root Meristem, Methods Mol Biol. 1761 (2018) 33–45. https://doi.org/10.1007/978-1-4939-7747-5_3.

[86] J. Hauslage, M. Görög, L. Krause, O. Schüler, M. Schäfer, A. Witten, L. Kesseler, M. Böhmer, R. Hemmersbach, ARABIDOMICS-A new experimental platform for molecular analyses of plants in drop towers, on parabolic flights, and sounding rockets, Rev Sci Instrum. 91 (2020) 034504. https://doi.org/10.1063/1.5120573.

[87] O. Schüler, A Molecular Characterization of the Response of Arabidopsis thaliana to a Simulated Microgravity Stimulus Using a Newly Constructed Hardware for Ground-Based Facilities, (2017).

[88] J. Cox, M. Mann, MaxQuant enables high peptide identification rates, individualized p.p.b.-range mass accuracies and proteome-wide protein quantification, Nat Biotechnol. 26 (2008) 1367–1372. https://doi.org/10.1038/nbt.1511.

[89] S. Tyanova, T. Temu, J. Cox, The MaxQuant computational platform for mass spectrometry-based shotgun proteomics, Nat Protoc. 11 (2016) 2301–2319. https://doi.org/10.1038/nprot.2016.136.

[90] L. Goeminne, Statistical methods for differential proteomics at peptide and protein level, (2019).

[91] T. Välikangas, T. Suomi, L.L. Elo, A systematic evaluation of normalization methods in quantitative label-free proteomics, Brief Bioinform. 19 (2018) 1–11. https://doi.org/10.1093/bib/bbw095.

[92] D.A. Stead, N.W. Paton, P. Missier, S.M. Embury, C. Hedeler, B. Jin, A.J.P. Brown, A. Preece, Information quality in proteomics, Brief Bioinform. 9 (2008) 174–88. https://doi.org/10.1093/bib/bbn004.

[93] C. Lazar, L. Gatto, M. Ferro, C. Bruley, T. Burger, Accounting for the Multiple Natures of Missing Values in Label-Free Quantitative Proteomics Data Sets to Compare Imputation Strategies, J Proteome Res. 15 (2016) 1116–25. https://doi.org/10.1021/acs.jproteome.5b00981.

[94] H. Wickham, ggplot2: Elegant Graphics for Data Analysis, 2nd ed. 2016, Springer International Publishing : Imprint: Springer, Cham, 2016. https://doi.org/10.1007/978-3-319-24277-4.

[95] K. Slowikowski, A. Schep, S. Hughes, S. Lukauskas, J.-O. Irisson, Z.N. Kamvar, T. Ryan,

D. Christophe, Y. Hiroaki, P. Gramme, Package ggrepel, Automatically Position Non-Overlapping Text Labels with 'ggplot2. (2018).

[96] H. Chen, P.C. Boutros, VennDiagram: a package for the generation of highly-customizable Venn and Euler diagrams in R, BMC Bioinformatics. 12 (2011) 35. https://doi.org/10.1186/1471-2105-12-35.

[97] M. Wu, L. Gu, TCseq: Time course sequencing data analysis. R package version 1.12. 0, (2020).

[98] B.T. Sherman, M. Hao, J. Qiu, X. Jiao, M.W. Baseler, H.C. Lane, T. Imamichi, W. Chang, DAVID: a web server for functional enrichment analysis and functional annotation of gene lists (2021 update), Nucleic Acids Res. 50 (2022) 216–21. https://doi.org/10.1093/nar/gkac194.

[99] W. Da Huang, B.T. Sherman, R.A. Lempicki, Systematic and integrative analysis of large gene lists using DAVID bioinformatics resources, Nat Protoc. 4 (2009) 44–57. https://doi.org/10.1038/nprot.2008.211.

[100] D. Schwartz, S.P. Gygi, An iterative statistical approach to the identification of protein phosphorylation motifs from large-scale data sets, Nat Biotechnol. 23 (2005) 1391–1398. https://doi.org/10.1038/nbt1146.

[101] R. Antoni, D. Dietrich, M.J. Bennett, P.L. Rodriguez, Hydrotropism: Analysis of the Root Response to a Moisture Gradient, Methods Mol Biol. 1398 (2016) 3–9. https://doi.org/10.1007/978-1-4939-3356-3_1.

[102] M. Schöller, E. Sarkel, J. Kleine-Vehn, E. Feraru, Growth Rate Normalization Method to Assess Gravitropic Root Growth, in: Root Development, Humana Press, New York, NY, 2018: pp. 199–208. https://doi.org/10.1007/978-1-4939-7747-5_15.

[103] C. Koncz, J. Schell, The promoter of TL-DNA gene 5 controls the tissue-specific expression of chimaeric genes carried by a novel type of Agrobacterium binary vector, Molec Gen Genet. 204 (1986) 383–396. https://doi.org/10.1007/BF00331014.

[104] S.J. Clough, A.F. Bent, Floral dip: a simplified method for Agrobacterium-mediated transformation of Arabidopsis thaliana, Plant J. 16 (1998) 735–43. https://doi.org/10.1046/j.1365-313x.1998.00343.x.

[105] X. Zhang, A.H. Smits, G.B.A. van Tilburg, H. Ovaa, W. Huber, M. Vermeulen, Proteome-wide identification of ubiquitin interactions using UbIA-MS, Nat Protoc. 13 (2018) 530–550. https://doi.org/10.1038/nprot.2017.147.

[106] R.P. Hellens, A.C. Allan, E.N. Friel, K. Bolitho, K. Grafton, M.D. Templeton, S. Karunairetnam, A.P. Gleave, W.A. Laing, Transient expression vectors for functional genomics, quantification of promoter activity and RNA silencing in plants, Plant Methods. 1 (2005) 13. https://doi.org/10.1186/1746-4811-1-13.

[107] I.A. Sparkes, J. Runions, A. Kearns, C. Hawes, Rapid, transient expression of fluorescent

fusion proteins in tobacco plants and generation of stably transformed plants, Nat Protoc. 1 (2006) 2019–2025. https://doi.org/10.1038/nprot.2006.286.

[108] S.-D. Yoo, Y.-H. Cho, J. Sheen, Arabidopsis mesophyll protoplasts: a versatile cell system for transient gene expression analysis, Nat Protoc. 2 (2007) 1565–1572. https://doi.org/10.1038/nprot.2007.199.

[109] D. Albrecht, O. Kniemeyer, A.A. Brakhage, R. Guthke, Missing values in gel-based proteomics, Proteomics. 10 (2010) 1202–11. https://doi.org/10.1002/pmic.200800576.

[110] Z. Hamid, K.D. Zimmerman, H. Guillen-Ahlers, C. Li, P. Nathanielsz, L.A. Cox, M. Olivier, Assessment of label-free quantification and missing value imputation for proteomics in non-human primates, BMC Genomics. 23 (2022) 496. https://doi.org/10.1186/s12864-022-08723-1.

[111] L. Jin, Y. Bi, C. Hu, J. Qu, S. Shen, X. Wang, Y. Tian, A comparative study of evaluating missing value imputation methods in label-free proteomics, Sci Rep. 11 (2021) 1760. https://doi.org/10.1038/s41598-021-81279-4.

[112] Y.V. Karpievitch, A.R. Dabney, R.D. Smith, Normalization and missing value imputation for label-free LC-MS analysis, BMC Bioinformatics. 13 Suppl 16 (2012) 5. https://doi.org/10.1186/1471-2105-13-S16-S5.

[113] Andrea Vega, Isabel Fredes, José O'Brien, Zhouxin Shen, Krisztina Ötvös, Rashed Abualia, Eva Benkova, Steven P Briggs, Rodrigo A Gutiérrez, Nitrate triggered phosphoproteome changes and a PIN2 phosphosite modulating root system architecture, EMBO Reports. 22 (2021) 51813. https://doi.org/10.15252/embr.202051813.

[114] M.M. Kamal, S. Ishikawa, F. Takahashi, K. Suzuki, M. Kamo, T. Umezawa, K. Shinozaki, Y. Kawamura, M. Uemura, Large-Scale Phosphoproteomic Study of Arabidopsis Membrane Proteins Reveals Early Signaling Events in Response to Cold, IJMS. 21 (2020) 8631. https://doi.org/10.3390/ijms21228631.

[115] K. Kammers, R.N. Cole, C. Tiengwe, I. Ruczinski, Detecting significant changes in protein abundance, EuPA Open Proteomics. 7 (2015) 11–19. https://doi.org/10.1016/j.euprot.2015.02.002.

[116] P.P. Roux, P. Thibault, The Coming of Age of Phosphoproteomics—from Large Data Sets to Inference of Protein Functions, Molecular & Cellular Proteomics. 12 (2013) 3453–3464. https://doi.org/10.1074/mcp.R113.032862.

[117] C.P.S. Kruse, A.D. Meyers, P. Basu, S. Hutchinson, D.R. Luesse, S.E. Wyatt, Spaceflight induces novel regulatory responses in Arabidopsis seedling as revealed by combined proteomic and transcriptomic analyses, BMC Plant Biol. 20 (2020) 237. https://doi.org/10.1186/s12870-020-02392-6.

[118] C.A. Schenck, V. Nadella, S.L. Clay, J. Lindner, Z. Abrams, S.E. Wyatt, A proteomics approach identifies novel proteins involved in gravitropic signal transduction, American

Journal of Botany. 100 (2013) 194–202. https://doi.org/10.3732/ajb.1200339.

[119] B.J. Feger, J.W. Thompson, L.G. Dubois, R.P. Kommaddi, M.W. Foster, R. Mishra, S.K. Shenoy, Y. Shibata, Y.H. Kidane, M.A. Moseley, L.S. Carnell, D.E. Bowles, Microgravity induces proteomics changes involved in endoplasmic reticulum stress and mitochondrial protection, Sci Rep. 6 (2016) 34091. https://doi.org/10.1038/srep34091.

[120] C. Mazars, C. Brière, S. Grat, C. Pichereaux, M. Rossignol, V. Pereda-Loth, B. Eche, E. Boucheron-Dubuisson, I. Le Disquet, F.J. Medina, A. Graziana, E. Carnero-Diaz, Microgravity induces changes in microsome-associated proteins of Arabidopsis seedlings grown on board the international space station, PLoS One. 9 (2014) 91814. https://doi.org/10.1371/journal.pone.0091814.

[121] L. Kaufman, P.J. Rousseeuw, Finding groups in data: an introduction to cluster analysis, John Wiley & Sons, 2009.

[122] J. Bennett, A. Weeds, CALCIUM AND THE CYTOSKELETON, British Medical Bulletin. 42 (1986) 385–390. https://doi.org/10.1093/oxfordjournals.bmb.a072156.

[123] B. Harrison, P.H. Masson, Do ARG1 and ARL2 form an actin-based gravity-signaling chaperone complex in root statocytes?, Plant Signaling & Behavior. 3 (2008) 650–653. https://doi.org/10.4161/psb.3.9.5749.

[124] L. Xi, Z. Zhang, S. Herold, S. Kassem, X.N. Wu, W.X. Schulze, Phosphorylation Site Motifs in Plant Protein Kinases and Their Substrates, in: X.N. Wu (Ed.), Plant Phosphoproteomics, Springer US, New York, NY, 2021: pp. 1–16. https://doi.org/10.1007/978-1-0716-1625-3_1.

[125] D. Bradley, P. Beltrao, Evolution of protein kinase substrate recognition at the active site, PLoS Biol. 17 (2019) e3000341. https://doi.org/10.1371/journal.pbio.3000341.

[126] X.-Y. Zhou, L. Song, H.-W. Xue, Brassinosteroids Regulate the Differential Growth of Arabidopsis Hypocotyls through Auxin Signaling Components IAA19 and ARF7, Molecular Plant. 6 (2013) 887–904. https://doi.org/10.1093/mp/sss123.

[127] R. Tejos, C. Rodriguez-Furlán, M. Adamowski, M. Sauer, L. Norambuena, J. Friml, PATELLINS are regulators of auxin-mediated PIN1 relocation and plant development in Arabidopsis thaliana, J Cell Sci. 131 (2018). https://doi.org/10.1242/jcs.204198.

[128] S. Penfield, S. Clements, K.J. Bailey, A.D. Gilday, R.C. Leegood, J.E. Gray, I.A. Graham, Expression and manipulation of phosphoenolpyruvate carboxykinase 1 identifies a role for malate metabolism in stomatal closure, The Plant Journal. 69 (2012) 679–88. https://doi.org/10.1111/j.1365-313X.2011.04822.x.

[129] mTORC1 signaling and the metabolic control of cell growth, Current Opinion in Cell Biology. 45 (2017) 72–82. https://doi.org/10.1016/j.ceb.2017.02.012.

[130] J. Van Leene, C. Han, A. Gadeyne, D. Eeckhout, C. Matthijs, B. Cannoot, N. De Winne, G. Persiau, E. Van De Slijke, B. Van De Cotte, E. Stes, M. Van Bel, V. Storme, F. Impens,

K. Gevaert, K. Vandepoele, I. De Smet, G. De Jaeger, Capturing the phosphorylation and protein interaction landscape of the plant TOR kinase, Nat. Plants. 5 (2019) 316–327. https://doi.org/10.1038/s41477-019-0378-z.

[131] L.R. Band, D.M. Wells, A. Larrieu, J. Sun, A.M. Middleton, A.P. French, G. Brunoud, E.M. Sato, M.H. Wilson, B. Péret, M. Oliva, R. Swarup, I. Sairanen, G. Parry, K. Ljung, T. Beeckman, J.M. Garibaldi, M. Estelle, M.R. Owen, K. Vissenberg, T.C. Hodgman, T.P. Pridmore, J.R. King, T. Vernoux, M.J. Bennett, Root gravitropism is regulated by a transient lateral auxin gradient controlled by a tipping-point mechanism, Proc Natl Acad Sci U S A. 109 (2012) 4668–73. https://doi.org/10.1073/pnas.1201498109.

[132] X. Wang, R. Yu, J. Wang, Z. Lin, X. Han, Z. Deng, L. Fan, H. He, X.W. Deng, H. Chen, The Asymmetric Expression of SAUR Genes Mediated by ARF7/19 Promotes the Gravitropism and Phototropism of Plant Hypocotyls, Cell Rep. 31 (2020) 107529. https://doi.org/10.1016/j.celrep.2020.107529.

[133] M. Dümmer, C. Michalski, C. Forreiter, P. Galland, Phenotypic Reversal in Arabidopsis thaliana: Sucrose as a Signal Molecule Controlling the Phenotype of Gravi- and Phototropism Mutants, J Plant Growth Regul. 35 (2016) 430–439. https://doi.org/10.1007/s00344-015-9550-5.

[134] N. S�ther, T.-H. Iversen, Gravitropism and starch statoliths in an Arabidopsis mutant, Planta. 184 (1991). https://doi.org/10.1007/BF00197897.

[135] D.Y. Sung, E. Vierling, C.L. Guy, Comprehensive expression profile analysis of the Arabidopsis Hsp70 gene family, Plant Physiol. 126 (2001) 789–800. https://doi.org/10.1104/pp.126.2.789.

[136] B.R. Harrison, P.H. Masson, ARL2, ARG1 and PIN3 define a gravity signal transduction pathway in root statocytes, Plant J. 53 (2008) 380–92. https://doi.org/10.1111/j.1365-313X.2007.03351.x.

[137] T.L. Yoder, H. Zheng, P. Todd, L.A. Staehelin, Amyloplast Sedimentation Dynamics in Maize Columella Cells Support a New Model for the Gravity-Sensing Apparatus of Roots, Plant Physiol. 125 (2001) 1045–1060. https://doi.org/10.1104/pp.125.2.1045.

[138] M. Zourelidou, I. Müller, B.C. Willige, C. Nill, Y. Jikumaru, H. Li, C. Schwechheimer, The polarly localized D6 PROTEIN KINASE is required for efficient auxin transport in *Arabidopsis thaliana*, Development. 136 (2009) 627–636. https://doi.org/10.1242/dev.028365.

[139] H.Q. Zheng, F. Han, J. Le, Higher Plants in Space: Microgravity Perception, Response, and Adaptation, Microgravity Sci. Technol. 27 (2015) 377–386. https://doi.org/10.1007/s12217-015-9428-y.

[140] Z. Yang, G. Guo, N. Yang, S.S. Pun, T.K.L. Ho, L. Ji, I. Hu, J. Zhang, A.L. Burlingame, N. Li, The change of gravity vector induces short-term phosphoproteomic alterations in

Arabidopsis, Journal of Proteomics. 218 (2020) 103720. https://doi.org/10.1016/j.jprot.2020.103720.

[141] N. Rayapuram, M. Jarad, H.M. Alhoraibi, J. Bigeard, A.A. Abulfaraj, R. Völz, K.G. Mariappan, M. Almeida-Trapp, M. Schlöffel, E. Lastrucci, L. Bonhomme, A.A. Gust, A. Mithöfer, S.T. Arold, D. Pflieger, H. Hirt, Chromatin phosphoproteomics unravels a function for AT-hook motif nuclear localized protein AHL13 in PAMP-triggered immunity, Proceedings of the National Academy of Sciences. 118 (2021) 2004670118. https://doi.org/10.1073/pnas.2004670118.

[142] K. Soga, C. Yamazaki, M. Kamada, N. Tanigawa, H. Kasahara, S. Yano, K.H. Kojo, N. Kutsuna, T. Kato, T. Hashimoto, T. Kotake, K. Wakabayashi, T. Hoson, Modification of growth anisotropy and cortical microtubule dynamics in Arabidopsis hypocotyls grown under microgravity conditions in space, Physiol Plant. 162 (2018) 135–144. https://doi.org/10.1111/ppl.12640.

[143] B.K. Drøbak, V.E. Franklin-Tong, C.J. Staiger, The role of the actin cytoskeleton in plant cell signaling, New Phytologist. 163 (2004) 13–30. https://doi.org/10.1111/j.1469-8137.2004.01076.x.

[144] S. Xu, Q. Wang, Y. Liu, Z. Liu, R. Zhao, X. Sheng, Latrunculin B facilitates gravitropic curvature of Arabidopsis root by inhibiting cell elongation, especially the cells in the lower flanks of the transition and elongation zones, Plant Signaling & Behavior. 16 (2021) 1876348. https://doi.org/10.1080/15592324.2021.1876348.

[145] P. Bork, E.V. Koonin, Protein sequence motifs, Current Opinion in Structural Biology. 6 (1996) 366–376. https://doi.org/10.1016/S0959-440X(96)80057-1.

[146] M. Zufferey, C. Montandon, V. Douet, E. Demarsy, B. Agne, S. Baginsky, F. Kessler, The novel chloroplast outer membrane kinase KOC1 is a required component of the plastid protein import machinery, Journal of Biological Chemistry. 292 (2017) 6952–6964. https://doi.org/10.1074/jbc.M117.776468.

[147] J.M. Stone, J.C. Walker, Plant Protein Kinase Families and Signal Transduction, Plant Physiol. 108 (1995) 451–457. https://doi.org/10.1104/pp.108.2.451.

[148] L. De Veylder, T. Beeckman, G.T.S. Beemster, L. Krols, F. Terras, I. Landrieu, E. Van Der Schueren, S. Maes, M. Naudts, D. Inzé, Functional Analysis of Cyclin-Dependent Kinase Inhibitors of Arabidopsis, Plant Cell. 13 (2001) 1653–1668. https://doi.org/10.1105/TPC.010087.

[149] F.A. Oluwafemi, A. Neduncheran, Analog and simulated microgravity platforms for life sciences research: Their individual capacities, benefits and limitations, Advances in Space Research. 69 (2022) 2921–2929. https://doi.org/10.1016/j.asr.2022.01.007.

[150] M. Böhmer, E. Schleiff, Microgravity research in plants: A range of platforms and options allow research on plants in zero or low gravity that can yield important insights into plant

physiology, EMBO Reports. 20 (2019) 48541. https://doi.org/10.15252/embr.201948541.

[151] B. Petrovská, H. Jeřábková, L. Kohoutová, V. Cenklová, Ž. Pochylová, Z. Gelová, G. Kočárová, L. Váchová, M. Kurejová, E. Tomaštíková, P. Binarová, Overexpressed TPX2 causes ectopic formation of microtubular arrays in the nuclei of acentrosomal plant cells, Journal of Experimental Botany. 64 (2013) 4575–4587. https://doi.org/10.1093/jxb/ert271.

[152] J.R. Lucas, S.L. Shaw, MAP65-1 and MAP65-2 promote cell proliferation and axial growth in Arabidopsis roots, The Plant Journal. 71 (2012) 454–63. https://doi.org/10.1111/j.1365-313X.2012.05002.x.

[153] L. Shi, Y. Wu, J. Sheen, TOR signaling in plants: conservation and innovation, Development. 145 (2018). https://doi.org/10.1242/dev.160887.

[154] J.C. Tovar, J.S. Hoyer, A. Lin, A. Tielking, S.T. Callen, S. Elizabeth Castillo, M. Miller, M. Tessman, N. Fahlgren, J.C. Carrington, Raspberry Pi–powered imaging for plant phenotyping, Applications in Plant Sciences. 6 (2018) 1031.

[155] J. Friml, M. Gallei, Z. Gelová, A. Johnson, E. Mazur, A. Monzer, L. Rodriguez, M. Roosjen, I. Verstraeten, B.D. Živanović, M. Zou, L. Fiedler, C. Giannini, P. Grones, M. Hrtyan, W.A. Kaufmann, A. Kuhn, M. Narasimhan, M. Randuch, N. Rýdza, K. Takahashi, S. Tan, A. Teplova, T. Kinoshita, D. Weijers, H. Rakusová, ABP1-TMK auxin perception for global phosphorylation and auxin canalization, Nature. 609 (2022) 575–581. https://doi.org/10.1038/s41586-022-05187-x.

[156] B.S. Mishra, M. Singh, P. Aggrawal, A. Laxmi, Glucose and auxin signaling interaction in controlling Arabidopsis thaliana seedlings root growth and development, PLoS One. 4 (2009) 4502. https://doi.org/10.1371/journal.pone.0004502.

[157] X. Che, B.L. Splitt, M.T. Eckholm, N.D. Miller, E.P. Spalding, BRXL4-LAZY1 interaction at the plasma membrane controls Arabidopsis branch angle and gravitropism, Plant J. 113 (2023) 211–224. https://doi.org/10.1111/tpj.16055.

[158] X. Yang, L. Song, H.-W. Xue, Membrane Steroid Binding Protein 1 (MSBP1) Stimulates Tropism by Regulating Vesicle Trafficking and Auxin Redistribution, Molecular Plant. 1 (2008) 1077–1087. https://doi.org/10.1093/mp/ssn071.

[159] X. Wang, Regulatory Functions of Phospholipase D and Phosphatidic Acid in Plant Growth, Development, and Stress Responses, Plant Physiology. 139 (2005) 566–573. https://doi.org/10.1104/pp.105.068809.

[160] Y. Li, W. Yuan, L. Li, H. Dai, X. Dang, R. Miao, F. Baluška, H.J. Kronzucker, C. Lu, J. Zhang, W. Xu, Comparative analysis reveals gravity is involved in the MIZ1-regulated root hydrotropism, Journal of Experimental Botany. 71 (2020) 7316–7330. https://doi.org/10.1093/jxb/eraa409.

Erklärung

Ich erkläre hiermit, dass ich mich bisher keiner Doktorprüfung unterzogen habe.

Frankfurt am Main, den …….. …….

Eidesstattliche Versicherung

Ich erkläre hiermit an Eides Statt, dass ich die vorgelegte Dissertation über

„Combining phosphoproteomics and high-throughput phenotyping for the identification of gravitropism-related proteins in *Arabidopsis thaliana*"

selbständig angefertigt und mich anderer Hilfsmittel als der in ihr angegebenen nicht bedient habe, insbesondere, dass alle Entlehnungen aus anderen Schriften mit Angabe der betreffenden Schrift gekennzeichnet sind.

Ich versichere, die Grundsätze der guten wissenschaftlichen Praxis beachtet, und nicht die Hilfe einer kommerziellen Promotionsvermittlung in Anspruch genommen zu haben.

Frankfurt am Main, den …….. …….